# The Identification and Characterization of Stem/Progenitor Cells in the Ovarian Surface Epithelium

Lisa Turchet

Thesis submitted to the
Faculty of Graduate and Postdoctoral Studies
in partial fulfillment of the requirements
for a doctoral degree in Cellular and Molecular Medicine.

Department of Cellular and Molecular Medicine
Faculty of Medicine
University of Ottawa

# DEDICATION

To my parents Enzo and Geri, my in-laws Pete and Liz and my husband Adam for their love and support.

# AUTHORIZATION

Chapter 2 appears in the journal Biology of Reproduction and is reproduced here with permission.

# ABSTRACT

When a follicle ovulates, the ovarian surface epithelium (OSE), which covers the surface of the ovary, is ruptured and then rapidly regenerates. Because of this cycle of wound and repair, we determined if the OSE contains a stem/progenitor cell population. We identified a population of OSE cells with progenitor cell characteristics that express the stem cell marker Stem Cell Antigen-1 (SCA-1). We determined the size of the SCA-1 expressing (SCA-1+) progenitor cell population is regulated by at least two ovulation-associated factors present in the follicular fluid: Transforming Growth Factor beta 1 (TGFB1) and Leukaemia-Inhibitory Factor. Ovulation triggers an epithelial-to-mesenchymal transition (EMT) in the OSE surrounding the ovulatory wound. Because TGFB1 is a known inducer of the EMT, and because the EMT plays a role in expanding stem cell populations in other epithelia, we determined if TGFB1 expands the SCA-1+ OSE progenitor cell population by triggering an EMT. Treatment with TGFB1 and overexpression of the EMT master gene, *SNAIL*, caused the OSE cells to undergo an EMT, but unlike TGFB1 treatment, SNAIL overexpression did not expand the SCA-1+ OSE population. Interestingly, EMT induced by SNAIL overexpression increased sphere formation by OSE cells, which indicated that it increased specific stem cell capabilities of the OSE. Because BRCA1 controls the size of the progenitor cell population in mammary epithelium, we determined if the OSE progenitor cell population is regulated by BRCA1. OSE with inactivated *Brca1* were more stem-like and expressed higher mRNA levels of the known stem cell markers *CD44*, *CD117*, *CD133* and *Sca-1* compared to OSE with functional *Brca1*. Inactivation of *Brca1* also increased the number of OSE cells with

surface expression of SCA-1. In addition, TGFB1 and SNAIL-overexpression decreased BRCA1 protein expression compared to controls. Besides providing the first report of a surface maker for OSE with stem-like properties, the results suggest that these cells may play a role in ovulatory wound healing as they are regulated by the EMT, and in ovarian cancer initiation as their numbers increase when BRCA1 is dysfunctional.

# TABLE OF CONTENTS

# LIST OF TABLES

# LIST OF FIGURES

# LIST OF ABBREVIATIONS

× *g*: times gravity
12L:12D: 12 hours light:12 hours dark
3D: three dimensional
ABC: ATP-binding cassette
ABCG2: ATP-binding cassette, subfamily G, member 2
AdCre: Ad5CMVCre recombinant adenovirus
AdGFP: Ad5CMVeGFP recombinant adenovirus
ANOVA: analysis of variance
AP-1: Activator Protein 1
ATP: Adenosine-5'-triphosphate
b-cat: Beta Catenin
BMP: Bone Morphogenetic Protein
bp: base pair
Brca1: breast cancer 1, early onset
Brca1int13rev: Brca1 intron 4 reverse
Brca1int4fwd: Brca1 intron 4 forward
BRCT domain: BRCA1 C Terminus domain
C-Terminal: Carboxyl-Terminal
CD117: v-kit Hardy-Zuckerman 4 feline sarcoma viral oncogene homolog (a.k.a. KIT)
CD133: Prominin 1
CD24: CD24 molecule
CD44: CD44 molecule (Indian blood group)
cDNA: complementary deoxyribonucleic acid
CMV: cytomegalovirus
$CO_2$: carbon dioxide
DAB: diaminobenzidine
DBS: donor bovine serum
ddH2O: double-distilled water
DNA: deoxyribonucleic acid
eCG: equine chorionic gonadotropin
ECL: enhanced chemiluminescence
EDTA: Ethylenediaminetetraacetic acid
EGF: Epithelial Growth Factor
eGFPL enhanced green fluorescent protein.
EMT: epithelial-to-mesenchymal transition
EOC: Epithelial Ovarian Cancer
EPCAM: Epithelial cell adhesion molecule

EpR: Epithelial Repressor
F: forward
FBS: fetal bovine serum
FE: Fimbria Epithelium
Foxc2: Forkhead Box Protein C2
FS: forward scatter
FSH: Follicle-stimulating Hormone
$FS^{high}$: high forward scatter
$FS^{low}$: low forward scatter
FTE: Fallopian Tube Epithelium
FVB/N:
GAPDH: Glyceraldehyde 3-phosphate dehydrogenase
GDF: Growth and Differentiation factor
*Gdf9*: *Growth/differentiation factor 9*
GDNF: Glial Cell-Derived Neurotrophic Factor
GFP: Green Fluorescent Protein
GPI-AP: Glycosyl Phosphatidylinositol-anchored Cell Surface Protein
h: hour
$H_2O_2$: Hydrogen Peroxide
H3K4: Histone H3 Lysine 4
hCG: human chorionic gonadotropin
HRP: Horseradish Peroxidase
i.p.: intraperitoneal
IGF2: Insulin-like Growth Factor II
IHC: immunohistochemistry
ITSS: Insulin-Transferrin-Sodium-Selenite Solution
IU: international units
kb: kilobase
KGF: Keratinocyte Growth Factor
KIT-: non-KIT expressing
Kit: v-kit Hardy-Zuckerman 4 feline sarcoma viral oncogene homolog (a.k.a. CD117)
KIT+: KIT expressing
L: liter
lacZ: β-galactosidase
LH: Luteinizing Hormone
LIF: Leukaemia-inhibitory Factor
loxP: locus of X-over P1
LSD1: lysine (K)-specific demethylase 1A
LY6A-: non-LY6A expressing
Ly6a: Lymphocyte antigen 6 complex, locus A (a.k.a. Sca-1)

LY6A+: LY6A expressing
MAPK: Mitogen-activated protein kinase
MaSC: Mammary Stem Cell
MDR1: multidrug-resistant protein 1
MeA: Mesenchymal Activator
mg: milligram
min: minute
ml: milliliter
mm: millimeter
MOSE: mouse ovarian surface epithelium
MP: main population
mW: milliwatts
N-Terminal: Amino-Terminal
Nanog: Nanog homeobox
ng: nanogram
nm: nanometers
Oct-4: Octamer-binding Transcription Factor 4
OSE: ovarian surface epithelium
OVGP1:oviductal glycoprotein 1
PAX8: Paired box gene 8
PBS: phosphate buffered saline
PCM: progenitor cell medium
PCR: polymerase chain reaction
PEI: polyethylenimine
*Ppia*: peptidylprolyl isomerase A (cyclophilin A)
Q-PCR: quantitate polymerase chain reaction
R: reverse
RANK: receptor activator of nuclear factor kappa B
RING domain:Really Interesting New Gene finger domain
RNA: ribonucleic acid
rpm: revolutions per minute
RT-PCR: reverse transcriptase polymerase chain reaction
Sca-1: Stem Cell Antigen-1 (a.k.a. Ly6a)
Scp3:Synaptonemal Complex Protein 3
sec: second
SEM: standard error of the mean
Slug: snail homolog 2 (Drosophila)
SMAD: Small Body Size (SMA) and Mothers Against Decapentaplegic (MAD) Homolog
SMAD3: SMAD family member 4
SMAD4: SMAD family member 4

Snail: snail homolog 1 (Drosophila)
SOV: superovulation
Sox2: Sex determining region Y-box 2
SOX9: SRY (sex determining region Y)-box 9
SP: side population
SP1: specificity protein 1
TBST: tris buffered saline with 0.05% Tween 20
TCF: T cell factor
TGFB: transforming growth factor beta
TGFB1: transforming growth factor beta 1
TSA: Tyramide Signal Amplification
Twist: twist homolog 1 (Drosophila)
U: units
VSELs: very small embryonic-like stem cells
wk: week
X-gal: 5-bromo-4-chloro-indolyl-β-D-galactopyranoside
Zeb: Zinc finger E-box-binding homeobox
µg: microgram
µl: microliter
µm: micrometer
µM: micromolar

# ACKNOWLEDGMENTS

First and foremost I would like to thank my supervisor and mentor, Barbara Vanderhyden. You provided guidance and direction when I lost my scientific way, you provided advice when I was not sure of the next step (both in the lab and in life) and you are a wonderful role model and mentor. You have influenced and enriched more than my scientific career and for that I am grateful. I will always look up to you.

Many thanks to my thesis advisory committee, Drs. Baltz, Sabourin, and McBurney, who always challenged me, kept me on my toes, and provided countless pieces of advice.

I have been fortunate to work with some wonderful people, many of whom have become life long friends. I'd like to thank my labmates. You were my colleagues, advisors, partners in crime, and most importantly my friends. Each of you provided advice and inspiration in your own way and for that I am grateful. I also would like to thank Olga Collins, Dr. Ken Garson, Colleen Crane and Elizabeth MacDonald for their patience, expertise, and willingness to teach. You were always there to answer my questions and have taught me so much.

Thank you to all my cheerleaders, especially my parents, my sisters, my in-laws and my Uncle Bill, who without hesitation believed I could do this and were always there to offer support, encouragement and a bottle of wine.

Finally, a special thanks to my husband, Adam, who I met at the beginning of graduate school and supported me every step of the way.

“A scientist in his laboratory is not a mere technician: he is also a child confronting natural phenomena that impress him as though they were fairy tales.”

- Marie Curie

# CHAPTER 1: INTRODUCTION

Covering the surface of the ovary is a rather unremarkable-looking simple epithelium, referred to aptly as the ovarian surface epithelium (OSE). The OSE is the least studied of the cell types that make up the ovary and, historically, its only function was thought to be rupturing during ovulation and healing afterwards. Today, the functional role of the OSE is steeped in controversy. Some researchers claim that even though it goes against ovarian biology dogma, cells within this epithelial layer are able to produce oocytes in the adult ovary (Johnson et al., 2004). Others report that OSE cells are capable of differentiating into granulosa cells, which are the cells that surround and support the oocyte as it matures (Mork et al., 2012). There is also evidence to suggest that OSE cells have the capacity to differentiate into cells that resemble the epithelium of the adjacent fallopian tube (Maines-Bandiera and Auersperg, 1997; Okamoto et al., 2009; Pothuri et al., 2010; Auersperg, 2011). All of these functions point to the potential existence of a stem population within the OSE. This thesis describes the first steps in defining a stem cell hierarchy: the discovery of a cell surface marker that identifies stem-like cells and the identification of different ways in which this putative stem cell population may be regulated.

## 1.1 The Ovary

The ovary is the principle functional organ in the female reproductive system and it plays two major physiological roles. First, the ovary is responsible for the propagation of the species through the growth and release of a mature oocyte for fertilization (McGee and

Hsueh, 2000). Second, it is responsible for synthesizing and releasing hormones that are essential for all aspects of female reproduction (Hirshfield, 1991).

The ovary contains a variety of cell types that work together to achieve the principle functions of the organ (Fig. 1.1). The ovarian stroma, which is the bulk of the ovarian mass, is made up of fibroblast-like stromal cells. Within the stroma the oocyte is surrounded by granulosa cells, which together with theca cells secrete growth factors and hormones to support folliculogenesis. Once the oocyte is ovulated, the granulosa and theca cells form the corpus luteum, which produces the hormones necessary to maintain the early stages of pregnancy. Finally, on the surface of the ovary, lies the focus of this thesis, the ovarian surface epithelium.

### *1.1.1 The Ovarian Surface Epithelium*

The OSE is a monolayer of squamous-to-cuboidal epithelial cells that covers the surface of the ovary. A basement membrane and a dense collagenous connective tissue layer called the tunica albuginea separates the OSE from the ovarian stroma (Auersperg et al., 2001).

With age the surface of the ovary becomes more irregular and OSE-lined surface invaginations and epithelial inclusion cysts form. The inclusion cysts are thought to be formed when invaginations pinch off and trap OSE cells inside the stroma (Auersperg, 2013). The vast majority of inclusion cysts are lined with OSE cells that appear to be similar to those seen on the surface of the ovary, but some contain ciliated columnar cells that resemble the fallopian tube epithelium (FTE). Interestingly, once OSE cells are

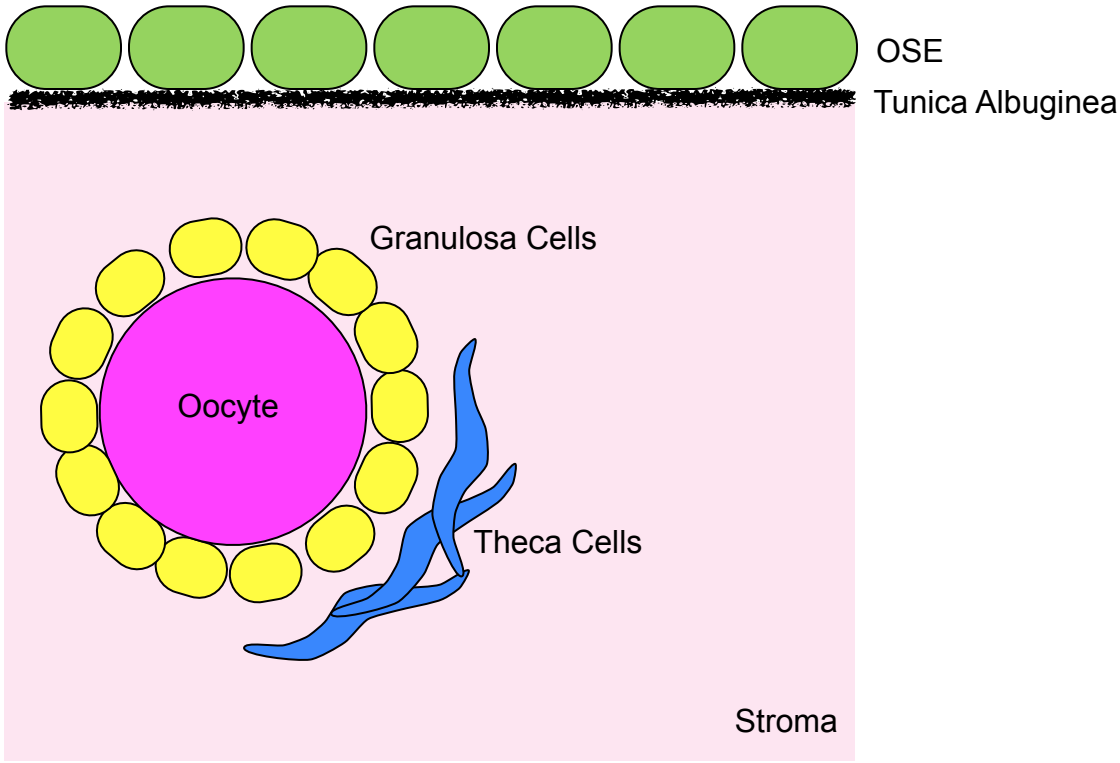


**Figure 1.1: Schematic diagram of the ovary.** Ovarian surface epithelial cells (OSE, green) are found on the surface of the ovary. The tunica albuginea (black line) separates the OSE from the ovarian stroma (light pink), which is made up of fibroblast-like stromal cells. Granulosa cells (yellow) surround the oocyte (magenta) and together with the theca cells (blue) support follicular growth. Not shown; corpus luteum.

trapped in the stroma and therefore exposed to a variety of growth factors and hormones, their gene expression profile changes to more closely resemble the FTE. OSE cells within inclusion cysts acquire the expression of proteins commonly expressed in FTE, including E-CADHERIN, EPCAM, PAX8, the oviduct specific glycoprotein OVGP1 and the presence of cilia (Maines-Bandiera and Auersperg, 1997; Okamoto et al., 2009; Pothuri et al., 2010; Auersperg, 2011). The same inclusion cysts can contain both cells that resemble the OSE cells on the surface of the ovary and cells that resemble FTE and so it is likely that the cells that resemble the FTE were derived from the OSE (Pothuri et al., 2010; Auersperg, 2011). This co-existence of OSE- and FTE-like cells within the same inclusion cysts implies that the OSE, under the right influences, can differentiate into cells that resemble the FTE.

The OSE takes part in cyclical ovulatory ruptures, which is the only defined function for this cell layer. Ovulation, with an emphasis on the impact on the OSE, will be described below.

### *1.1.2 Ovulation*

Ovulation is the process by which a mature oocyte, along with its attached cumulus cells, is expelled from the ovary. It can be broken down into three phases: the pre-ovulatory phase, the ovulatory phase and the post-ovulatory phase.

In the non-ovulating ovary the cells of the OSE are relatively quiescent and slowly dividing. During the pre-ovulatory phase, the follicle that contains the soon-to-be ovulated oocyte swells to form a pronounced bulge on the surface of the ovary, with the point of

ovulation being called a stigma. The OSE cells covering the growing follicle have been shown to proliferate more than OSE cells located distal to the growing follicle (Gaytán et al., 2005; Burdette et al., 2006).

The surge of luteinizing hormone (LH) that triggers ovulation causes the follicle to secrete proteolytic enzymes which degrade the follicle at the surface of the ovary (Murdoch and Martinchick, 2004). As the pressure builds, the follicle ruptures and the oocyte and follicular fluid are expelled. Electron microscope studies reveal that, in many species, OSE cells degenerate and are sloughed off the follicular surface shortly before ovulatory rupture (Auersperg et al., 2001). This cyclic loss of OSE cells may be due to apoptosis induced by prostaglandins produced by the pre-ovulatory follicle (Ackerman and Murdoch, 1993; Murdoch, 1995; Barnett et al., 2006), or by DNA damaged caused by inflammatory mediators and reactive oxygen species that are byproducts of follicular rupture (Shukovski and Tsafriri, 1994; Murdoch, 1999; Kodaman and Behrman, 2001; Murdoch and Martinchick, 2004). In culture OSE cells have been shown to produce proteases, which have been proposed to break down the extracellular matrix and follicle wall (Kruk et al., 1994). It is unclear if this proteolytic activity is required for ovulation as OSE cells undergo apoptosis and are sloughed off the surface of the follicle before it ruptures, although they may exert their effects on the extracellular matrix before they are lost.

Following ovulation, the remnants of the follicle transform into a corpus luteum and the ovarian wound begins to heal. The remaining OSE cells that surround the wound site undergo an epithelial-to-mesenchymal transition and resemble fibroblasts (Salamanca et al., 2004; Ahmed et al., 2006; Gotfredson and Murdoch, 2007). This transformation imparts the

cells with the ability to migrate and contract to heal the gap in the epithelium (Kruk and Auersperg, 1992). OSE cells may also be responsible for replacing the ruptured extracellular matrix as they have been shown to synthesize the necessary components (Kruk and Auersperg, 1992; Auersperg et al., 1994; Kruk and Auersperg, 1994; Kruk et al., 1994; Salamanca et al., 2004).

### *1.1.3 Stem Cells In The OSE*

A stem cell is defined by its ability to robustly self-renew and differentiate into all the cells of its lineage. In many tissues, like the mammary gland, there exists a stem cell hierarchy (Woodward et al., 2005). When stem cells divide they give rise to daughter cells that are either stem cells (through the process of self-renewal) or progenitor cells. Progenitor cells exhibit less robust self-renewal capacity when compared to stem cells and produce differentiated the daughter cells that make up the lineage.

The OSE possesses many characteristics that suggest that it may contain a stem/ progenitor cell subpopulation. The OSE is cyclically ruptured during ovulation and then regenerates to heal the ovarian wound. This process of tissue homeostasis, as seen in other epithelial tissues, is typically maintained by the presence of stem or progenitor cells (Blanpain et al., 2007). Also, OSE cells can adopt both a mesenchymal or an epithelial phenotype, indicating that OSE cells can alter their state of differentiation along pathways leading to fibroblast-like cells to heal ovulatory wound or aberrant epithelial phenotypes like FTE when trapped in inclusion cysts (Auersperg et al., 2001). Finally, it has recently been demonstrated in mice that shortly after birth, the OSE gives rise to the granulosa cells

that surround follicles that are active during adult life (Mork et al., 2012) and may be a source of oocytes in the adult ovary (Johnson et al., 2004). It is therefore likely that the OSE contains at the very least a unipotent progenitor cell capable of replacing OSE cells lost during ovulation, and may even contain multipotent stem or progenitor cells capable of producing FTE-like cells found in inclusion cysts, fibroblast-like cells seen during ovulatory wound repair, granulosa cells perinatally and/or oocytes postnatally.

Recently, a putative somatic stem/progenitor cell in the OSE has been described (Szotek et al., 2008). Label retention was used to identify and isolate slowly-cycling or quiescent cells in the OSE that express epithelial and mesenchymal markers and are enriched within the side population (SP). The SP phenotype, which is discussed in more detail in Chapter 2, is based on the exclusion of Hoechst dye and has been associated with stem/progenitor cells in a variety of tissues and cancers, including ovarian cancer (Goodell et al., 1996; Szotek et al., 2006; Ono et al., 2007). In addition, the label retaining stem/ progenitor cells were observed to proliferate after ovulation, which indicates that they may respond to the estrous cycle (Szotek et al., 2008).

In any discussion of stem cells in the ovary or OSE, it is difficult to ignore the body of research surrounding oogonial stem cells which are cells that are thought to give rise to new oocytes in the adult mouse ovary (summarized in Table 1.1). Johnson et al. (2004) proposed in a controversial paper that there may be an oogonial stem cell, also known as a germline stem cell, on the surface of the ovary that is the source of oocytes in the adult mouse (Johnson et al., 2004). This finding is in direct contrast to the basic doctrine of reproductive biology that females cease oocyte production before birth and as a result are

**Table 1.1: Summary of Ovarian Stem Cell Literature.** A summary of the source or location of the proposed ovarian stem cell, the isolation method, the markers identified and the product or cell type proposed to be produced by the ovarian stem cells.

| Source | Isolation Method | Markers | Product | Ref. |
|---|---|---|---|---|
| Hilar MOSE - Junction of OSE, Hilum and fallopian tube | Enzymatic, FACS | ALDH1, LGR5, LEF1, CD133, CK6B | MOSE, more susceptible to transformation | Flesken-Nikitin et al., 2013 |
| MOSE (tend to be on side closest to fallopian tube) | Enzymatic, FACS | SCA-1 | MOSE | Gamwell et al., 2012 |
| MOSE | Label retention, dye exclusion | Side Population, label retention | MOSE | Szotek et al., 2008 |
| MOSE (E11.5 and birth - P5) | Cell tracking with IF | FOXL2 | Granulosa cells (medullary and cortical) | Mork et al., 2012 |
| MOSE | Visualized with IHC, ovarian cortex pieces transplanted | MVH (mouse VASA homolog) | oocytes | Johnson et al., 2004 |
| MOSE (aged mice) | GFP reporter mice (cell tracking) | Stra8, Dazl | Oocytes (NOBOX, form follicles) | Niikura et al, 2009 |
| Any cell within neonatal or young adult mouse ovary | MACS on dispersed ovary | DDX4 | Oocytes, offspring | Zou et al., 2009 |
| Any cell within adult mouse ovary, oocytes excluded by size | FACS on dispersed ovary | DDX4 | oocytes | White et al., 2012 |
| Ovarian cortical tissue (HOSE, TA, stroma, primordial follicles) from reproductive age women | FACS on dispersed cortical tissue | DDX4 | oocytes | White et al., 2012 |
| HOSE or TA | Scrapping and culturing or IHC studies | morphology | Oocytes (CK5-, SP + surface, presence of polar body) | Bukovsky et al., 2005, 2008 |
| HOSE from women with no follicles or oocytes (premature ovarian failure or menopausal) OSE from adult rabbit, sheep and monkey | Scrapping and culturing | Size (small round bubble like) "VSELs" | Oocytes (OCT4A, OCT4B, C-KIT, VASA, ZP2, ZP4, DAZL, GDF9, NANOG, Stella) | Virant-Klum et al., 2008, 2011, Parte et al., 2011 |

Abbreviations: FACS - fluorescence activated cell sorting, HOSE - human ovarian surface epithelium, IF - immunofluorescence, MACS - magnet assisted cell sorting, TA - tunica albuginea.

born with a finite set of oocytes (Anderson and Hirshfield, 1992). Similarly, Bukovsky and colleagues claim that the tunica albuginea located directly below the OSE is capable of producing new primordial follicles in the postnatal ovary (Bukovsky et al., 1995; Bukovsky et al., 2004; Bukovsky et al., 2008). This claim is partially supported by a recent report that, in mice, the OSE can produce granulosa cells within the first few days after birth, although in this study, the oocytes that were surrounded by the OSE-derived granulosa cells were already present within the ovarian stroma before birth (Mork et al., 2012). The location of the germline stem cells on the surface of the ovary was called into question by Johnson et al. (2005), the same authors who had advocated that concept a year earlier. Instead, they proposed that the putative oocyte-producing cell was found in the bone marrow and peripheral blood of adult female mice (Johnson et al., 2005), although in subsequent publications from this and other research groups, the oocyte-producing cells were again proposed to be within the ovarian cortex, which contains OSE cells as well as the tunica albuginea. In mice, some groups have had success generating oocytes from germline stem cells that are capable of producing viable progeny (Johnson et al., 2005; Zou et al., 2009; Pacchiarotti et al., 2010).

Recent studies have reported the isolation of germline stem cells from OSE of postmenopausal women and women with premature ovarian failure which express developmental embryonic markers including Oct-4, VASA, Nanog, c-Kit and Sox-2 (Virant-Klun et al., 2009; Virant-Klun et al., 2011). These cells are capable of developing embryoid body-, oocyte- and blastocyst-like structures in culture (Virant-Klun et al., 2008; Virant-Klun et al., 2011). In addition, germline stem cells have been isolated from ovarian

cortical tissue of women of reproductive age (White et al., 2012). In some reports, the germline stem cells have a smaller volume than the surrounding somatic cells and are referred to as very small embryonic-like stem cells (VSELs) (Parte et al., 2011; Virant-Klun et al., 2011; Bhartiya et al., 2012). The topic of de novo oocyte generation in the adult ovary is still a controversial one, and it remains to be seen if the presence of germline stem cells can be demonstrated clearly enough to convince the many skeptics.

## 1.2 Stem Cell Antigen 1: Structure and Function

Stem cell markers are surface antigens that allow researchers to identify and isolate/ enrich for cells that display the functional properties of stem or progenitor cells. Molecular stem cell markers, which are used to identify stem cells but not always to isolate then, often play a role in maintaining the characteristics of stem cells, or "stemness". For example, expression of the classic embryonic stem cell marker NANOG, a transcription factor named after *Tír na nÓg* the mythical land of the ever young, is required to maintain both human and mouse embryonic stem cells in an undifferentiated state (Calloni et al., 2013). Surface stem cell markers, are expressed on the surface of cells and can be used, in combination with functional tests of stemness, to isolate or enrich for cells that behave like stem cells. For example Stem Cell Antigen-1 (SCA-1, also known as LY6A), is cell-surface protein that is used to isolate murine hematopoietic stem cells (Spangrude et al., 1988; Okada et al., 1992) and is a focus of this thesis.

SCA-1 is a 18-kDa mouse glycosyl phosphatidylinositol-anchored cell surface protein (GPI-AP) that is encoded by two strain-specific alleles of the *Ly6* gene which are

members of the *Ly6* gene family (LeClair et al., 1986; Palfree and Hämmerling, 1986; McGrew and Rock, 1991; Holmes and Stanford, 2007). The function of SCA-1 is not well understood, but other proteins encoded by members of the *Ly6* gene family localize to lipid rafts in the plasma membrane (Stefanová et al., 1991) and because of this localization, are thought to play critical roles in cell signalling by excluding or concentrating key signalling molecules (Horejsí et al., 1999; Simons and Toomre, 2000; Holmes and Stanford, 2007), as well as regulating receptor recycling and degradation (Le Roy and Wrana, 2005). Like other GPI-APs, SCA-1 may regulate cell signalling via receptor-ligand binding or other protein-protein interactions although no SCA-1 specific ligand has been identified (Holmes and Stanford, 2007).

SCA-1 is perhaps best known as a hematopoietic stem cell marker in mice (Spangrude et al., 1988; Okada et al., 1992). Outside of the hematopoietic system it is expressed in a mixture of mouse stem, progenitor and differentiated cell types, including cells in the dermis, uterus, brain and mammary gland (Miles et al., 1997; Ma et al., 2002a; Ma et al., 2002b; Hanson et al., 2003).

SCA-1 null mice appear to be phenotypically normal, with no reported defects in fertility (Stanford et al., 1997). With age, potential defects in stem/progenitor cell populations of various organs become apparent, though there are no reported defects found in the ovary (Holmes and Stanford, 2007). It has been proposed that the loss of SCA-1 favours differentiation signals at the expense of self-renewal which over time can lead to stem cell exhaustion (Holmes and Stanford, 2007). One example of this can be found in the muscle of SCA-1 deficient mice. Young, SCA-1 deficient mice exhibit larger muscle fibers,

which may be a result of enhanced myoblast proliferation (Mitchell et al., 2005; Kafadar et al., 2009). With age, the size of the muscle fibers in these mice are decreased, perhaps because the increased myoblast proliferation in early life exhausted the muscle stem cell pool (Mitchell et al., 2005; Holmes and Stanford, 2007).

A number of potential human *SCA-1* orthologs have been identified, many of which are encoded by genes that are localized to the region of chromosome 8 that is syntenic with the region where mouse *Ly6* genes reside (Bamezai, 2004), but a human *SCA-1* homolog has not been identified (Holmes and Stanford, 2007). In fact, the 500 kb region that contains the gene that encodes for *Sca-1* was deleted during the speciation between mouse and rat (Holmes and Stanford, 2007). While there is no human equivalent to SCA-1, the fact that it identifies stem/progenitor cells in many different adult mouse tissues and cancers makes it a useful tool in understanding stem/progenitor cell biology.

## 1.3 Transforming Growth Factor Beta 1

Transforming Growth Factor Beta 1 (TGFB1), which is a major focus of the research described in this thesis, is a member of the Transforming Growth Factor Beta (TGFB) superfamily, a structurally conserved but functionally diverse group of proteins. These proteins are widely distributed throughout the body and are involved in numerous physiological processes during both pre- and postnatal life (Massagué, 1992).

### *1.3.1 The TGFB Superfamily*

Members of the TGFB superfamily have been further classified into several

subfamilies. These include the prototypic TGFB subfamily (comprising TGFB1, TGFB2, and TGFB3), the bone morphogenetic protein (BMP) subfamily, the growth and differentiation factor (GDF) subfamily, the activin/inhibin subfamily, the glial cell-derived neurotrophic factor (GDNF) subfamily, as well as several additional members such as anti-Müllerian hormone and NODAL.

In addition to the ligands, there are five type II TGFB receptors and seven type I TGFB receptors which exist as dimers on the cell surface and interact upon ligand binding (Attisano and Wrana, 2002; Derynck and Zhang, 2003). Once a ligand binds to the type II receptor, it activates the type I receptor through phosphorylation to activate the kinase domain (Attisano and Wrana, 2002; Derynck and Zhang, 2003). Each of the ligands in the TGFB superfamily interact with these receptors and combinations of ligand-receptor interactions result in activation of different signalling pathways within the cell such as the Smad and MAPK pathways (Derynck and Zhang, 2003). As a result, the TGFB superfamily regulates a number of processes such as the establishment of the body plan and tissue differentiation through regulation of cell proliferation, differentiation and migration (Attisano and Wrana, 2002; Derynck and Zhang, 2003).

### *1.3.2 TGFB1 In The Ovary*

In the rodent and human ovary the expression of TGFB1 is first detected in preantral follicles and continues to be present through the subsequent stages of follicular development (Knight and Glister, 2006). In rodents and humans, the three prototypic TGFB isoforms (TGFB1, TGFB2 and TGFB3) are produced by theca, granulosa and OSE cells

(Berchuck et al., 1992; Knight and Glister, 2006). The type I and type II TGFB receptors are ubiquitously expressed in most cell types in the ovary, including the OSE (Berchuck et al., 1992).

Since OSE cells secrete TGFB1, and express the components required for TGFB signalling, the OSE may be controlled by autocrine TGFB1 signalling (Berchuck et al., 1992). TGFB1 may also act in a paracrine manner as OSE cells come into contact with TGFB1 that is secreted by the granulosa or theca cells and diffused through the ovarian stroma (Knight and Glister, 2006). In addition, TGFB1 is present in the follicular fluid (Fried and Wramsby, 1998; Fried et al., 1998; Ouellette et al., 2005), and since at ovulation OSE cells are exposed to follicular fluid, this is an additional means by which the OSE may be exposed to ovarian TGFB1.

Regardless of the source, like activin and inhibin, TGFB1 is a known regulator of normal OSE cell function. TGFB1 inhibits OSE cell proliferation in vitro (Berchuck et al., 1992; Ismail et al., 1999; Choi et al., 2001), which may prevent the overproliferation of OSE cells during ovulatory wound healing. Interestingly, exactly how TGFB1 inhibits OSE cell proliferation is unknown, although it does not trigger apoptosis in vitro (Havrilesky et al., 1995). Previous studies have suggested that it may cause a decrease in cyclin-dependent kinase levels which would result in a cell cycle arrest in the G1 to S-phase stage of DNA replication (Massagué, 1992). TGFB1 can counteract the growth stimulatory effect of TGF-alpha or epidermal growth factor (EGF) on OSE (Vigne et al., 1994; Nilsson et al., 2001). TGFB1 also decreases the expression of the Kit ligand and Keratinocyte Growth Factor (KGF) mRNA, both of which code for proteins that, when increased in OSE cells, have a

stimulatory effect on cell proliferation (Ismail et al., 1999; Nilsson et al., 2001). While it is proposed that the role of TGFB1 during ovulation is to control the proliferation rate of the OSE, little is known about the effect of TGFB1 on other aspects of OSE cell function.

### *1.3.3 The Epithelial-to-Mesenchymal Transition*

TGFB1 is a prototypic inducer of the epithelial-to-mesenchymal transition (EMT), which is a phenotypic shift where closely associated, stationary epithelial cells take on a more mesenchymal phenotype and gain the ability to migrate (Zavadil and Böttinger, 2005; Lee et al., 2006; Savagner, 2010). This process plays an important role during embryonic development and tissue regeneration and repair in the adult (Lee et al., 2006; Savagner, 2010).

As epithelial cells undergo EMT, they lose the characteristics of epithelial cells and gain molecular, morphological and/or functional characteristics found in mesenchymal cells. Epithelial cells are normally found in one cell thick layers of cells which are arranged in an orderly fashion by regularly spaced cell junctions. In the OSE, which is one cell layer thick and therefore considered a simple epithelium, these cell junctions are made up of desmosomes, junctional proteins (Siemens and Auersperg, 1988), integrins (Kruk et al., 1994; Cruet et al., 1999) and cadherins (Sundfeldt et al., 1997). The cell junctions allow epithelial cells to enclose 3D structures, like an ovary in the case of the OSE. Besides maintaining the cell layer, the cell junctions inhibit movement of cells away from the monolayer. Epithelial sheets are polarized and the apical and basal surfaces of the sheet have different functions, or, as seen in the OSE, adhere to different substrates.

In contrast to epithelial cells, mesenchymal cells form irregular structures that are not uniform in composition or cell density. The cell-to-cell adhesions are less strong than those seen in epithelial layers, which allows for the increased migration that is characteristic of mesenchymal cells (Savagner, 2010). Rather than the apical-basal polarity seen in epithelial cell layers, mesenchymal cells tend to have front to back leading edge polarity and have a more elongated and extended cell shape (Lee et al., 2006).

Experimentally, the occurrence of an EMT can be detected by an increase in the proteins typically expressed in mesenchymal cells along with a decrease in the expression of proteins associated with epithelial cells. In addition, a change in cell morphology, namely the detection of loosely associated elongated cells, and functional tests that detect an increased ability to migrate, invade and resist anoikis are also used. The proteins, morphological characteristics and functional traits commonly used to detect an EMT are summarized in Table 1.2.

The signalling pathways that initiate the EMT involve the activity of many different members of the TGFB superfamily. When TGFB1 binds to a type II receptor, the type I receptor is activated through phosphorylation (Derynck and Zhang, 2003). The kinase domain on the receptor is then activated and it mediates the phosphorylation of SMAD3 (Derynck and Zhang, 2003). Phosphorylated SMAD3 then binds to SMAD4 and recruits to the promotor region of epithelial or mesenchymal genes, either an epithelial repressor or a mesenchymal activator, respectively (Fuxe et al., 2010). Once recruited, these complexes repress the expression of epithelial genes, like *E-cadherin* and/or promote the expression of mesenchymal genes like *Vimentin* (Figure 1.2).

**Table 1.2: Markers of the epithelial-mesenchymal transition**

| **Proteins That Increase** |
|---|
| SNAIL |
| SLUG |
| TWIST |
| FIBRONECTIN |
| VIMENTIN |
| N-CADHERIN |
| **Proteins That Decrease** |
| E-CADHERIN |
| CYTOKERATIN |
| OCCLUDIN |
| DESMOPLAKIN |
| **Functional Markers** |
| Elongation of cell shape |
| Increased cell scattering |
| Increased migration |
| Increased invasion |
| Resistance to anoikis |

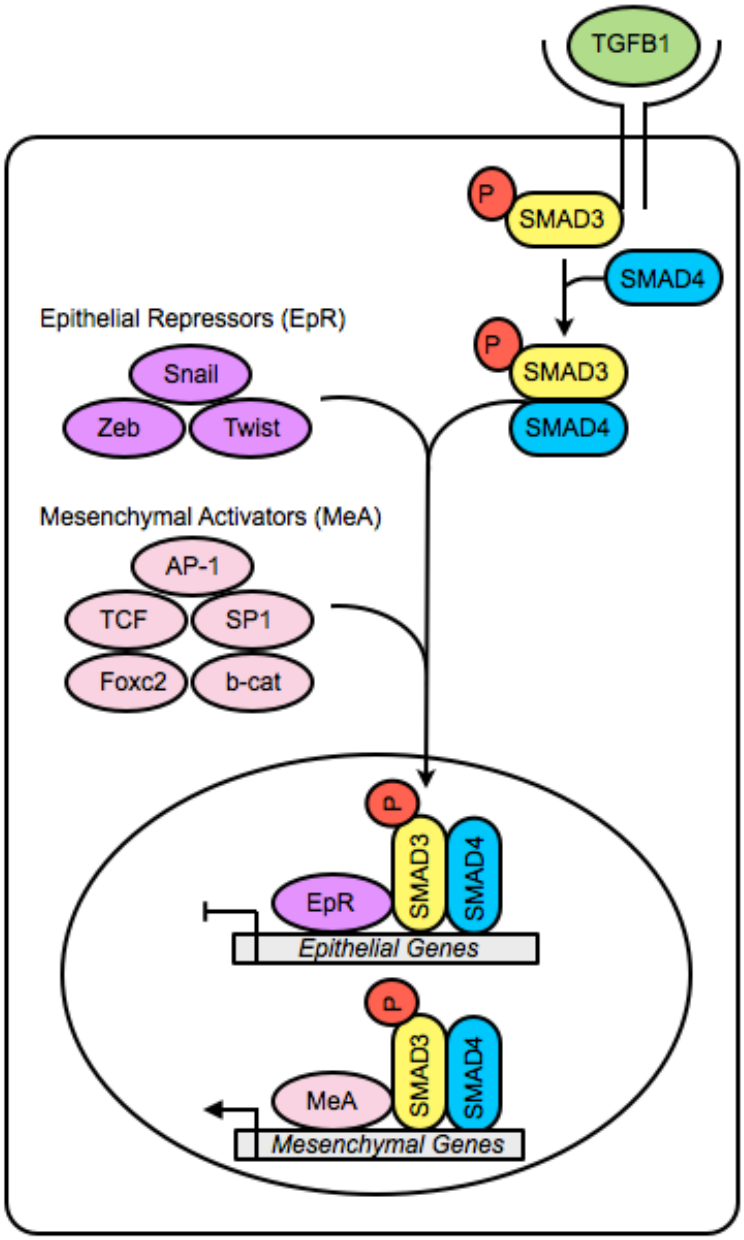


**Figure 1.2: A schematic diagram of SMAD-mediated TGFB1 signaling.** When TGFB1 binds to its receptor, it triggers the phosphorylation of SMAD3. Phospho-SMAD3 then recruits SMAD 4. The phospho-SMAD3/SMAD4 complex recruits either epithelial repressors (EpR) or Mesenchymal Activator (MeA) transcription factors and translocates to the nucleus where they bind to and repress the promotors of epithelial genes or activate the promoters of mesenchymal genes, respectively. Adapted from Fuxe et al., 2010.

During the postovulatory repair process, OSE cells undergo an EMT which can be triggered in vitro by EGF and collagen, both of which are present at the ovulation site (Salamanca et al., 2004). Similarly, embedding OSE cells in collagen gels or other 3D matrices, which mimics the environment to which OSE cells are exposed when they are displaced by ovulation, can also trigger an EMT (Kruk and Auersperg, 1992; Kruk et al., 1994; Ohtake et al., 1999). In addition, TGFB1, a prototypic inducer of the EMT, is an autocrine and paracrine regulator of OSE cell function (Berchuck et al., 1992; Knight and Glister, 2006) and can induce an EMT in OSE cells in vitro (Zhu et al., 2010). The EMT seen at the time of ovulation is thought to facilitate the repair of the ovulatory wound (Ahmed et al., 2006) and is a part of normal OSE physiology.

### *1.3.4 EMT And Stem Cells*

In recent years, the EMT has been proposed to regulate stemness in both normal and cancerous tissues. Mani et al. (2008) provided the first reported evidence of the link between the EMT and stem cells using the stem cell hierarchy in the mammary gland as a model system. The mammary gland is a tree-like structure with hollow branches. These branches have an inner layer of luminal epithelial cells that face the lumen and are enclosed by an outer layer of myoepithelial cells. Ductal luminal cells line the ducts of the mammary gland while lobular luminal cells form secretory acinar structures at the end of the branches and, with pregnancy, become alveolar cells to produce milk. A stem/progenitor cell hierarchy has been demonstrated in this tissue. In simple terms, at the top of the hierarchy are the mammary stem cells (MaSCs), which are capable of reconstituting complete and

functional mammary glands in cleared mammary fat pads (Asselin-Labat et al., 2008). The MaSCs give rise to luminal progenitor cells, which produce only the inner layer of luminal epithelial cells, and myoepithelial progenitor cells, which give rise to only the outer layer of myoepithelial cells of the ducts (Asselin-Labat et al., 2008).

In human immortalized mammary epithelial cells (HMLEs), EMT, when induced by treatment with TGFB1 or overexpression of the EMT-associated transcription factors SNAIL and TWIST, resulted in most, if not all of the HMLEs adopting a $CD44^{high}CD24^{low}$ phenotype that is characteristic of MaSCs and also breast cancer stem cells (Mani et al., 2008). In addition, these EMT-induced $CD44^{high}CD24^{low}$ cells had a greater capacity for mammosphere formation, which is another indicator that they exhibit characteristics of MaSCs. MaSCs isolated from mouse or human mammary glands, or human mammary carcinomas express markers of mesenchymal cells (Mani et al., 2008) which further strengthens the link between the EMT and stem cells in both normal and cancerous tissues. These findings are in agreement with results from a research group in France who reported similar results around the same time as Mani et al. (Morel et al., 2008). Similarly, another research group recently determined that EMT caused by RANK overexpression also resulted in an increase in the number of $CD44^{high}CD24^{low}$ human MaSCs and promoted tumourigenesis and metastasis (Palafox et al., 2012).

Recently this correlation between EMT and the generation of MaSCs has been strengthened by a report that mouse MaSCs generated by EMT can reconstitute complete and functional mammary glands in cleared mammary fat pads (Guo et al., 2012). In these experiments EMT was induced by the overexpression of SLUG, a SNAIL-related

transcription factor. Interestingly, while the induction of EMT alone was enough to convert a luminal progenitor cell into a fully functional MaSC, it was not sufficient to convert a differentiated luminal cell into a MaSC (Guo et al., 2012). To convert differentiated luminal cells into MaSCs, overexpressing the stem cell transcription factor SOX9, in combination with overexpression of either SLUG or SNAIL was required (Guo et al., 2012). In addition co-expression of SLUG and SOX9 greatly increased the tumourigenic and metastatic potential of human breast cancer cells (Guo et al., 2012). While the bulk of the research thus far has been done in the mammary gland, there is emerging evidence that the link between EMT and stem cell regulation may translate to other epithelial stem cell populations, like in the intestine (Horvay et al., 2011). In addition, because an EMT is observed in the OSE surrounding the ovulatory wound site (Salamanca et al., 2004; Ahmed et al., 2006; Gotfredson and Murdoch, 2007), an EMT may be responsible for creating OSE cells with stem/progenitor cell capabilities.

## 1.4 Epithelial Ovarian Cancer

Ovarian cancer is the most lethal gynaecological malignancy and the fifth leading cause of cancer-associated deaths in women. Over the past 20 years the overall cure rate has remained approximately 30% (Seton-Rogers, 2011). Only 20% of ovarian cancer patients are diagnosed when the tumours are limited to the ovary (stage 1) (Romero and Bast, 2012). At this stage, 90% of the patients can be cured by standard therapy which includes cytoreductive surgery followed by platinum and taxane based chemotherapy (Romero and Bast, 2012). After the disease metastasizes to the pelvic organs (stage 2),

organs within the abdomen (stage 3) or organs outside the peritoneal cavity (stage 4) it is much harder to cure (Romero and Bast, 2012).

In the vast majority (70%) of patients, the standard treatment results in a reduction in their tumour burden, and in half of those patients that initially respond to the treatment, no evidence of the disease can be detected up to 5 months after the treatment is finished (Romero and Bast, 2012). Unfortunately, all too often, a small number of chemoresistant cancer cells survive the treatment and are the source of chemoresistant tumours that eventually lead to the death of the patient. Therefore late diagnosis and the persistence of drug-resistant cancer cells have contributed to the lack of improvement in the cure rate.

Epithelial ovarian cancer (EOC) accounts for approximately 90% of ovarian cancers. Currently there are two proposed tissues of origin for EOC, the OSE and the fallopian tube epithelium (FTE), specifically the fimbria (Fig. 1.3). Historically, the OSE was thought to be the sole source of EOC tumours, but in 2001 the FTE was proposed to be the source of hereditary EOC (Piek et al., 2001). Hereditary EOC, which will be discussed in greater detail below, represents 10% of EOC cases and occurs in women with germline mutations in the *Breast Cancer-1, early onset* (*BRCA1*) gene (Weberpals et al., 2008). When the ovary and fallopian tubes were removed prophylactically in 12 BRCA1 mutation carriers, 11 of the 12 specimens had hyperplastic lesions in the FTE, specifically the fimbria, called serous tubal intraepithelial carcinomas (STICs) (Piek et al., 2001). None of the control specimens contained STICs (Piek et al., 2001). Subsequently, STICs were found in 70% of women with EOC irrespective of family history which led to the hypothesis that FTE is the source of some sporadic EOC tumours as well (Kindelberger et al., 2007). There

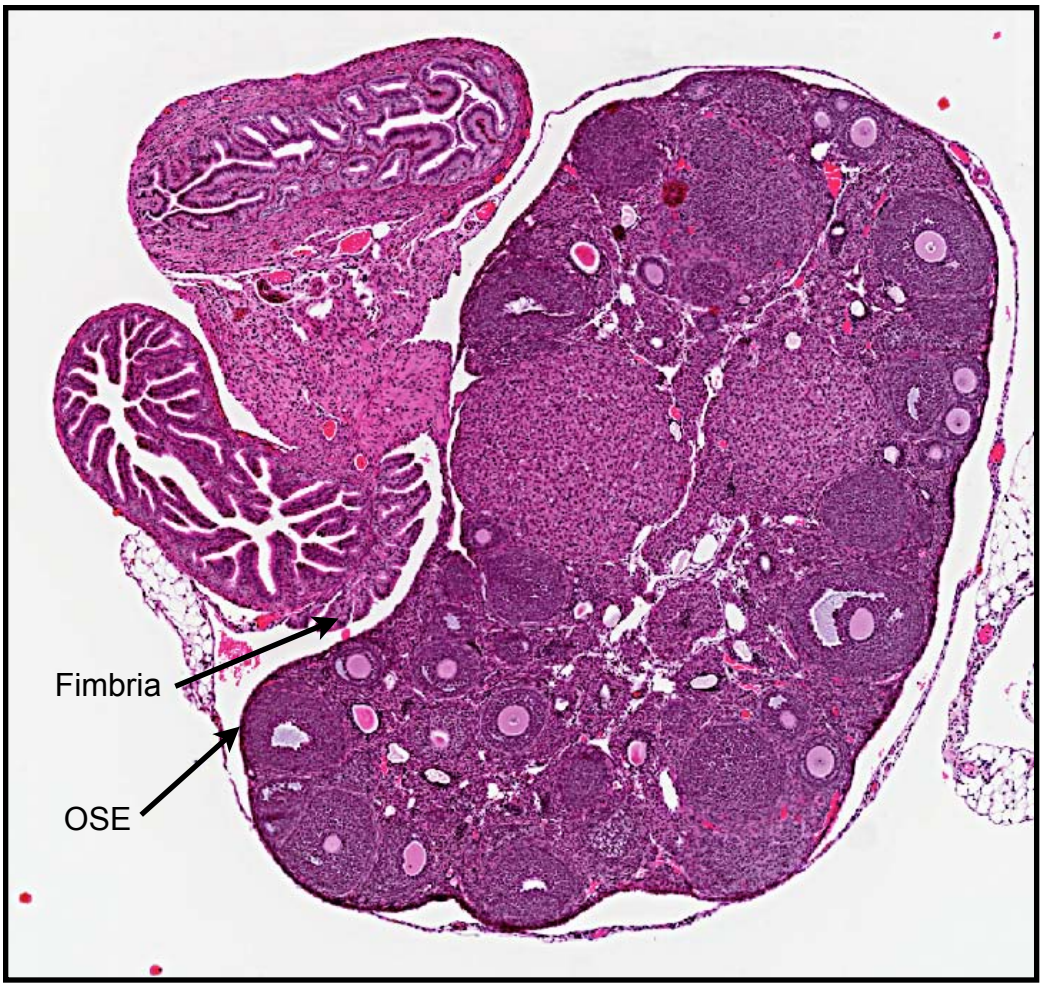


**Figure 1.3: The proposed tissues of origin of epithelial ovarian cancer.** A hematoxylin and eosin stained 3 μm thick section of a paraffin embedded mouse ovary. The ovarian surface epithelium (OSE) and the fimbria are both hypothesized to be tissues of origin for epithelial ovarian cancer (indicated with arrows). The ovary is the kidney shaped structure on the right and the fallopian tube (oviduct) is in the upper left portion of the image. Like the fimbria of the human fallopian tube, the infindibulum of the mouse oviduct has an exteriorized layer of epithelium that is immediately adjacent to the OSE. (Gamwell, unpublished results)

has since been a flurry of research activity, focused mainly on demonstrating that the FTE is the sole source of EOC (Jarboe et al., 2008). Many of the arguments used for either perspective apply to both hypotheses and there is not a single piece of evidence that is 100% in favour of only the FTE or the OSE as the origin of EOC (reviewed in Auersperg, 2013). Therefore, the current evidence would support origins of EOC from both the ovary and the FTE.

### *1.4.1 Ovulation Is An EOC Risk Factor*

Ovulation is the largest non-genetic risk factor for developing ovarian cancer and has been shown to have an impact on both the OSE and the FTE (Burdette et al., 2006; Murdoch et al., 2008; King et al., 2011). There are three major hypotheses linking events associated with ovulation to EOC risk. The tear and repair hypothesis states that over time the continuous damage and repair of the OSE triggered by ovulation increases the likelihood of DNA replication errors leading to genomic instability (Fathalla, 1971). The gonadotropin hypothesis postulates that excessive gonadotropin exposure, specifically FSH and LH which spike during ovulation, lead to increased proliferation of the OSE and/or inhibit apoptosis in damaged cells (Cramer and Welch, 1983; Konishi et al., 1999). Finally, the inflammation hypothesis, which combines and adds to the previous two hypotheses, states that inflammation induced by ovulation may generate oxidative stress that is further exacerbated by cellular proliferation and the effects of FSH and LH, leading to DNA damage and replication error (Fleming et al., 2006). Ovulatory wounds are repaired in an ischemia-reperfusion associated manner and also recruit leukocytes to the wound site on the

surface of the ovary (Murdoch et al., 2008). Both processes generate inflammatory molecules to which OSE cells are exposed (Murdoch et al., 2008).

There are several lines of epidemiological evidence to support the link between ovulation and EOC risk. Over the last 100 years, the incidence of EOC has increased (Fleming et al., 2006). At the same time the estimated average number of ovulations a women experiences has also increased (Fleming et al., 2006). Similarly, a significant correlation was found between the number of ovulations and EOC risk as women who had EOC had more ovulations during their reproductive lifetimes than women who did not have EOC (Purdie et al., 2003).

Further support for the link between ovulation and EOC can be found in non-primate mammals. EOC is rare in non-primate mammals, likely because most animals do not normally reach a high total ovulation number as they only ovulate a few times a year, in response to mating, or in the presence of a male. The only species other than humans that frequently develop EOC are hens, specifically laying hens which are hyperovulated to produce eggs on a daily basis (Fredrickson, 1987).

Pregnancy, lactation and oral contraceptives decrease the risk of EOC, and all suppress ovulation (Risch et al., 1983; Nasca et al., 1984; Shu et al., 1989; Whittemore et al., 1992; Whittemore, 1993; Adami et al., 1994; Risch et al., 1994; Rodriguez et al., 1998; Riman et al., 2002). Each year of oral contraceptive use is associated with a 7% reduction in the relative risk of developing EOC. Interestingly, the use of progestin-only oral contraceptives, which do not suppress ovulation, provides more protection than combined oral contraceptive pills which do suppress ovulation (Risch, 1998). Each month of

pregnancy and breastfeeding reduces EOC risk by approximately 2.5% (Gwinn et al., 1990). The difference in risk reduction seen with pregnancy, lactation, and different formulations of oral contraceptives implies that the protection afforded by pregnancy and oral contraceptive pills cannot be explained merely by a reduction in ovulation. While the epidemiological evidence indicates that ovulation is a risk factor, and not the only risk factor for EOC, more basic research into the impact of ovulation on the tissues of origin of ovarian cancer is needed.

## 1.5 Brca1

Hereditary EOC represents approximately 10% of cases, with the majority of these women carrying germline mutations in the *Breast Cancer-1, early onset* (*BRCA1*) gene (Weberpals et al., 2008). *BRCA1* mutation carriers have a 15-60% increased risk of developing ovarian cancer. In addition, in 40-72% of cases of non-hereditary or sporadic EOC, *BRCA1* is inactivated through hypermethylation, loss of heterozygosity, or haploinsufficiency (Weberpals et al., 2008). Therefore BRCA1 dysfunction is seen in both hereditary and sporadic forms of EOC. The consequence of BRCA1 dysfunction in sporadic EOC and the specific mechanisms underlying the increased risk of ovarian cancer in *BRCA1* mutation carries are not well defined but a better understanding of the function and regulation of BRCA1 may provide some answers.

BRCA1 is a 220kD phosphoprotein that contains an N-terminal RING domain that has E3 ubiquitin ligase activity and a C-terminal BRCT domain that facilitates phospho-protein binding (Mueller and Roskelley, 2003). BRCA1 can interact with a variety of

different proteins, like tumour suppressors, DNA repair proteins and cell cycle regulators (Weberpals et al., 2008). The majority of the mutations found in *BRCA1* mutation carriers are found in the RING and BRCT domains, which indicates that they play a role in suppressing breast and ovarian cancer (Weberpals et al., 2008).

While BRCA1 is known to play a role in cell cycle regulation, cell signalling, and proliferation and differentiation pathways (Weberpals et al., 2008), it is perhaps best known for its role in homologous recombination, which is a major mechanism for protecting the integrity of the genome of proliferating cells (Roy et al., 2012). This form of high-fidelity DNA damage repair uses the undamaged sister chromatid to carry out repair of the double stranded DNA breaks (Roy et al., 2012).

Expression levels of the BRCA1 protein are regulated by a variety of mechanisms. Most known modes of regulation are related to the cell cycle. BRCA1 expression is higher in replicating cells than in non-replicating cells (Gudas et al., 1996). Because of this, factors that alter the proliferation rate of cells have been proposed to directly regulate BRCA1 expression, though upon closer study the alteration in BRCA1 expression was due to the altered proliferation rate and not a direct action of the factor. For example, estrogen has been shown to increase the levels of BRCA1 expression in human breast and ovarian cancer cell lines (Spillman and Bowcock, 1996; Romagnolo et al., 1998), but in these studies the increase in BRCA1 expression has been attributed to an increase in the proliferation rate of cells treated with estrogen, and not to a direct effect of estrogen (Marks et al., 1997; Romagnolo et al., 1998).

BRCA1 expression levels have been shown to change depending on the cell cycle.

BRCA1 is degraded in a proteasome-dependent manner during the G1 phase of the cycle (Roy et al., 2012). When the cell starts DNA replication in preparation for cell division, BRCA1 levels rise, and stay high during the G2 phase, as the newly synthesized DNA is checked for errors and repaired (Roy et al., 2012). This pattern of BRCA1 expression is in keeping with its role in homologous recombination.

Recent research by Wu et al. (2012) has provided an additional way BRCA1 may be regulated which links the EMT with epigenetic regulation of BRCA1 expression. In the presence of Wnt ligands, the EMT transcription factors Slug and Snail are upregulated in breast cancer cells. Slug or Snail then recruit LSD1, a histone demethylase, which binds to the *BRCA1* promoter. LSD1 has been shown to suppress BRCA1 expression by removing methyl groups from histone H3 lysine 4 (H3K4) (Lu et al., 2011).

### *1.5.1 Brca1 Mediated Regulation Of Stem Cells*

Recently a new function for BRCA1 has been identified. BRCA1 was originally hypothesized to act as a stem/progenitor cell regulator by Foulkes (2004). This hypothesis gained support when BRCA1 knockdown in mammary epithelial cells was shown to increase the fraction of cells displaying stem cell markers (Furuta et al., 2005; Liu et al., 2008; Lim et al., 2009; Proia et al., 2011), suggesting that loss of BRCA1 function enhances mammary stem cell characteristics. In addition, in the mammary gland and breast cancer cell lines, expression of CD44, CD113 and CD117 has been shown to be controlled by BRCA1 (Furuta et al., 2005; Liu et al., 2008; Lim et al., 2009; Proia et al., 2011). Current evidence suggests that loss of BRCA1 in mammary tissue may result in the

accumulation of genetically unstable breast stem cells, providing prime targets for further carcinogenic events (Furuta et al., 2005; Liu et al., 2008; Lim et al., 2009; Proia et al., 2011). Determining if BRCA1 can control the differentiation of stem/progenitor cells in other tissues would provide further evidence that BRCA1 can act as a stem cell regulator.

## 1.6 Rationale and Specific Aims

RATIONALE

Many lines of evidence suggest that the OSE may contain a stem/progenitor cell population. The OSE is cyclically ruptured during ovulation and then regenerates to heal the ovarian wound. This process of tissue homeostasis, as seen in other epithelial tissues, is typically maintained by the presence of stem or progenitor cells (Blanpain et al., 2007). Also, the OSE can adopt both a mesenchymal or an epithelial phenotype, indicating that OSE cells can alter their state of differentiation along pathways leading to fibroblast-like cells to heal ovulatory wound or aberrant epithelial phenotypes like FTE when trapped in inclusion cysts (Auersperg et al., 2001). Finally, it has recently been demonstrated that, shortly after birth, the OSE gives rise to granulosa cells found in follicles that are active during adult life (Mork et al., 2012) and may be a source of oocytes in the adult ovary (Johnson et al., 2004). It is therefore likely **the OSE contains at the very least a unipotent progenitor cell capable of replacing OSE lost during ovulation and we hypothesize that OSE progenitor cells can be identified by a surface marker.**

The OSE surrounding the ovulatory wound site are exposed to factors in the follicular fluid and undergo an EMT in response to the rupture (Salamanca et al., 2004;

Ahmed et al., 2006). It has been recently demonstrated that the EMT can increase the number of cells with stem cell characteristics in the mammary gland (Mani et al., 2008; Guo et al., 2012). **We therefore hypothesize that factors in the follicular fluid and/or the induction of an EMT can regulate the MOSE progenitor cell population.**

Finally, germline deleterious mutations in *BRCA1* result in an increased risk for developing EOC and BRCA1 dysfunction is a hallmark of the majority of sporadic EOC tumours (Weberpals et al., 2008). Given that BRCA1 regulates the size of a mammary gland progenitor cell population (Furuta et al., 2005; Liu et al., 2008; Lim et al., 2009; Proia et al., 2011) **we hypothesize that this tumour suppressor can also regulate progenitor cells in the OSE.** To address these hypotheses we have the following specific aims.

SPECIFIC AIMS

AIM 1: To identify cell surface stem cell markers that enrich for MOSE with stem/ progenitor cell characteristics.

AIM 2: To determine the effect of ovulation on MOSE progenitor cells by characterizing their response to factors in the follicular fluid and the induction of an EMT.

AIM 3: To determine whether BRCA1 controls the number of MOSE progenitor cells.

The results from these experiments will allow us to discover cell surface markers that identify progenitor cells in the OSE and to further characterize the ways in which the progenitor cells may be regulated. By identifying and characterizing a progenitor cell

population in the OSE, we hope to gain insight into the aetiology of OSE derived ovarian cancer and provide a starting point for more in depth studies of the differentiation potential of the OSE.

# CHAPTER 2: THE MOUSE OVARIAN SURFACE EPITHELIUM CONTAINS A POPULATION OF LY6A (SCA-1) EXPRESSING PROGENITOR CELLS THAT ARE REGULATED BY OVULATION ASSOCIATED FACTORS.

*Lisa F. Gamwell**[1,2],*Olga Collins*[1,2], *and Barbara C. Vanderhyden*[1,2],

1. Center for Cancer Therapeutics, Ottawa Hospital Research Institute, Ottawa, ON, Canada, K1H 8L6.
2. Department of Cellular and Molecular Medicine, Faculty of Medicine, University of Ottawa, Ottawa, ON, Canada, K1H 8M5.

Published in BIOLOGY OF REPRODUCTION (2012) 87(4):80, 1–10, Published online before print 22 August 2012. DOI 10.1095/biolreprod.112.100347

**Contributions of Collaborators**

Olga Collins performed the experiments investigating the effects of cytokines on proliferation, sphere formation, sphere morphology and diameter in addition to the sphere passaging experiment. She also performed the proliferation assays on SOV vs control and eCG + hCG vs. control MOSE.

*I am in the process of assuming my married name, Gamwell. While this thesis is submitted under my maiden name Turchet, this manuscript was published under my married name.

## 2.1 Abstract

The ovarian surface epithelium, a single layer of poorly differentiated epithelial cells, covers the surface of the ovary and is ruptured during ovulation. Little is known about the changes that occur in this layer before or during ovulation, and even less is known about the regenerative processes that occur after the surface is ruptured to release a mature oocyte. Recently, a population of mouse ovarian surface epithelial (MOSE) cells that exhibit progenitor/stem cell characteristics has been identified, though neither a genetic marker nor how these cells are regulated has been determined. We have identified a defined population of MOSE cells with progenitor cell characteristics that express the stem cell marker lymphocyte antigen 6 complex, locus A (LY6A; also known as stem cell antigen-1 [SCA-1]). By testing the effect of factors found in the follicular fluid at ovulation on proliferation, sphere formation, and LY6A expression, we have determined that the size of the LY6A expressing (LY6A+) progenitor cell population is regulated by at least two ovulation-associated factors present in the follicular fluid: transforming growth factor beta 1 and leukaemia-inhibitory factor. Our work has identified a population of LY6A+ MOSE progenitor cells on the surface of the ovary that may play a role in ovulatory wound healing.

## 2.2 Introduction

The ovarian surface epithelium (OSE) is a monolayer of squamous-to-cuboidal epithelial cells covering the surface of the ovary. Its only defined function in healthy ovaries is during the rupture-wound repair process associated with ovulation (Auersperg et al., 2001; Murdoch and Van Kirk, 2002). Little is known about the changes occurring in the OSE before or during ovulation, and even less is known about the regenerative processes that occur after the surface is ruptured to release the mature oocyte. Ovulation is induced by a surge of the gonadotropic hormone, luteinizing hormone, and is associated with extensive architectural remodelling of the follicular structure, the overlying extracellular matrix, and the layer of OSE cells. This remodelling culminates in apoptotic degradation of the monolayer of OSE cells at the apex of the ovulating follicle, extrusion of the ovum, and repair of the epithelial wound. OSE cells in close contact with the apical wall of the preovulatory follicle secrete enzymes that lead to localized OSE cell apoptosis (Osterholzer et al., 1985; Ackerman and Murdoch, 1993). It is hypothesized that the cells exfoliated from the dome of those follicles are replenished by progenitor cell replication and migration from the wound edges (Osterholzer et al., 1985; Burdette et al., 2006). Many studies have determined the effect of growth factors and hormones on the growth rate of OSE cells (Ismail et al., 1999; Wong and Leung, 2007), but how these findings apply to ovulatory wound closure is unknown.

Like most epithelia, the OSE requires replacement throughout the lifetime of the individual. This process of tissue homeostasis is typically maintained by the presence of somatic progenitor cells (Blanpain et al., 2007). Progenitor cells are defined by their ability

to self-renew and differentiate along the lineages of their tissue of origin (Moore et al., 2006). Many adult tissues contain progenitor cells for which the main function is to maintain tissue homeostasis by replacing cells damaged by injury or age. Progenitor cells have been reported in bone marrow and brain and many epithelia, including lung, cornea, epidermis, intestine, prostate, and mammary gland (Blanpain et al., 2007).

Despite several reports of putative stem/progenitor cells in the ovarian epithelium that may support neo-oogenesis (Johnson et al., 2004; Bukovsky et al., 2008; Virant-Klun et al., 2008; White et al., 2012), only one report to date suggests the presence of stem/ progenitor cells in the ovarian epithelium in the context of ovulatory wound repair (Szotek et al., 2008). In that recent report, Szotek et al. (Szotek et al., 2008) identified a population of mouse OSE (MOSE) cells that exhibits asymmetric label retention, colony formation, and enrichment by flow cytometric isolation of the side population (SP), but how these cells contribute to ovulatory wound repair was not determined. If a progenitor cell population does exist in the MOSE, no markers have been published, and the regulation and function of these progenitor cells during ovulation in the normal ovary have not been determined.

Using established stem/progenitor cell assays, we have identified a defined population of MOSE cells with progenitor cell characteristics. This population of putative progenitor cells expresses the stem cell marker lymphocyte antigen 6 complex, locus A (LY6A), also known as stem cell antigen-1 (SCA-1). This population is regulated by at least two factors found in the follicular fluid at the time of ovulation, indicating an important role for these cells in facilitating ovulatory wound repair.

## 2.2 Materials and Methods

*Experimental Animals*

FVB/N mice (Jackson Laboratory) were the source of MOSE cells for all experiments. The mice were housed under a 12L:12D photoperiod with free access to food and water. All animal experiments described in the present study were performed according to the Guidelines for the Care and Use of Animals established by the Canadian Council on Animal Care, with protocols approved by the University of Ottawa Animal Care Committee.

*Isolation And Culture Of MOSE Cells*

To establish primary cultures of MOSE cells, ovaries were individually dissected from randomly cycling, 6-wk-old FVB/N female mice. For each primary culture, 10–20 mice were used. The ovaries were rinsed twice with PBS (Hyclone), then incubated in 0.25% Trypsin/PBS (0.5 ml/ovary; Invitrogen) in a 15-ml Falcon tube at 37°C at 5% CO2 for 30 min to remove the MOSE layer. ‘‘MOSE media’’ (a-Minimum Essential Medium [Hyclone] supplemented with 4% heat-inactivated 3:1 donor bovine serum:fetal bovine serum [DBS:FBS; PAA Laboratories, Inc.], 5 U/ml of penicillin and 0.005 mg/ml of streptomycin solution [Sigma-Aldrich], 0.1 μg/ml of gentamicin [Invitrogen], and 1 μg/ml of insulin-transferrin-sodium-selenite solution [ITSS; Roche]) was added to inactivate the trypsin, and the tube was agitated gently by hand to remove the MOSE cells from the ovaries. The supernatant containing the MOSE cells was centrifuged at 1000 rpm for 5 min, and the cells were resuspended in the appropriate medium. If freshly isolated MOSE cells

were used, the cells were processed for the appropriate assay.

Superovulation (SOV) was induced by i.p. administration of 5 IU of equine chorionic gonadotropin (eCG; Calbiochem), followed by i.p. administration of 5 IU of human chorionic gonadotropin (hCG; Sigma) 46 h later (Nagy et al., 2003). To limit the contamination of MOSE cultures by blood, immune, and stromal cells exposed by the ovulatory wound, the mice were euthanized 72 h after hCG injection for MOSE cell isolation as described above.

For primary cultures, the MOSE cells were plated on tissue-culture plates (Becton-Dickinson) in MOSE medium at 37°C with 5% $CO_2$. After 24 h, the medium and any floating cells were removed from the culture and replaced with fresh MOSE medium. The cultures were passaged (trypsin and gentle agitation at 90% confluency) two to four times before use in experiments. When passaging was not necessary, the medium was changed by half every 4 days. All in vitro MOSE experiments were carried out at least three times using a minimum of two different isolations of MOSE cells with a passage number of less than 30.

*SP Analysis*

The MOSE cells were released from tissue-culture dishes at 90% confluency with trypsin and gentle agitation and then passed through a 40-μm cell strainer to achieve a single-cell suspension. They were then incubated for 10 min at 37°C with or without the drug pump inhibitor verapamil (7.5 μM), and the fluorescent dye Hoechst 33342 (Invitrogen) was then added at a concentration of 5 μg/ml. The cells were incubated at 37°C

for 90 min, during which time the cells were gently mixed every 15 min to prevent cell clumping. After the 90-min exposure to the Hoechst dye, the cells were pelleted by centrifugation for 5 min at 300 × *g*, the Hoechst dye was removed, and the cells were resuspended in cold 2% DBS:FBS in PBS. Dead cells were labeled by the addition of 2 μg/ml of propidium iodide, and cells that took up this dye were gated out of the analysis. SP cells were identified and electronically gated on their characteristic light-scatter properties and singular Hoechst 33342 red versus blue fluorescence emission pattern after excitation with 100 mW of 355-nm ultraviolet light on a MoFlo cell sorter (Beckman Coulter, Inc.). SP fluorescence emissions were directed toward a 610-nm dichroic filter, then captured simultaneously through both a 424/44-nm band-pass filter (blue) and a 575/26-nm (red) filter on a linearly amplified fluorescence scale (Preffer et al., 2002). Main population (MP) cells, which due to retention of the dye have a higher red and blue fluorescence than the SP, were gated as shown in Figure 2.1A.

*Follicular Fluid And Cytokines*

Bovine follicular fluid was collected and kindly provided as a gift from Dr. Marc-André Sirard, (Université de Laval, Québec, PQ). Bovine ovaries were collected from a commercial slaughterhouse and transported to the laboratory in a thermoflask containing a warm, 0.9% saline solution supplemented with 100 000 IU/L penicillin, 100 mg/L streptomycin, and 250 μg/L amphotericin B (Sigma-Aldrich). The follicular fluid was collected by aspiration of five individual preovulatory follicles (diameter, 12–22 mm) with an 18-gauge needle attached to a 10-ml disposable syringe. The follicular fluid was

centrifuged at 1000 × *g* for 5 min to remove any cellular debris and stored at -80°C. Activated transforming growth factor beta 1 (TGFB1) levels were measured in the five bovine follicular fluid samples using a Quantikine Human TGFB1 ImmunoAssay (R&D Systems, Inc.) following the manufacturer's protocol. The TGFB1 concentration in the samples was 1.3–4.8 ng/ml, which falls within the range found in human follicular fluid (Fried et al., 1998). Based on the volume of follicular fluid obtained (1–2 ml) and dilutions of follicular fluid previously reported in the literature (Doyle and Donadeu, 2009), the samples were diluted 1:10 in MOSE medium.

The cytokines used were mouse insulin-like growth factor II (IGF2; 30 ng/ ml), human TGFB1 (10 ng/ml), and mouse leukaemia-inhibitory factor (LIF; 20 ng/ml; all from Sigma-Aldrich), which are present in human follicular fluid at the following concentrations: IGF2, 75–83.7 ng/ml (Hsieh et al., 2009); TGFB1, 1.75–5.81 ng/ml (Fried et al., 1998); and LIF, 0.43–2.89 ng/ml (Arici et al., 1997). The concentration of LIF used in the present study was chosen taking into account its ability to inhibit the spontaneous differentiation of mouse embryonic stem cells (Nagy et al., 2003).

*Proliferation Assays*

Cells were plated at a density of $1 \times 10^4$ cells/ml in MOSE medium, and viable cells were counted using a Vi-CELL XR Cell Viability Analyzer (Beckman Coulter, Inc.) at the reported time points. When follicular fluid or cytokines were used in the assay, cells were allowed to adhere to the tissue culture plate for 24 h before the treatments were added.

*Sphere Culture Conditions And Manipulations*

To assess the ability of individual cells to form spheres in culture, MOSE cells were released from tissue-culture plates at 90% confluency with trypsin or were removed from freshly dissected ovaries as described above. The cells were then passed through a 40-μm cell strainer and suspended as single cells in a 1:1 mixture of methylcellulose (to prevent cell aggregation) and ‘‘progenitor cell medium’’ (PCM; 1:1 Dulbecco modified Eagle medium:Ham F12, with a B27 supplement; Invitrogen) at a density of $2 \times 10^4$ cells/ml per well of a 24-well tissue culture plate. Sphere formation and morphology were monitored weekly using a dissecting microscope, and spheres were counted with the aid of a grid placed under the culture dish. Sphere-forming efficiency was calculated as the percentage of single cells capable of sphere formation. The diameter of the spheres was determined using a microscope fitted with a micrometer. To determine the effect of factors found in the follicular fluid at the time of ovulation on the sphere parameters (number, size, and morphology), IGF2 (30 ng/ml), TGFB1 (10 ng/ml), and LIF (20 ng/ml) were added to the PCM before the addition of methylcellulose, $2 \times 10^4$ cells were plated at the above mentioned cell density for each factor, and the sphere parameters were assessed after 28 days in culture.

For passaging, spheres were released from methylcellulose by dilution with an equal volume of medium and then pelleted using centrifugation for 5 min at $300 \times g$. After the sphere pellet was washed twice briefly with PBS, the spheres were dissociated with trypsin and gentle agitation. The dissociated spheres were then passed through a 40-μm cell strainer to achieve a single-cell suspension. These single cells were then placed back into

sphere-culture conditions for new sphere formation. To serially passage the spheres, this process was repeated.

*Magnetic Bead Assisted Cell Separation*

The MOSE cells were released from tissue culture plates at 90% confluency by nonenzymatic dissociation (MULTICELL Cell Stripper; Wisent Bioproducts), passed through a 40-μm cell strainer, and then separated into LY6A-expressing (LY6A+) and non-LY6A-expressing (LY6A-) fractions or KIT-expressing (KIT+) and non-KIT-expressing (KIT-) fractions using an anti-LY6A or an anti-KIT MicroBead kit with a MiniMAC separator and MS columns (Miltenyi Biotech) following the manufacturer's protocol. The antibodies were added to a single-cell suspension and incubated at 4°C for 10 min. Excess antibody was washed away by the addition of 5 ml of wash buffer (PBS [pH 7.2], 0.5% bovine serum albumin, and 2 mM ethylenediaminetetra-acetic acid), followed by a 10-min centrifugation at 1500 rpm to remove the supernatant. The cells were resuspended in fresh wash buffer, and the magnetic beads were added. Following a 15-min incubation at 4°C, the cells were washed and then resuspended in 500 μl of wash buffer and applied to an MS column in a magnetic holder. To increase the purity of the positive fraction, the eluted cells were passed through a second column.

*Gene Expression Analysis*

The RNA was extracted using an RNeasy Mini Kit (Qiagen) following the manufacturer's instructions. RNA was quantified, and cDNA was made by reverse

transcriptase PCR (RT-PCR) from 1000 ng of RNA using the OneStep RT-PCR Kit (Qiagen). Gene expression was determined by relative quantitative PCR (Q-PCR) performed on an ABI 7500 FAST qRT-PCR machine (Applied Biosystems) using the Fast SYBR Green Master Mix (Invitrogen) following the manufacturer's instructions. The real-time thermal cycler program was 95°C for 10 min, followed by 40 cycles of 95°C for 10 sec and 60°C for 30 sec. Primer pairs to amplify murine *Ly6a* (forward [F], 5'- GAC CCT GGA GGC ACA CAG CC-3'; reverse [R], 5'-CAT GTG GGA ACA TTG CAG GAC CCC-3'), *Kit* (F, 5'-GAT CTG CTC TGC GTC CTG TT-3'; R, 5'-CTT GCA GAT GGC TGA GAC G-3'), *Nanog* (F, 5'-CCT GAT TCT TCT ACC AGT CCC A-3'; R, 5'-GGC CTG AGA GAA CAC AGT CC-3'), and *Ppia* (F, 5'-AGG GTG GTG ACT TTA CAC GC-30; R, 5'-GAT GCC AGG ACC TGT ATG CT-3') were designed using OligoPerfect primer design software (Invitrogen). The expression level of *Ppia* mRNA was used as the endogenous control.

*Flow Cytometry For LY6A Expression*

The MOSE cells were released from tissue-culture dishes at 90% confluency using nonenzymatic dissociation (MULTICELL Cell Stripper), a single-cell suspension was achieved by passing the cells through a 40-μm cell strainer, and the cells were incubated for 30 min at 4°C with an anti-LY6A antibody conjugated to the allophycocyanin fluorophore (Miltenyi Biotech). After unbound antibody was washed away by the addition of 5 ml of wash buffer and centrifugation for 5 min at 300 × *g*, the percentage of cells with surface expression of LY6A was determined using a MoFlo cell sorter.

*Immunohistochemistry (IHC)*

Histological sections were deparaffinized and rehydrated, and then high temperature antigen retrieval was performed in sodium citrate buffer (pH 6; Antigen Unmasking Solution; Vector Laboratories) in a pressure cooker (Tender Cooker; Nordic Ware). Endogenous peroxidase activity was blocked by 3% hydrogen peroxide in methanol for 30 min. LY6A expression was visualized with a monoclonal rat anti-LY6A primary antibody and a polyclonal goat anti-rat secondary antibody (BD553333 and BD554016, respectively; both from BD Biosciences) using a signal amplification kit (TSA Biotin System; PerkinElmer), following the manufacturer's instructions. Developing was performed with diaminobenzidine (DAB) as a substrate (0.2% DAB, 0.001% $H_2O_2$; Sigma-Aldrich). Sections were counterstained with Harris hematoxylin (Fisher Scientific) and mounted with Permount (Fisher Scientific). Images were obtained with the ScanScope CS system and ImageScope software (both from Aperio).

*Statistical Analyses*

Based on the number of conditions tested, a Student t-test or an ANOVA with a Tukey post-test was used to determine statistical significance ($P < 0.05$). Error bars indicate the SEM.

## 2.3 Results

*MOSE Contains A Verapamil-Sensitive SP*

Based on a previous report in the literature that the MOSE contains an SP identified by flow cytometry (Szotek et al., 2008), SP analysis was used to enrich for potential MOSE progenitor cells. The identification of an SP is based on differential exclusion of the DNA-binding dye Hoechst 33342 (Challen and Little, 2006). Hoechst 33342 enters live cells, where it can be actively pumped out by ATP-binding cassette transporters like the multidrug-resistant protein 1 (MDR1) and the ATP-binding cassette, subfamily G, member 2 (ABCG2) (Challen and Little, 2006). It is thought that stem/progenitor cells express a large number of these pumps to protect themselves from toxins and, therefore, are able to pump out the dye faster than non-stem cells (Challen and Little, 2006). This technique is especially useful when no genetic stem/progenitor cell markers are known, and it is routinely used to enrich for stem/progenitor-like cells in both normal and cancerous tissues (Goodell et al., 1996; Wulf et al., 2001; Preffer et al., 2002; Welm et al., 2002; Al-Hajj et al., 2003; Bhatt et al., 2003; Jonker et al., 2005; Haraguchi et al., 2006; Szotek et al., 2006; Ono et al., 2007; Szotek et al., 2008; Hosonuma et al., 2011). On average, we found that the MOSE cells grown in culture contained an SP that constitutes approximately 3% of the whole MOSE cell population (Fig. 2.1A). Verapamil, a nonspecific drug pump inhibitor, abolished the SP phenotype, which indicated that the SP cells were correctly gated (Fig. 2.1B).

A comparison of growth rates in culture was made between the SP, the MP, and the mixed MOSE cell population from which the SP and the MP were isolated, which

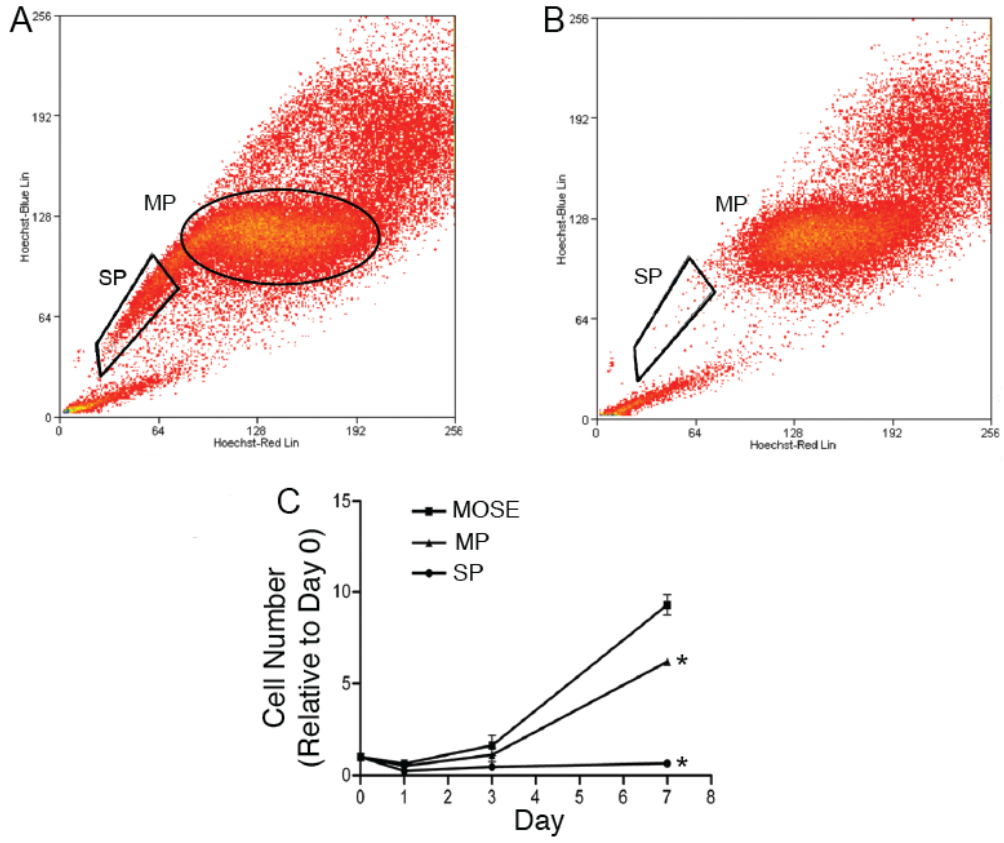


**Figure 2.1: MOSE cells were analyzed by flow cytometry for the presence of an SP.** **A:** The SP gate is denoted by the black box. A total of $4 \times 10^4$ events are shown. **B:** SP analysis of MOSE cells pretreated with the drug pump inhibitor verapamil, with a black box indicating the same SP gate as shown in A. A total of $3 \times 10^4$ events are shown. **C:** A comparison of the proliferation rates of MOSE, MP, and SP adherent cultures in MOSE medium. Error bars indicate the SEM. *$P < 0.05$ compared to MOSE and MP.

was kept on ice while the cell sort was being performed (Fig. 2.1C). On Day 7 of culture after sorting, the MOSE cells exhibited a 9-fold increase in cell number, and the MP showed a 6-fold increase in cell number, when compared to Day 1. The SP cells did not proliferate during the initial 7 days after sorting but eventually began to proliferate after 4 wk. The difference in proliferation rate between the SP, the MP, and MOSE population suggests that the SP may be a distinct population of MOSE cells.

*LY6A Surface Expression Marks MOSE Cells With Enhanced Sphere-Forming Ability*

To identify potential genetic progenitor cell markers for the MOSE, Q-PCR was used to compare the mRNA expression levels of known stem/progenitor cell markers in the SP to the MP. LY6A, KIT (also known as CD117), and NANOG are critically involved in self renewal (Osawa et al., 1996; Storm et al., 2007), and they have been used as markers of hematopoietic stem cells (LY6A and KIT) (Welm et al., 2002), breast stem cells (LY6A) (Welm et al., 2002), and embryonic stem cells (NANOG) (Noaksson et al., 2005). Whereas the MP and SP both expressed mRNAs for the stem/progenitor cell markers, the SP expressed significantly higher levels of *Ly6a* and *Kit* mRNA (5-fold and 3-fold higher, respectively), and a trend toward higher levels of *Nanog* mRNA (2.5-fold higher) was found when compared to the MP (Fig. 2.2A). Based on these results, further investigation focused on LY6A and KIT as potential markers of a population of MOSE cells enriched with progenitor cell characteristics.

To test whether surface expression of LY6A or KIT enriches for MOSE cells with progenitor cell characteristics, we used an established, quantifiable in vitro system for

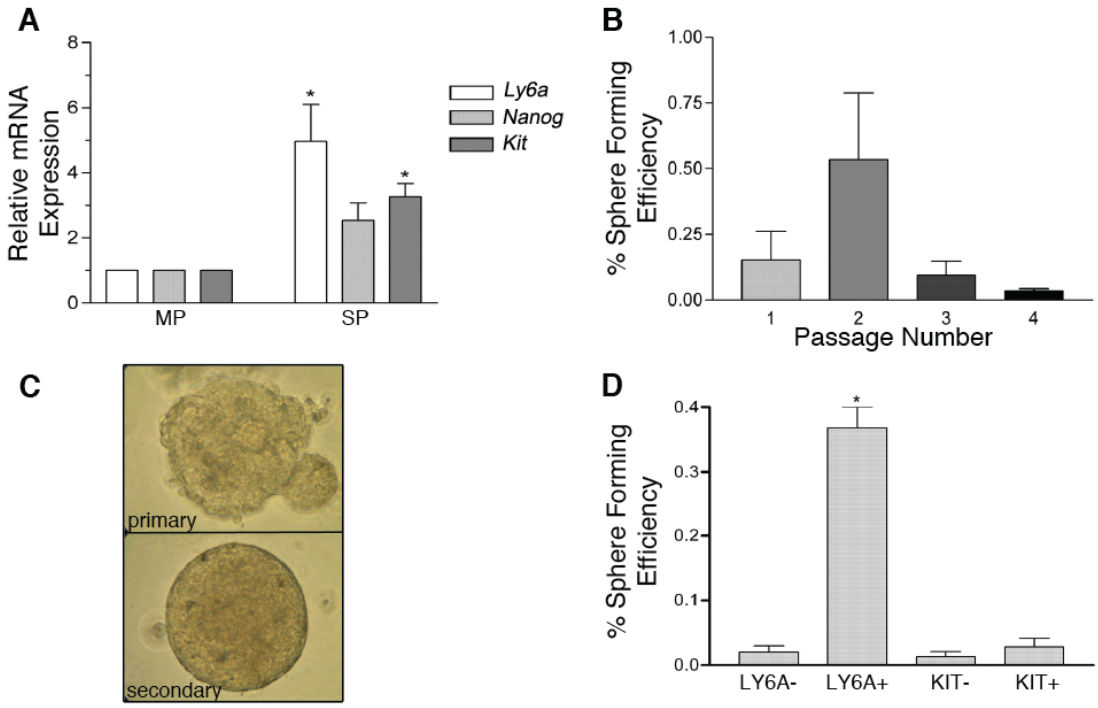


**Figure 2.2: Putative progenitor cells in MOSE cultures. A:** The SP expresses significantly higher levels of Ly6a and Kit mRNA when compared to the MP. A trend is observed toward higher levels of Nanog mRNA. Relative transcript levels were determined by Q-PCR. *P < 0.05 compared to MP. **B:** Freshly isolated MOSE cells form spheres when placed in sphere-forming culture conditions. The spheres were dissociated and replated three times and evaluated for efficiency of sphere formation, as indicated by the percentage of plated cells that formed spheres. **C:** Morphology of spheres changes with passage. Primary spheres have an irregular shape, whereas secondary spheres are spherical and compact. Original magnification ×400. **D:** MOSE cells were sorted for LY6A and KIT expression, and the percentages of cells that formed spheres were determined. Error bars indicate the SEM. *P < 0.05 compared to LY6A-.

testing “stemness”. The capacity for sphere formation has been used to indicate the presence of cells with stem/progenitor cell characteristics in a variety of tissues (Reynolds and Weiss, 1996; Weiss et al., 1996; Dontu et al., 2003; Woodward et al., 2005; Liao et al., 2007). To ensure that sphere formation was not an artifact of in vitro culture, we assessed the sphere-forming ability of freshly isolated MOSE cells. When $5 \times 10^4$ freshly isolated MOSE cells were placed directly into sphere-forming cultures, a small percentage (0.19% ± 0.11%) formed spheres. These spheres could be passaged at least three times ($2 \times 10^4$ cells plated each time), suggesting the presence of cells with self-renewal capacity (Fig. 2.2B). Whereas the mean number of spheres formed tended to decrease with passaging (passage 2, 0.53%; passage 3, 0.09%; and passage 4, 0.03%), the difference was not statistically significant. Primary spheres had an irregular shape, but after one passage, the spheres were more uniform, with tightly associated cells (Fig. 2.2C).

Because enrichment of sphere-forming ability indicates an enrichment of cells with stem/progenitor cell characteristics, the sphere-forming assay was used to test the putative progenitor cell markers LY6A and KIT. Cultured MOSE cells were separated based on surface expression of LY6A or KIT into LY6A+ and LY6A- fractions (0.89% and 99.1%, respectively) or KIT+ and KIT- fractions (2.3% and 97.7%, respectively) using magnetic bead assisted cell separation. The LY6A+ fraction expressed 240-fold higher levels of *Ly6a* mRNA compared to the LY6A- fraction, and the KIT+ fraction expressed 125-fold higher levels of *Kit* mRNA compared to the KIT- fraction. The fractions were resuspended as single cells ($2.4 \times 10^5$ cells from each fraction were plated) and tested for sphere formation in methylcellulose. Spheres were quantified after 28 days. LY6A+ cells formed 18-fold

more spheres compared to all other fractions (Fig. 2.2D). The sphere-generating efficiencies of the KIT+ and KIT- MOSE fractions were not statistically different. Taken together, these results indicated that the LY6A+ fraction is enriched for cells with stem/ progenitor cell characteristics.

*LY6A+ MOSE Cells Are Present As Rare Cells On The Ovarian Surface In Vivo*

To visualize LY6A+ MOSE cells on the surface of the ovary in vivo, immunohistochemistry (IHC) for LY6A expression was performed on ovaries excised from 6-wk-old, normally cycling mice. Occasional LY6A+ cells were found within the MOSE layer, with an average of less than one LY6A+ cell per section (Fig. 2.3A). LY6A+ MOSE cells did not appear to be associated with any particular underlying structure (i.e., follicle or corpus luteum) and tended to be more cuboidal (Fig. 2.3A) relative to the rest of the surface, which was covered by squamous (LY6A-) epithelial cells (Fig. 2.3B). The oocytes of primordial follicles also appeared to stain for LY6A expression (Fig. 2.3A).

*SOV In Vivo Increases The Proliferation Rate Of MOSE In Vitro*

To examine the effects of ovulation on the OSE, MOSE cells were isolated 72 h after hCG injection from SOV mice (SOV MOSE) and, at the same time, from mice that were cycling normally. Once the primary cultures were established (each primary culture was passaged twice), the proliferation rate of the SOV MOSE was compared to the control MOSE (Fig. 2.4A). SOV MOSE had a significantly faster proliferation rate at Day 11 than the control MOSE (doubling time: SOV MOSE, 4.3 days; control MOSE, 6.5 days). To

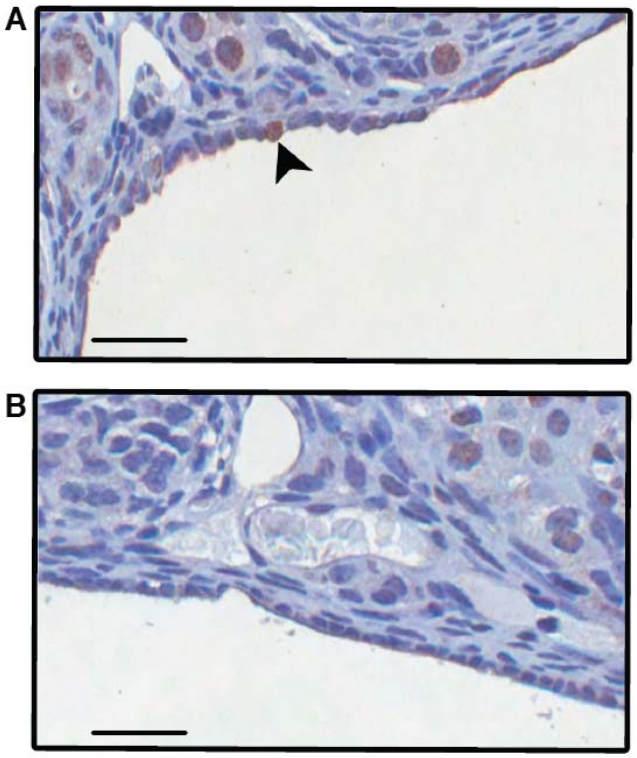


**Figure 2.3: Detection of LY6A+ cells on the surface of the ovary. A:** A rare cell in the ovarian surface epithelium expressing LY6A (brown staining, indicated by arrow head) is shown following detection by IHC. Oocytes in primordial follicles in the ovarian cortex also stain positively for LY6A**. B:** An area of the same ovary section depicting MOSE cells where LY6A+ cells are not detected. Bar = 25μm.

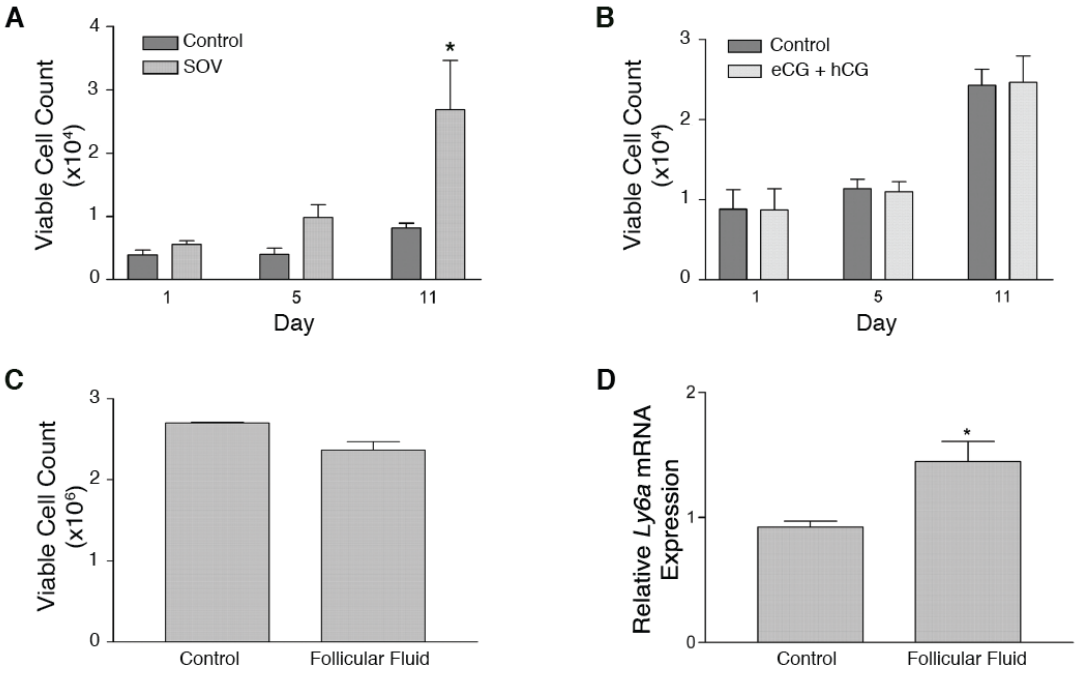


**Figure 2.4: The role of SOV on MOSE cell proliferation and LY6A expression. A:** The rate of proliferation of primary MOSE cells isolated from ovaries that had been superovulated compared to primary MOSE isolated from normally cycling mice (control). **B:** Proliferation of MOSE cells treated in vitro with eCG and hCG. **C:** Proliferation of MOSE treated with 10% bovine follicular fluid. **D:** Q-PCR detection of Ly6A transcripts in MOSE cells treated with 10% follicular fluid. Error bars indicate SEM. * indicates significant difference from control, $P < 0.05$ compared to control.

determine if exposure to the SOV hormones caused the difference in proliferation rate, cultured MOSE cells were treated in vitro with eCG and hCG in the same sequence as used for the SOV in vivo. The hormones did not alter the proliferation rate of the MOSE (Fig. 2.4B), nor did treatment with a range of concentrations of estradiol (data not shown), indicating that other aspects of SOV, like the follicular fluid, may be responsible for the longer-term effects on the proliferation rate.

*Follicular Fluid Increases* Ly6A *MRNA Expression In MOSE*

Because follicular fluid is expelled and bathes the MOSE surrounding the ovulatory wound, we next studied the effect of follicular fluid on MOSE proliferation. We were unable to collect sufficient murine follicular fluid, so MOSE cells were cultured with bovine follicular fluid collected from the preovulatory follicles of heifers. Each of the five follicular fluid samples was diluted 1:10 in MOSE medium and tested independently. After 7 days, the cells were counted to assess proliferation, and RNA was extracted for Q-PCR analysis. Whereas treatment with 10% follicular fluid did not alter the growth rate of MOSE (Fig. 2.4C), it did significantly increase the expression of *Ly6a* mRNA by 50% (Fig. 2.4D) indicating that follicular fluid expelled during ovulation may regulate the size of the LY6A+ MOSE cell population or alter the expression level in those cells that already express LY6A.

*Ovulation-Associated Factors Regulate The LY6A+ MOSE Fraction*

As a follicle grows, several proteins accumulate in the follicular fluid, including

IGF2, TGFB1, and LIF (Arici et al., 1997; Fried et al., 1998; Ouellette et al., 2005; Knight and Glister, 2006; Hsieh et al., 2009). The effect of each of these factors on MOSE proliferation was determined after 7 days in adherent MOSE cell cultures. LIF increased proliferation by 1.8-fold during that period compared to control, whereas IGF2 had no effect and TGFB1 significantly decreased MOSE proliferation 2-fold (Fig. 2.5A).

To determine the effect of IGF2, TGFB1, and LIF on sphere formation, MOSE cells were plated in sphere-forming conditions with each factor added to the culture medium. For each factor, $2 \times 10^4$ MOSE cells were plated. The number of spheres was counted and compared to untreated controls. Despite opposing effects on cell proliferation, both TGFB1 and LIF significantly increased the number of spheres formed (by 6.4-fold and 3.6-fold, respectively) (Fig. 2.5B). LIF also stimulated the formation of significantly larger, more compact spheres when compared to untreated controls (average diameter, 75.6 and 58.5 μm, respectively), whereas the addition of TGFB1 caused significantly smaller (average diameter, 45.5 μm), more loosely associated spheres (Fig. 2.5, C and D). Spheres that formed in the presence of IGF2 did not differ significantly in number, size, or morphology when compared to the controls.

Because the LY6A+ MOSE fraction is enriched for sphere-forming cells, we investigated the effect of LIF and TGFB1 on LY6A expression. Interestingly, even though LIF caused an increase in the number of spheres formed, exposure to LIF for 1 wk in culture significantly decreased *Ly6a* mRNA expression 2.5-fold (Fig. 2.5E). In comparison, TGFB1 increased *Ly6a* mRNA expression 6-fold (Fig. 2.5F) and almost tripled the percentage of LY6A+ MOSE cells, as determined by flow cytometry (Fig. 2.5G). These

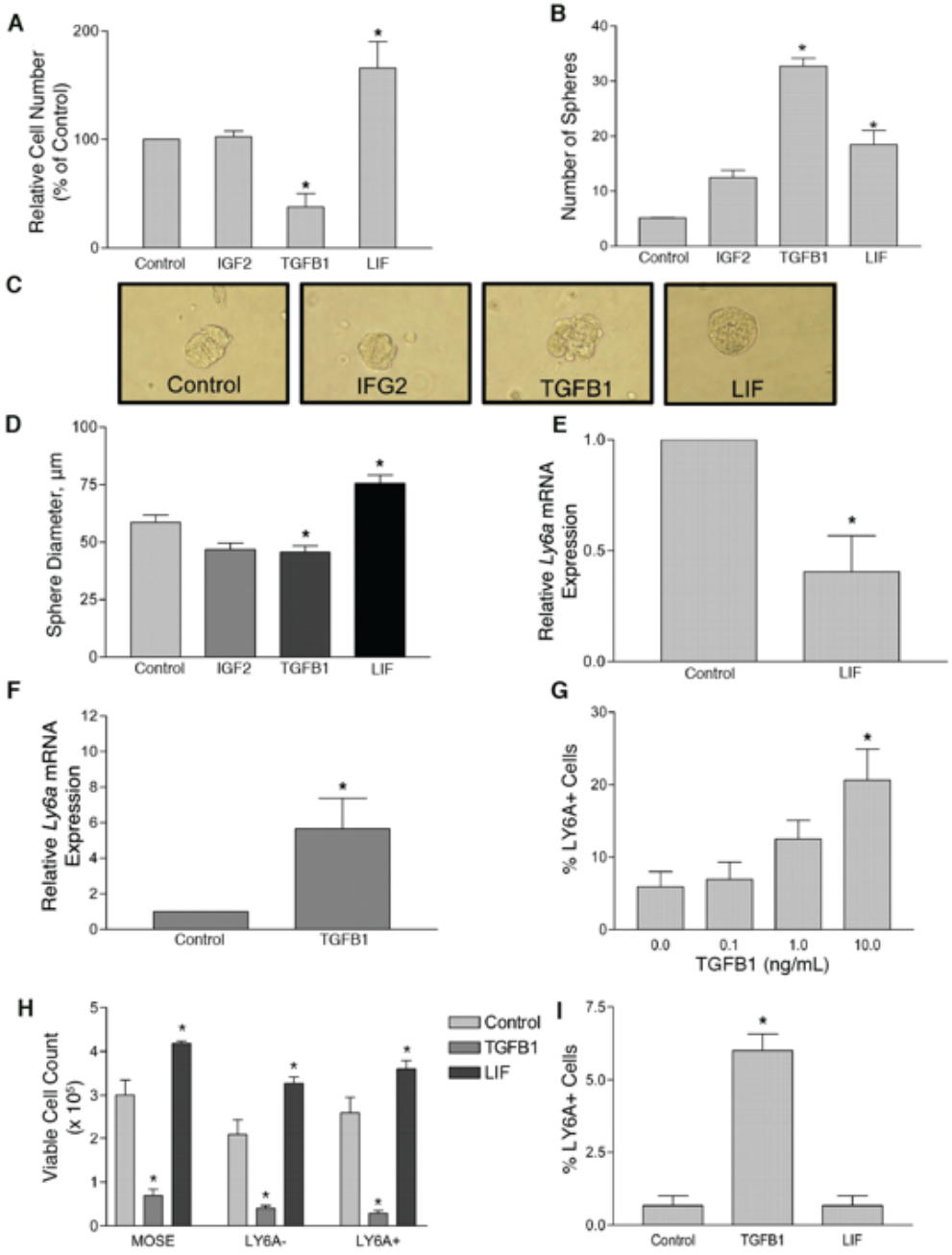


**Figure 2.5: Phenotypic changes in MOSE following treatment with IGF2, LIF or TGFB1. A-D:** Following treatment with IGF2, LIF or TGFB1, the proliferation of adherent MOSE (A), the sphere-forming capability of MOSE cells (B), the sphere morphology (C), and average sphere diameter were determined (D) were determined. **E and F:** Q-PCR analysis comparing *Ly6a* mRNA levels in adherent MOSE in MOSE media (control) to MOSE treated with LIF for 7 days (E) or TGFB1 for 7 days (F). **G:** The percentage of LY6A+ MOSE in adherent cultures treated with a range of TGFB1 doses for 7 days as detected by flow cytometry. **H:** Proliferation assay comparing the effect of TGFB1 and LIF on MOSE cells (MOSE), and MOSE cells sorted for LY6A expression. **I:** The percentage of LY6A+ MOSE that are present 7 days after plating LY6A- MOSE in adherent cultures with or without treatment with TGFB1 or LIF. Error bars indicate SEM. * indicates significant difference from the relevant control group, $P < 0.05$ compared to the relative control group.

data suggest that TGFB1 may act to increase the number of spheres formed by expanding the LY6A+ MOSE fraction.

To investigate this further, the effect of TGFB1 and LIF on the proliferation of LY6A- and LY6A+ MOSE cells was tested by placing both unsorted MOSE cells that were passed through the cell sorter without being gated and sorted LY6A- and LY6A+ MOSE cells into adherent cultures and exposing them to TGFB1 or LIF. After 7 days, TGFB1 significantly reduced proliferation in all cell populations, whereas LIF increased proliferation compared to controls (Fig. 2.5H). Because TGFB1 did not increase the proliferation of the LY6A+ MOSE cells, this suggested that TGFB1 may expand the LY6A + MOSE fraction by causing LY6A- MOSE cells to express LY6A. To test this directly, LY6A- MOSE cells were cultured in MOSE medium and treated with TGFB1 or LIF for 7 days, then reassessed by flow cytometry to determine the percentage of cells that express LY6A. Six percent of TGFB1-treated LY6A- cells expressed LY6A after 7 days of culture, whereas the percentage of control (untreated) or LIF-treated cells that expressed LY6A did not significantly differ from zero as determined by a one-sample t-test (Fig. 2.5I).

## 2.4 Discussion

We have isolated a subpopulation of MOSE cells based on the verapamil-sensitive efflux of Hoechst dye and have reported, to our knowledge for the first time, that this subpopulation shows enhanced expression of LY6A, a stem cell maker. LY6A+ MOSE cells can be detected on the surface of the mouse ovary in vivo. When compared to LY6A- MOSE cells, LY6A+ MOSE cells have enhanced sphere-forming efficiency (an indication

of self-renewal and differentiation). These characteristics suggest that this cell population is enriched for progenitor cell activity. The behaviour of these putative MOSE progenitor cells is regulated by at least two factors found in follicular fluid, TGFB1 and LIF, indicating that they may play a role in ovulatory wound healing.

Given the limited evidence for distinct subpopulations of cells in the OSE, we initiated the present study using methodologies that have been effective in isolating stem/ progenitor cells from other adult tissues. Initial experiments have shown that the MOSE contains a verapamil-sensitive SP, a phenotypic marker that has been used to identify many somatic and cancer stem cells (Goodell et al., 1996; Wulf et al., 2001; Preffer et al., 2002; Al-Hajj et al., 2003; Bhatt et al., 2003; Jonker et al., 2005; Challen and Little, 2006; Haraguchi et al., 2006; Szotek et al., 2006; Ono et al., 2007; Szotek et al., 2008; Hosonuma et al., 2011). The ability to efflux substances is thought to be protective against a variety of chemicals, allowing somatic stem cells to survive long term in the body (Rossi et al., 2008). The size of the SP we report is in keeping with the only other report of a MOSE SP (Szotek et al., 2008). The SP cells proliferate at a slower rate, which is also consistent with the finding by Szotek et al. (Szotek et al., 2008) that label-retaining cells, which proliferate slowly, are enriched in the SP. The difference in proliferation rate between the MP and MOSE cells is likely because the MOSE cells were not passed through the cell sorter and were more robust than the MP when placed into culture.

Although previous studies have identified a putative stem cell population in the OSE that may be involved in neo-oogenesis (Johnson et al., 2004; Bukovsky et al., 2008; Virant-Klun et al., 2008; White et al., 2012), no indication regarding what role these cells

may play in ovulation has been reported. Similarly, Szotek et al. (Szotek et al., 2008) reported the presence of label-retaining cells juxtaposed to sites of ovulation, but their importance to ovulation or ovulatory wound repair was not investigated. In the present study, we have attempted to isolate and characterize these cells to enable an examination of their role in ovulation. Herein, we have shown that a small subpopulation of MOSE cells expresses the genetic marker, LY6A, known as SCA-1 in the stem cell field. LY6A is the most commonly used genetic marker for enrichment for murine hematopoietic stem cells (Spangrude et al., 1991; Okada et al., 1992), and it has been used to prospectively isolate murine progenitor or stem cells from such diverse tissues as vascular endothelium, bone, mammary gland, prostate, skeletal muscle, heart, dermis, liver, and lung (reviewed in Holmes and Stanford, 2007). Whereas studies with transgenic mouse lines using the LY6A promotor to drive lacZ, green fluorescent protein (GFP), or enhanced GFP (eGFP) expression have shown that it is expressed in many tissues (Miles et al., 1997; Ma et al., 2002a; Ma et al., 2002b; Hanson et al., 2003), the present study is to our knowledge the first report of LY6A expression in the ovary, perhaps because the single cells seen on the surface of the ovary by IHC are easily missed when screening organs for X-gal staining or GFP or eGFP expression, or because the ovaries were not closely examined in the other studies. In addition to the MOSE, LY6A staining was seen in the oocytes of primordial follicles. LY6A expression has not been previously reported in oocytes, and this observation raises the intriguing possibility of a connection between this progenitor population and neo-oogenesis, as proposed previously (Johnson et al., 2004; Bukovsky et al., 2008; White et al., 2012).

The LY6A+ MOSE cells have a higher sphere-forming efficiency than LY6A- MOSE cells, suggesting that LY6A surface expression marks a population of cells with progenitor cell characteristics. The sphere-forming assay tests the two fundamental properties of progenitor cells: the ability to self- renew and the ability to differentiate. When spheres are formed from a single-cell suspension in methylcellulose, which prevents aggregation, all cells in the sphere originate from that single cell. By definition, progenitor cells are able to produce the differentiated progeny that make up the cell types within the sphere, so the number of spheres formed reflects the number of progenitor cells in the culture. Sphere formation was first used to isolate neural progenitor cells (Reynolds and Weiss, 1996; Weiss et al., 1996); it has since been used to isolate mammary gland progenitor cells (Dontu et al., 2003; Woodward et al., 2005; Liao et al., 2007). The fact that not every LY6A+ MOSE cell forms spheres indicates that there may be other, as-yet-undiscovered progenitor cell markers that would more efficiently enrich for MOSE cells with progenitor cell characteristics.

The MOSE cells, when taken directly off the surface of the ovary and placed into sphere culture conditions, have the ability to form spheres that can be passaged at least three times. The ability to passage spheres suggests that the cells are undergoing asymmetric division, because within the mixed ball of cells, there remains at least one cell with the ability to produce spheres. If all the cells within a sphere could produce secondary spheres, a dramatic increase in sphere-forming efficiency would be expected; however, this was not seen.

The MOSE requires repeated, localized replacement during the reproductive life

span of the ovary. It remains unclear how the MOSE regenerates in response to ovulatory wounding, but at least two processes are possible: 1) Every cell in the MOSE has the same capacity to proliferate to close the wound, or 2) a small population of cells are stimulated to divide and produce differentiated daughter cells in response to some aspect of ovulation. Our results, and the work of others in rodents and nonhuman primates (Gaytán et al., 2005; Burdette et al., 2006; Szotek et al., 2006; Wright et al., 2008a), support the second process, and we propose that a small population of progenitor cells participates in wound repair following ovulation.

We have shown that SOV, which causes a supraphysiological number of ovulation sites, causes a lasting increase in the proliferative capacity of the MOSE. This is consistent with the long-standing hypothesis that ovulation has a mitogenic effect on the OSE and is therefore a risk factor for ovarian cancer (Fathalla, 1971). The gonadotropins responsible for SOV, estrogen, and 10% follicular fluid failed to directly increase MOSE proliferation in vitro. Determining what is responsible for the increase in proliferation in primary cultures from SOV ovaries may provide information about the etiology of ovarian cancer.

Both LIF and TGFB1, the levels of which are increased in follicular fluid in response to ovulation-inducing gonadotropins (Arici et al., 1997; Fried et al., 1998; Ouellette et al., 2005; Knight and Glister, 2006), increased the proportion of cells that form spheres, but their mechanisms of action differ. In addition to promoting sphere formation, LIF increased proliferation of the total population of MOSE cells and also increased proliferation of sorted LY6A- and LY6A+ MOSE cells. This effect on proliferation explains why LIF, in addition to producing more spheres, also produced larger spheres. It also

explains the reduced *Ly6a* mRNA expression compared to controls, because LIF expanded the LY6A+ sphere-forming population but also expanded the LY6A- MOSE cell population. This suggests the intriguing possibility that this growth factor is able to promote both the expansion of the MOSE progenitor cell population as well as the proliferation of their progeny during ovulatory wound repair. The decrease in Ly6a mRNA caused by LIF treatment may be a reflection of LY6A+ MOSE cells being diluted by the proliferative effects of LIF on the LY6A- cells, because the majority of cells in a mixed MOSE population do not express LY6A. Additionally, LIF may be acting to expand a population of sphere-forming MOSE cells that express a still undiscovered progenitor cell marker.

The TGFB1 decreased proliferation of mixed MOSE cells, LY6A- MOSE cells, and LY6A+ MOSE cells; resulted in the production of smaller spheres; and increased both *Ly6a* mRNA and the proportion of MOSE cells expressing LY6A compared to control. It also induced LY6A surface expression in LY6A- MOSE cells, something that LIF was not able to do. This indicates that TGFB1 increases both the number of spheres formed and the number of LY6A+ cells by inducing LY6A expression in MOSE cells that previously did not express the marker.

Given the opposing effects of LIF and TGFB1 on both proliferation and expression of LY6A in MOSE, it was not surprising that the application of a 1:10 dilution of bovine follicular fluid, containing both of these factors (and others), did not alter the proliferation of MOSE in vitro. A determination of the relative concentration of these and other factors in murine follicular fluid and an improved understanding of the time course of the response to these factors may improve our understanding of their putative roles in the modulation of

MOSE during ovulatory wound repair.

Finally, TGFB1 is a prototypic inducer of the epithelial-to-mesenchymal transition (EMT), a process by which epithelial cells adopt a mesenchymal phenotype(Zavadil and Böttinger, 2005). The EMT plays an important role during development and wound healing; in fact, in response to ovulation, OSE cells surrounding the ovulatory wound adopt a mesenchymal phenotype (Auersperg et al., 2001). Recently, TGFB1 and the EMT have been associated with the conversion of mammary epithelial cells into mammary stem cells (Mani et al., 2008; Guo et al., 2012), and the maintenance of naturally occurring mammary stem cells requires the expression of transcription factors that are upregulated as a result of an EMT (Guo et al., 2012). Our results suggest that a similar process may be occurring in the OSE, and this process is the focus of current studies.

In conclusion, the MOSE contains an LY6A+ population of cells that has enhanced progenitor cell characteristics (increased sphere-forming efficiency). This population is regulated by two factors found in follicular fluid, TGFB1 and LIF. Our findings that TGFB1 can convert LY6A- MOSE cells into LY6A+ progenitor cells and that LIF can induce the expansion of LY6A+ MOSE progenitor cells while also stimulating proliferation of LY6A- MOSE cells provide a new perspective on how LY6A expression and ovulatory wound healing may be regulated.

## 2.5 Acknowledgements

The authors are grateful to Dr. Marc-André Sirard (Université de Laval, Québec, PQ) for providing the bovine follicular fluid and Paul Oleynik and Caroline Vergette

(StemCore Laboratories, Ottawa, ON) who assisted with the flow cytometry.

# CHAPTER 3: TGFB1 INDUCES AN EPITHELIAL-TO-MESENCHYMAL TRANSITION AND EXPANDS A PROGENITOR CELL POPULATION IN THE OVARIAN SURFACE EPITHELIUM

*Lisa F. Gamwell**[1,2], *Olga Collins*[1], *Maria Merziotis*[1], *Kenneth Garson*[1] *and Barbara C. Vanderhyden*[1,2,]

1. Center for Cancer Therapeutics, Ottawa Hospital Research Institute, Ottawa, ON, Canada, K1H 8L6.

2. Department of Cellular and Molecular Medicine, Faculty of Medicine, University of Ottawa, Ottawa, ON, Canada, K1H 8M5.

Formatted for submission to the journal Stem Cells.

**Contributions of Collaborators:**
Olga Collins performed replicate TGFB1 treatments, gene expression analysis and performed the migration assays. Maria Merziotis performed the western blots on TGFB1 treated MOSE. Dr. Kenneth Garson assisted with virus production and MOSE infection.

* While this thesis is submitted under my maiden name Turchet, this manuscript will be published under Gamwell, my married name.

## 3.1 Abstract

The ovarian surface epithelium (OSE) is a layer of epithelial cells lining the surface of the ovary. When the ovary ovulates, the OSE is ruptured and rapidly regenerates itself. This process, while not well understood, is associated with a local epithelial-to-mesenchymal transition (EMT) in the OSE surrounding the wound site. Recently, Stem Cell Antigen-1 (SCA-1) has been identified as a surface marker that enriches for OSE cells with progenitor cell characteristics. In addition, TGFB1, a cytokine present at the ovulatory wound site, has been shown to expand the SCA-1 expressing (SCA-1+) OSE population. Because TGFB1 is a known inducer of the EMT, and because the EMT plays a role in expanding stem cell populations in other epithelia, we determined whether TGFB1 expands the SCA-1+ OSE progenitor cell population by triggering an EMT. Both treatment with TGFB1 and overexpression of the EMT master gene, SNAIL, caused the OSE cells to adopt a mesenchymal phenotype, but unlike TGFB1 treatment, SNAIL overexpression stimulated cell proliferation and did not expand the SCA-1+ OSE population nor did it alter the size distribution of the OSE. Interestingly, EMT induced by SNAIL overexpression did increase sphere formation by OSE cells, which indicates that it increases the stem cell capabilities of the OSE. Our results suggest that the EMT, which occurs in OSE at the ovulation site, may cause an increase in the number of OSE progenitor cells as a means to facilitate ovulatory wound repair.

## 3.2 Introduction

Each time the ovary ovulates, the ovarian surface epithelium (OSE) is ruptured. The resultant ovulatory wound is quickly healed, although the process controlling this is poorly understood. Recently, the presence of an OSE progenitor cell population has been reported in the literature (Szotek et al., 2008; Gamwell et al., 2012). The number of OSE with progenitor cell characteristics have been found to increase after ovulation (Szotek et al., 2008), indicating that this progenitor cell population is controlled in some way by ovulation. In addition, OSE progenitor cells express the stem cell marker Stem Cell Antigen-1 (SCA-1, also known as LY6A) which to date is the only surface marker identified for this progenitor cell population (Gamwell et al., 2012), although a small cell size has recently been proposed as a marker of OSE cells with the ability to produce oocyte-like cells (Parte et al., 2011; Virant-Klun et al., 2011; Bhartiya et al., 2012).

The SCA-1 expressing (SCA-1+) OSE progenitor cell population is expanded by Transforming Growth Factor Beta 1 (TGFB1), a factor found in the follicular fluid at ovulation (Fried and Wramsby, 1998; Fried et al., 1998; Ouellette et al., 2005; Knight and Glister, 2006; Gamwell et al., 2012). We have previously shown that TGFB1 causes the OSE cells to assume a more stem-like phenotype, as seen by an increase in sphere formation, but it also expands the SCA-1+ progenitor cell population by converting cells that do not exhibit surface expression of SCA-1 (SCA-1-) into SCA-1+ cells (Gamwell et al., 2012). Determining how TGFB1 controls this switch from SCA-1- to SCA-1+ could provide valuable insight into how this progenitor cell population is regulated and provide insight into how ovulatory wounds are healed.

TGFB1 is a well known inducer of the epithelial-to-mesenchymal transition (EMT) where polarized epithelial cells transition into migratory mesenchymal cells (Kalluri and Weinberg, 2009). As the EMT progresses, protein markers associated with epithelial cells, like E-Cadherin and cytokeratins are lost while expression of members of the family of EMT master genes (e.g. *Snail*, *Slug*, and *Twist*) and *Vimentin* is gained (Kalluri and Weinberg, 2009; Savagner, 2010). In the adult, the EMT often occurs during tissue repair and regeneration as it allows terminally differentiated epithelial cells to change their function to reconstruct tissues following injury or inflammation (Kalluri and Weinberg, 2009). In the OSE, an EMT occurs in response to ovulation with OSE cells near the wound site assuming a mesenchymal phenotype to enable them to migrate and proliferate to close the wound (Auersperg et al., 2001; Salamanca et al., 2004; Ahmed et al., 2006; Gotfredson and Murdoch, 2007).

Recently, the EMT has been shown to promote stemness in mammary epithelial cells (Mani et al., 2008; Morel et al., 2008; Guo et al., 2012; Palafox et al., 2012). When mammary epithelial cells are induced to undergo an EMT they not only acquire mesenchymal characteristics, but they also resemble mammary epithelial stem cells with the expression of epithelial stem cell markers and an increased ability to form mammospheres and reconstitute functional mammary glands in cleared mammary fat pads (Mani et al., 2008; Morel et al., 2008; Guo et al., 2012; Palafox et al., 2012).

Because TGFB1 increases the ability of OSE to form spheres, increases the expression SCA-1, a marker of OSE progenitor cells (Gamwell et al., 2012), and is a potent inducer of the EMT, we determined whether TGFB1 is able to expand the OSE progenitor

cell population through an EMT and specifically through the expression of the EMT master gene, *Snail*.

## 3.3 Materials and Methods

*Experimental Animals*

FVB/N mice (Jackson Laboratory) were the source of mouse OSE (MOSE) cells for most of the experiments. The TgN(UbGFP)6752Dag mice (referred to as UbGFP mice, kindly provided as a gift from Dr. Douglas Gray, Ottawa Hospital Research Institute, Ottawa, ON), express enhanced green fluorescent protein (eGFP) under the control of the human ubiquitin promotor (Tsirigotis et al., 2001) and were used as the source of eGFP+ donor MOSE cells. NOD.SCID mice (NOD.CB17-Prkdc$^{scid}$/NcrCrl, Charles Rivers Laboratories, Wilmington, MA) were used as recipient animals in cell transfer experiments. The mice were housed with 12 hour light/dark cycle with free access to food and water. All animal experiments described in this study were performed according to the Guidelines for the Care and Use of Animals established by the Canadian Council on Animal Care with protocols approved by the University of Ottawa Animal Care Committee.

*MOSE Isolation, Culture And Manipulations*

MOSE isolation and culture have been previously described (Gamwell et al., 2012). Briefly, MOSE cells were isolated from 6-wk-old female mice using gentle trypsinization (0.25% Trypsin/0.5 ml PBS/ovary; Invitrogen, Burlington, ON). For each primary culture, 10–20 mice were used. MOSE were grown in ‘MOSE media’ and maintained on tissue

culture plates (Becton-Dickinson, Mississauga, ON) as described (Gamwell et al., 2012). All in vitro MOSE experiments were carried out at least three times using a minimum of two different isolations of MOSE cells with a passage number of less than 20.

To test the effects of TGFB1 on RNA and protein expression, MOSE were treated with TGFB1 (10 ng/mL; human TGFB1, Sigma-Aldrich, Oakville, ON) for 7 days as previously described (Gamwell et al., 2012). Cell morphology was assessed and documented using the EVOS XL Core microscope system (Advanced Microscopy Group, Bothell, WA). The effect of TGFB1 on proliferation was assessed by treating MOSE (10,000 cells/mL) with a range of TGFB1 concentrations (0, 1, 10, 50, and 100 ng/mL) and counting viable cells after 48 hours using a Vi-CELL XR Cell Viability Analyzer (Beckman Coulter, Brea, CA). When growth curves were performed, MOSE were plated (10,000 cells/mL) and viable cells were counted using a Vi-CELL Analyzer 1, 2, 3, and 4 days after cells were plated.

*In Vivo Repopulation*

MOSE cells were isolated from UbGFP mice as described above and, once established in short-term culture, the eGFP+ MOSE cells were sorted by magnetic beads into SCA-1+ and SCA-1- fractions. Briefly, MOSE were released from tissue culture plates by non-enzymatic dissociation (MULTICELL Cell Stripper, Wisent Bioproducts, Montreal, PQ), passed through a 40 μm cell strainer and then separated into SCA-1+ and SCA-1- fractions using an anti-SCA-1 MicroBead kit with a MiniMAC separator and MS columns (Miltenyi Biotec, Cambridge, MA) following the manufacturer's protocol and as previously

described (Gamwell et al., 2012). To increase the purity of the positive fraction, the eluted cells were passed through a second column.

The separated fractions were injected under the bursa of the ovaries of 6-8 week old recipient mice (5 female NOD.SCID mice, 40,000 cells/ovary) using a microsurgical procedure described previously (Clark-Knowles et al., 2007; Laviolette et al., 2010). SCA-1+ cells were transplanted to one ovary and SCA-1- cells were transplanted to the contralateral ovary of each mouse. The ovaries (with ovarian bursa and fat pad intact) along with the attached oviduct were removed after five weeks, fixed in formalin and paraffin-embedded so eGFP expression could be detected by immunohistochemistry. Three micrometer sections were cut with a microtome and mounted on Superfrost Plus slides (Fisher Scientific, Nepean, ON).

*Immunohistochemistry (IHC)*

Histological sections were deparaffinized and rehydrated and then high temperature antigen retrieval was performed in pH6 sodium citrate buffer (Antigen Unmasking Solution; Vector Laboratories, Burlington, ON) in a pressure cooker (Tender Cooker; Nordic Ware, Minneapolis, MN). Endogenous peroxidase activity was blocked by 3% hydrogen peroxide in ddH2O for 30 minutes and non-specific antibody binding was blocked with Protein Block, Serum-Free (Dako, Burlington, ON; all IHC reagents from Dako unless specified otherwise). A polyclonal rabbit eGFP primary antibody (Ab6556, AbCam, Toronto, ON) was diluted in Antibody Diluent with Background Reducing Components at a concentration of 1:200 and incubated on the tissues for 1 hour at room

temperature. After washing away unbound primary antibody, the sections were incubated with the Anti-Rabbit Envision+ System-HRP Labelled Polymer, washed and then immersed for 5 min in 250 ml of diaminobenzidine (DAB) chromogen solution (Sigma-Aldrich) with 50 µl of 30% hydrogen peroxide. Sections were counterstained with Harris hematoxylin (Fisher Scientific) and mounted with Permount (Fisher Scientific). Images were obtained with the ScanScope CS system and ImageScope software (Aperio, Vista, CA).

*Flow Cytometry*

The numbers of cells with surface expression of SCA-1 were determined using antibodies against SCA-1 and flow cytometric procedures as described in (Gamwell et al., 2012). The relative volume of different populations of MOSE cells was estimated by comparing their forward scatter (FS), as the FS is determined to a large extent by the volume of the scattering particles (Tzur et al., 2011).

*Gap Closure Migration Assay*

Migration was assessed using a Gap Closure Migration Assay (Radius 24-Well Cell Migration Assay, Cell BioLabs, San Diego, CA) following the manufacturer's directions. Prior to placing cells in the migration wells, cells were pretreated with MOSE media in the absence or presence of 10 ng/ml TGFB1 for 5 days. Cells (100,000/well) were then plated in 500 uL of MOSE media or MOSE media with 10 ng/ml TGFB1. The cells were allowed to attach for 24 hours and confluency was confirmed before the disc insert was removed, at which point the media was replaced. The control MOSE received MOSE media and the

TGFB1 treated MOSE received MOSE media with 10 ng/ml TGFB1 for the duration of the migration assay. Images were taken using the EVOS XL Core microscope system immediately after the insert was removed (0h) and after 33 hours.

*Gene Expression Analysis*

RNA isolation and quantitative real-time PCR (Q-PCR) were carried out as described in Gamwell et al. (2012). The primer sequences used to detect *Snail, Slug, Twist, Vimentin, E-Cadherin, Cytokeratin* and *Ppia* (endogenous control) are listed in Table 3.1. The primer sequence used to detect *Sca-1* has been previously described (Gamwell et al., 2012).

*Western Blot Analysis*

Protein was isolated using ProteoJET Mammalian Cell Lysis Reagent (Fisher Scientific) following the manufacturer's directions. Lysates (60 ng) were run on precast NuPAGE 4-12% Bis-Tris gels (Invitrogen) and transferred to Immobilon-P membranes (Millipore, Billerica, MA). Blots were blocked with 5% milk in Tris-buffered saline with 0.05% Tween 20 (TBST) for at least 1 hour at room temperature. Blots were then probed with antibodies against SNAIL (1:200, ab82849, AbCam), E-CADHERIN (1:5000, 610182, BD Transduction Laboratories, Mississauga, ON), and GAPDH (1:80,000, Ab8245, AbCam). For primary antibodies raised in mice, a rabbit anti-mouse secondary antibody was used (E-CADHERIN, 1:2500; BRCA1 and GAPDH, 1:20,000; Ab6728, Abcam). For primary antibodies raised in rabbits (SNAIL), a donkey anti-rabbit secondary antibody was

**Table 3.1:** Primer Sequences

| Gene | Forward Primer (5'-3') | Reverse Primer (5'-3') |
|---|---|---|
| *Snail* | GTC TGC ACG ACC TGT GGA A | CAG GAG AAT GGC TTC TCA CC |
| *Slug* | TGC AAG ATC TGT GGC AAG G | CAG TGA GGG CAA GAG AAA GG |
| *Twist* | AGC TAC GCC TTC TCC GTC T | TCC TTC TCT GGA AAC AAT GAC A |
| *Vimentin* | CGC CCAG GCC AAG CAG GAG TC | CGC TCC AGG GAC TCG TTA GTG C |
| *E-Cadherin* | ATC CTC GCC CTG CTG ATT | ACC ACC GTT CTC CTC CGTA |
| *Cytokeratin 19* | TGA CCT GGA GAT GCA GAT TG | CCT CAG GGC AGT AAT TTC CTC |
| *Ppia* | AGG GTG GTG ACT TTA CAC GC | GAT GCC AGG ACC TGT ATG CT |

used (1:10,000, 711-035-152, Cedarlane, Burlington, ON). Both primary and secondary antibodies were diluted in 5% milk in TBST and incubated with the membranes for 1 hour at room temperature. Detection was performed with ECL Plus (GE LifeSciences, Baie d'Urfe, PQ) following the manufacturer's protocol. Images were taken using a DE500 MultiImage FC Light Cabinet and were analyzed using AlphaEase FC (both from Alpha Innotech Corporation, Johannesburg, SA).

*Viral Production And Infection*

The pBp-SNAIL plasmid was obtained from AddGene (Cambridge, MA) and has been previously described (Yang et al., 2004). The CMV-driven puromycin resistance expression vector pLPCX (ClonTech, Mountain View, CA) was used as a control. The viruses were produced by cotransfection of 293T/17 cells (American Type Culture Collection, Manassas, VA) with the pBp-SNAIL or pLPX vectors along with pHIT60, a CMV-driven *gag-pol* expression plasmid (Soneoka et al., 1995) and pHIT123, a CMV-driven ecotropic *env* expression plasmid (Soneoka et al., 1995). Transfections of 15,000,000 293T/17 cells were carried out using polyethylenimine (PEI, 7.5mM, pH 7.4, Polysciences, Warrington, PA) and the following plasmid ratios 2:1.3:1.25 μg of pBp-SNAIL/pLPCX:pHIT60:pHIT123. Virus was harvested by collecting media from the transfected cultures 48h post transfection and 500 μL of the filtered virus containing media was used to infect two different MOSE primary cultures (200,000 cells). Transfections were carried out in duplicate in the presence of 10 μg/ml of polybrene (Sigma-Aldrich). Following infection, cells were selected with 4 μg/ml puromycin. The infected MOSE lines

are referred to as pLPCX (vector control, 4 lines total) and pBp-SNAIL (4 lines total).

*Sphere Forming Assays*

MOSE cells were released from tissue culture plates at 90% confluency with trypsin, passed through a 40-μm cell strainer and suspended as single cells in a 1:1 mixture of methylcellulose (to prevent cell aggregation) and progenitor cell media (Gamwell et al., 2012) at a density of 20,000 cells/ml per well of a 12-well tissue culture plate. The bottom of each well was coated with a thin layer of 1% agarose in progenitor cell media to prevent the cells from adhering to the bottom of the culture plate. Sphere formation and morphology were monitored and documented using the EVOS microscope system and the number of spheres in 3 random fields per well was counted.

*Statistical Analyses*

Based on the number of conditions tested, a Student t-test or an ANOVA (one-way or two-way depending on the experimental design) with a Tukey's post-test was used to determine statistical significance ($P<0.05$). Error bars indicate the SEM.

## 3.4 Results

*Transplanted SCA-1+ But Not SCA-1- MOSE Are Detected On The Surface Of The Ovary 5 Weeks After Intrabursal Injection*

MOSE with surface expression of the stem cell marker SCA-1 are more stem-like than MOSE without expression of the marker (Gamwell et al., 2012). To confirm that

SCA-1 marks a MOSE progenitor cell population, we tested the repopulation potential of SCA-1+ MOSE and therefore their potential for self-renewal and/or proliferation in vivo. SCA-1+ and SCA-1- MOSE isolated from UbGFP mice express eGFP and can be identified when introduced into recipient mice that do not express eGFP. SCA-1+ or SCA-1- cells were injected between the surface of the ovary and the bursal membrane in contralateral ovaries. Five weeks after surgery, the presence of eGFP expressing cells was determined by IHC. Cells expressing eGFP could be detected on the surface of recipient ovaries where SCA-1+ cells had been introduced under the bursa (Figure 3.1D). eGFP-expressing cells could not be detected on the surface of ovaries that had been injected with SCA-1- MOSE (Figure 3.1C). These findings suggest that only SCA-1+ MOSE cells can attach and survive on the surface of the ovary.

*TGFB1 Expands The FS$^{low}$ MOSE Population, Which Is Enriched With SCA-1+Progenitor Cells*

TGFB1 expands the SCA-1+ progenitor cell population by converting SCA-1- MOSE into SCA-1+ MOSE (Gamwell et al., 2012). To expand on this result, MOSE cells were treated with a range of TGFB1 concentrations (0-10 ng/mL). The percentage of MOSE cells with surface expression of SCA-1 was found to increase in a dose-dependent manner as the concentration of TGFB1 increased (Fig. 3.2C, "All Cells"), but reached significance only at 10 ng/mL. At that concentration of TGFB1, the percentage of SCA-1+ MOSE almost tripled compared to control, untreated cells.

Careful flow cytometric analysis revealed two populations of MOSE cells based on

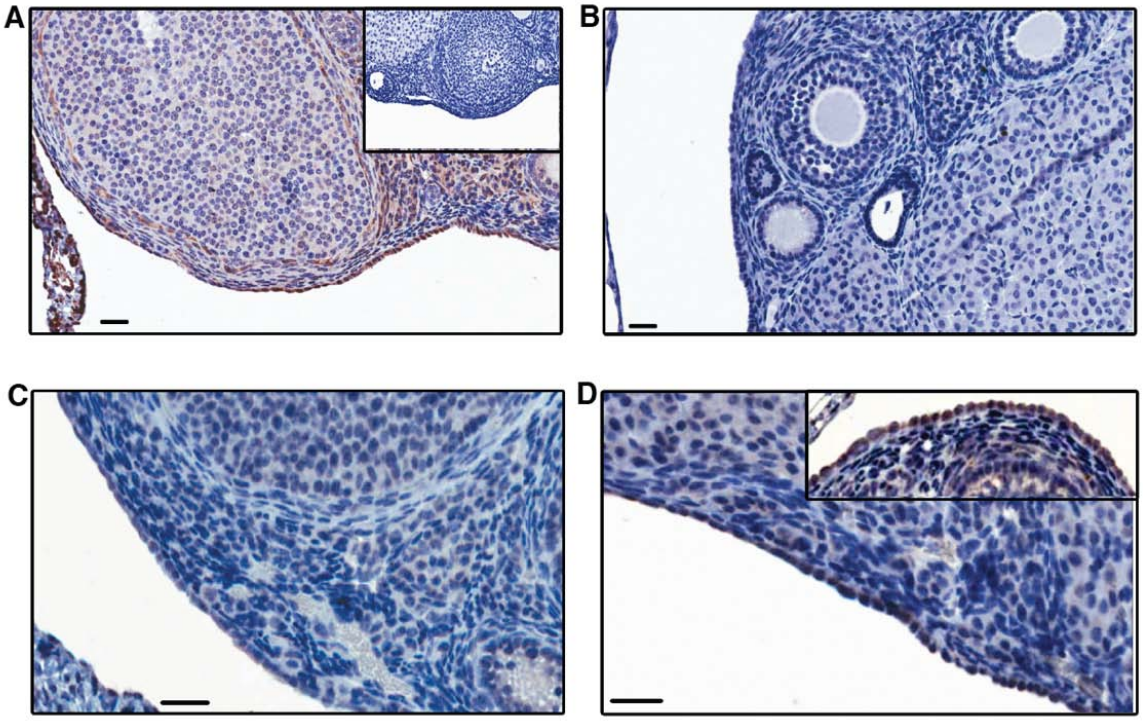


**Figure 3.1: Engraftment of SCA-1-expressing MOSE on the surface of the ovary of a recipient NOD.SCID mouse. A:** IHC for eGFP expression on a cross-section of an ovary from a UbGFP mouse. Brown staining, as seen in the MOSE, indicates eGFP expression. Inset shows the no primary antibody control. **B:** A cross-section from an uninjected ovary from a NOD.SCID mouse. **C,D:** IHC for eGFP expression on a cross-section of a NOD.SCID ovary transplanted with 4 x $10^4$ eGFP+ SCA-1- cells (C) or 4 x $10^4$ eGFP+ SCA-1+ cells (D), collected 5 weeks after intrabursal injection. Brown staining indicates cells positive for eGFP. Inset in D shows eGFP expression in a cross-section of an ovary from a different NOD.SCID mouse transplanted with eGFP+ SCA-1+ cells. Scale bars = 25μm.

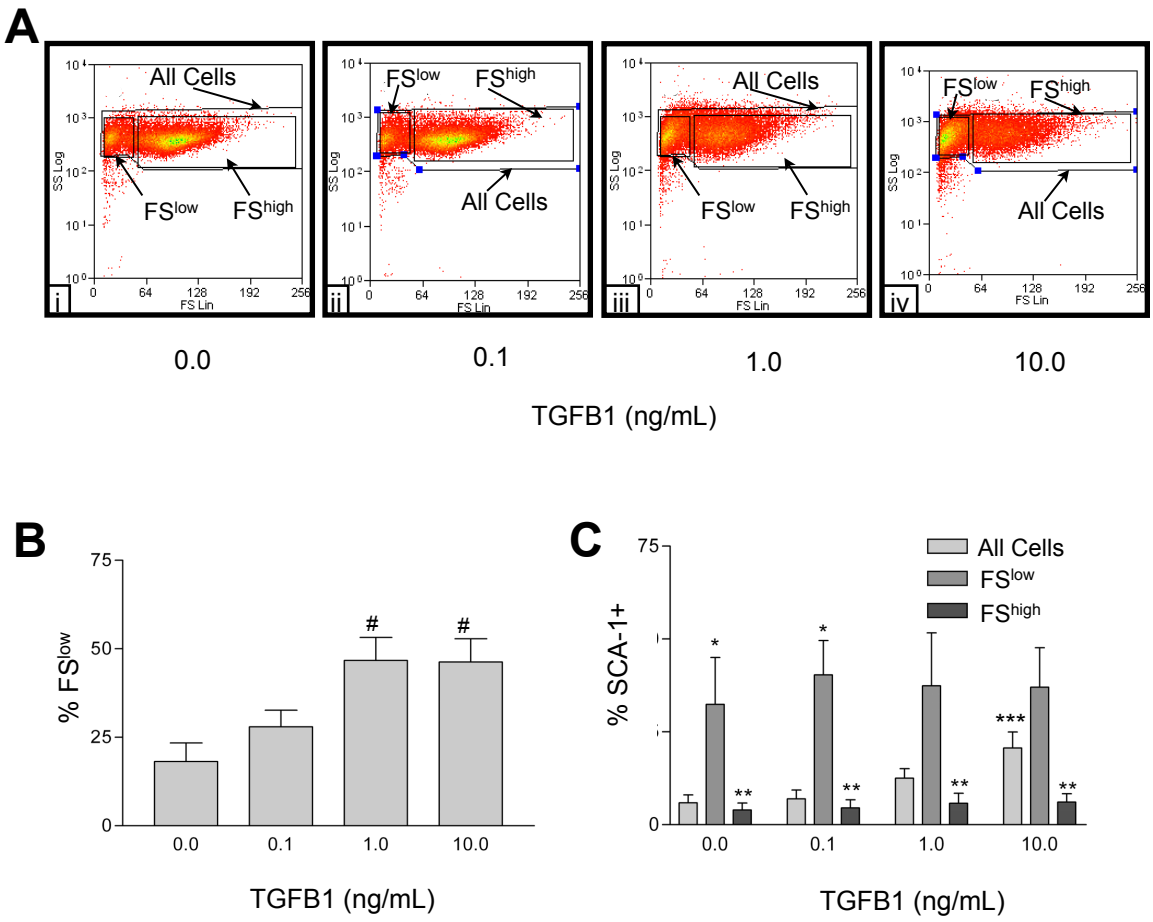


**Figure 3.2: Flow cytometric analysis of the effect of TGFB1 on the percentage of SCA-1+ and FS$^{low}$ MOSE.** **A:** Representative Side Scatter (SS) vs. Forward Scatter (FS) flow cytometry profile of MOSE treated with increasing concentrations of TGFB1 for 7 days. FS$^{low}$ and FS$^{high}$ indicates population of cells with a low or high FS respectively. All Cells represents all live cells (including FS$^{low}$ and FS$^{high}$). **B:** Graphical representation of the average percentage of FS$^{low}$ cells in MOSE treated with increasing concentrations of TGFB1 for 7 days. # indicates $p<0.05$ compared to control (0 ng/mL TGFB1). **C:** Graphical representation of the average percentage of SCA-1+ MOSE in the All Cells, FS$^{low}$ and FS$^{high}$ gates indicated in A. * indicates $p<0.05$ compared to All Cells at a given concentration of TGFB1. ** indicates $p<0.05$ compared to FS$^{low}$ at a given concentration of TGFB1. *** indicates $p<0.05$ compared to control (All Cells, 0 ng/mL TGFB1).

forward scatter vs. side scatter (FS vs. SS, Fig. 3.2A[i]). One group clustered around a lower FS ($FS^{low}$) which indicated these cells had a smaller cell volume, compared to the second group which had a higher FS ($FS^{high}$) and therefore larger volume. As the concentration of TGFB1 in the culture media increased, the percentage of cells falling within the $FS^{high}$ gate decreased, while the percentage of cells within the $FS^{low}$ gate increased (Fig. 3.2 A[i-iv]). The percentage of cells in the $FS^{low}$ gate is represented graphically in Fig. 3.2B and was significantly increased at the two highest concentrations of TGFB1. When the percentage of SCA-1+ cells within the $FS^{low}$ gate, the $FS^{high}$ gate and the "All Cells" gate were compared at each TGFB1 concentration, SCA-1+ cells were found to be enriched in the $FS^{low}$ gate (Fig. 3.2C). The enrichment of SCA-1+ MOSE in the $FS^{low}$ population was statistically significant compared to $FS^{high}$ in untreated cells and at all TGFB1 concentrations. The $FS^{low}$ population was also significantly enriched compared to "All Cells" without TGFB1 and at the lowest TGFB1 concentration, with a strong trend for an increase at the two highest concentrations of TGFB1.

Interestingly, as the concentration of TGFB1 increased, the proportion of SCA-1+ MOSE in the $FS^{low}$ and $FS^{high}$ gates remained the same (Fig. 3.2c), while the proportion of SCA-1+ MOSE in the total population (All Cells) increased. Therefore it appears that TGFB1 not only increases the proportion of SCA-1+ MOSE (Fig. 3.2C, All Cells) but it also alters the size distribution of MOSE cells as determined by FS. In addition, cells with a relatively small cell volume (as determined by FS) are more likely to be SCA-1+ compared to cells with a larger cell volume, regardless of the absence or presence of TGFB1.

*TGFB1 Induces A Reversible EMT In The MOSE*

We previously showed that treatment with TGFB1 expands the SCA-1+ MOSE progenitor cell population by converting a SCA-1- cells into SCA-1+ progenitor cells (Gamwell et al., 2012). In a variety of tissues TGFB1 induces EMT, which is required for the remodelling of tissues during embryogenesis, during certain types of wound healing and during the acquisition of malignant traits by carcinoma cells (Ahmed et al., 2007). Recently, the EMT has been shown to generate cells with many of the properties of stem cells (Liao et al., 2007; Mani et al., 2008; Guo et al., 2012; Palafox et al., 2012). We therefore determined whether an EMT, triggered by TGFB1, was driving the conversion from a normal MOSE cell to a MOSE cell with stem-like characteristics.

To determine whether MOSE cells undergo an EMT in response to TGFB1 treatment, MOSE cells were treated with 10 ng/ml of TGFB1. After 7 days the MOSE cells exhibited a mesenchymal phenotype (Fig. 3.3A) and upregulated *Snail* mRNA 5-fold (Fig. 3.3B) while downregulating *E-Cadherin* and *Cytokeratin 19* mRNA 2-fold and 4-fold respectively (Fig. 3.3C). There was no change in *Slug*, *Twist*, or *Vimentin* transcript abundance (Fig. 3.3B). The EMT was reversible as removing TGFB1 caused the mRNA levels of *Snail* and *Cytokeratin 19* to return to that of untreated MOSE (Fig. 3.3D). In addition to the changes in mRNA abundance, TGFB1 treatment caused a 4-fold increase in SNAIL protein expression and a 2-fold decrease in E-CADHERIN protein levels as determined by western blotting and densitometric analysis (Fig 3.4A,B).

When epithelial cells take on a mesenchymal phenotype they often gain the ability to migrate. To determine if MOSE induced to undergo an EMT gained the ability to migrate

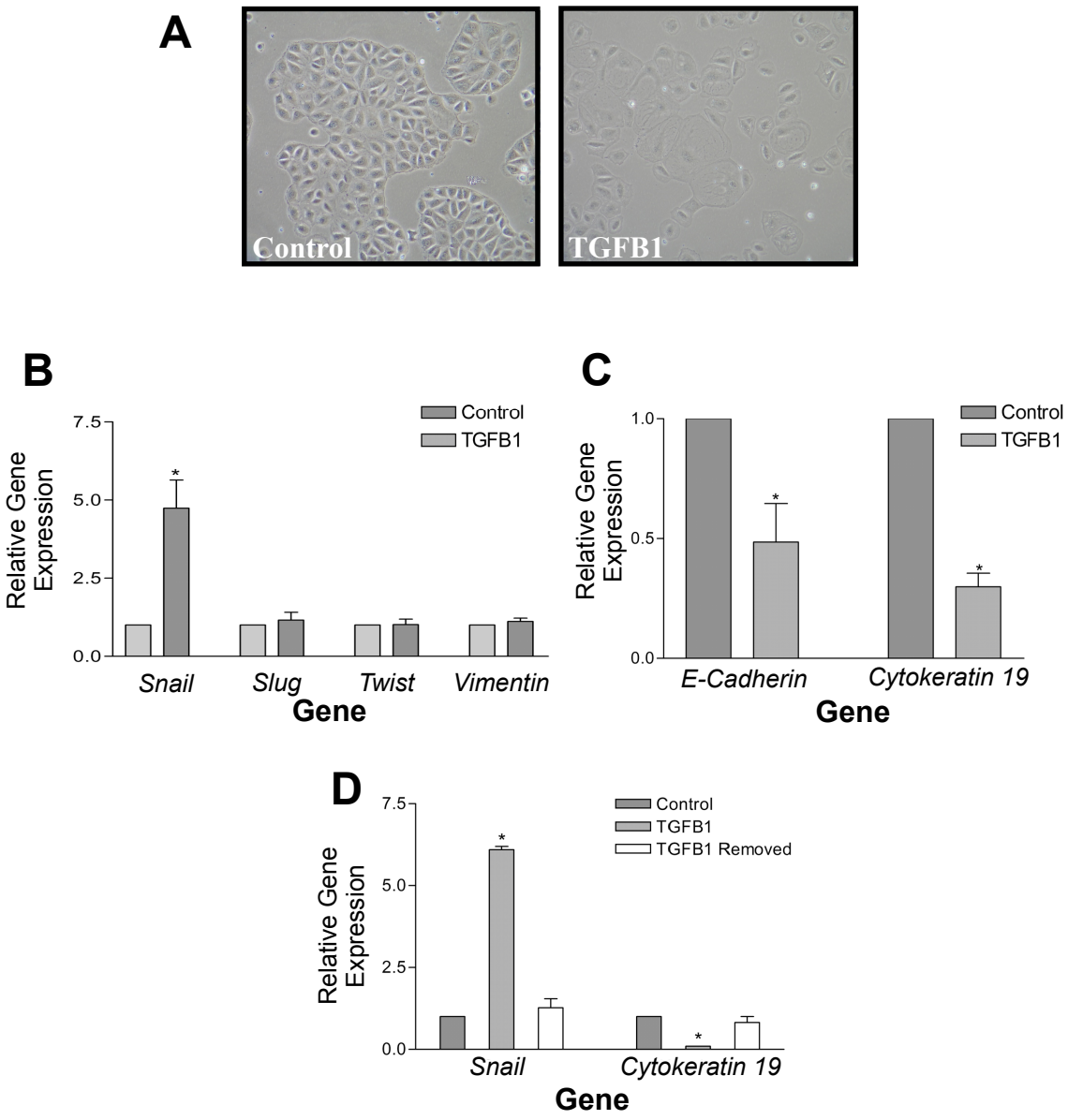


**Figure 3.3: The effect of TGFB1 treatment on morphology and gene expression.**
**A:** Representative phase contrast images of MOSE cells grown in MOSE media (control) and in MOSE media with TGFB1 (10 ng/mL, 7 days). Original magnification is 20x. **B, C:** Q-PCR analysis comparing the expression of mRNAs commonly upregulated (B) or downregulated (C) in mesenchymal cells compared to epithelial cells. MOSE grown in MOSE media (Control) or in the presence of TGFB1 (10 ng/mL, 7 days) were compared. **D:** Q-PCR detecting the relative expression of *Snail* and *Cytokeratin 19* mRNA in MOSE treated with 10 ng/mL TGFB1 for 7 days (TGFB1), MOSE treated with TGFB1 for 7 days, and then grown in the absence of TGFB1 for 7 days (TGFB1 removed) as compared to MOSE cells grown in MOSE media (Control). *indicates $p<0.05$ compared to control.

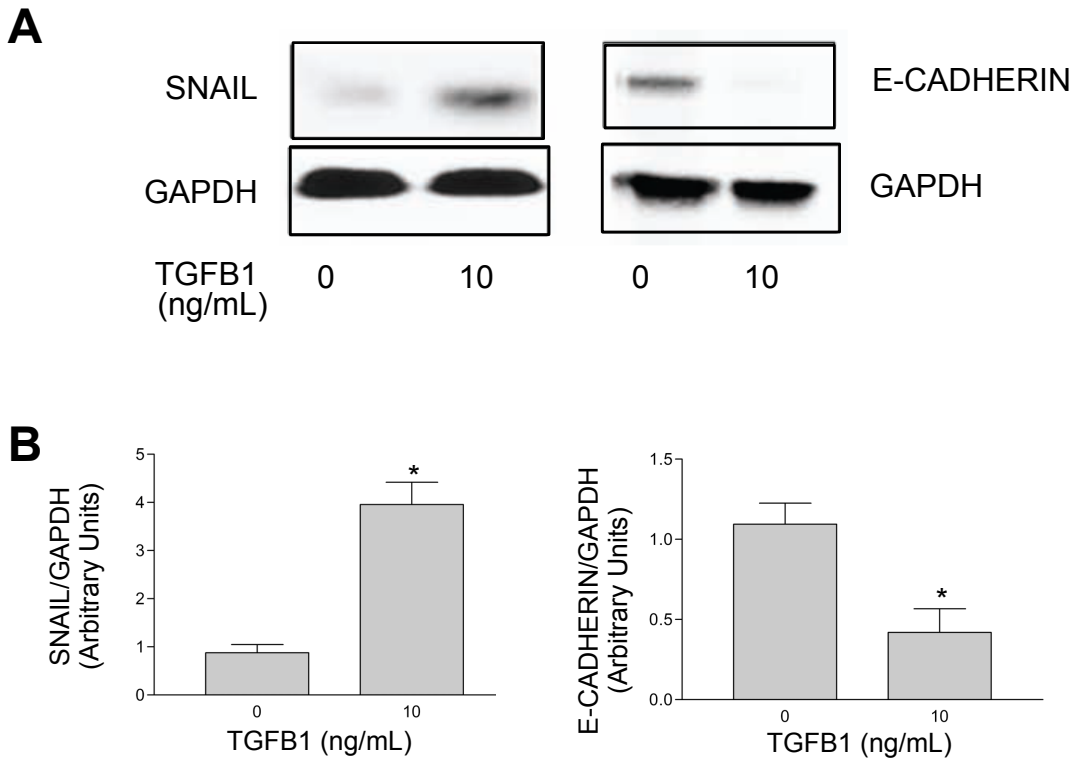


**Figure 3.4: Protein expression analysis in TGFB1-treated MOSE. A:** Western blot analysis of expression of SNAIL and E-CADHERIN in MOSE treated with TGFB1 (10 ng/mL, 7 days) and control MOSE. GAPDH is used as a loading control. **B:** Densitometric analysis of three Western blots indicative of that shown in A. * indicates $p < 0.05$ compared to control.

we compared the ability of TGFB1-treated and control MOSE cells to migrate into a gap. TGFB1 enhanced the ability of MOSE cells to migrate during a gap closure migration assay (Fig 3.5A). This enhanced migration was not caused by an increase in proliferation because MOSE treated with 10 ng/ml TGFB1 for 48 hours were strongly growth inhibited, reducing the cell number by 60% compared to control (untreated) cells (Fig. 3.5B). Proliferation was also significantly inhibited at 1, 50 and 100 ng/mL of TGFB1.

*Overexpression Of SNAIL Induces EMT In The MOSE*

TGFB1 has a variety of effects on cells including cell growth, differentiation, apoptosis, and cellular homeostasis (Kalluri and Weinberg, 2009). To study the effect of EMT on the MOSE progenitor cell population, separate from any other effects of TGFB1, we overexpressed SNAIL in the MOSE cells using a Maloney-based retrovirus. SNAIL was chosen, rather than SLUG or TWIST, because only *Snail* mRNA was upregulated by TGFB1 while the other two transcription factors were not. SNAIL overexpression has been shown to be sufficient to induce an EMT in other epithelial cell types (Batlle et al., 2000; Cano et al., 2000).

Transduction with the control pLPCX puromycin resistance vector or the pBp-SNAIL vector, resulted in puromycin resistant colonies in all 4 replicates. Cells were maintained in puromycin-containing media throughout the experiments. To confirm SNAIL overexpression, protein was isolated from the uninfected MOSE, the pLPCX infected MOSE and the pBp-SNAIL infected MOSE and the level of SNAIL was determined by western blotting. MOSE cells infected with the pLPCX vector express

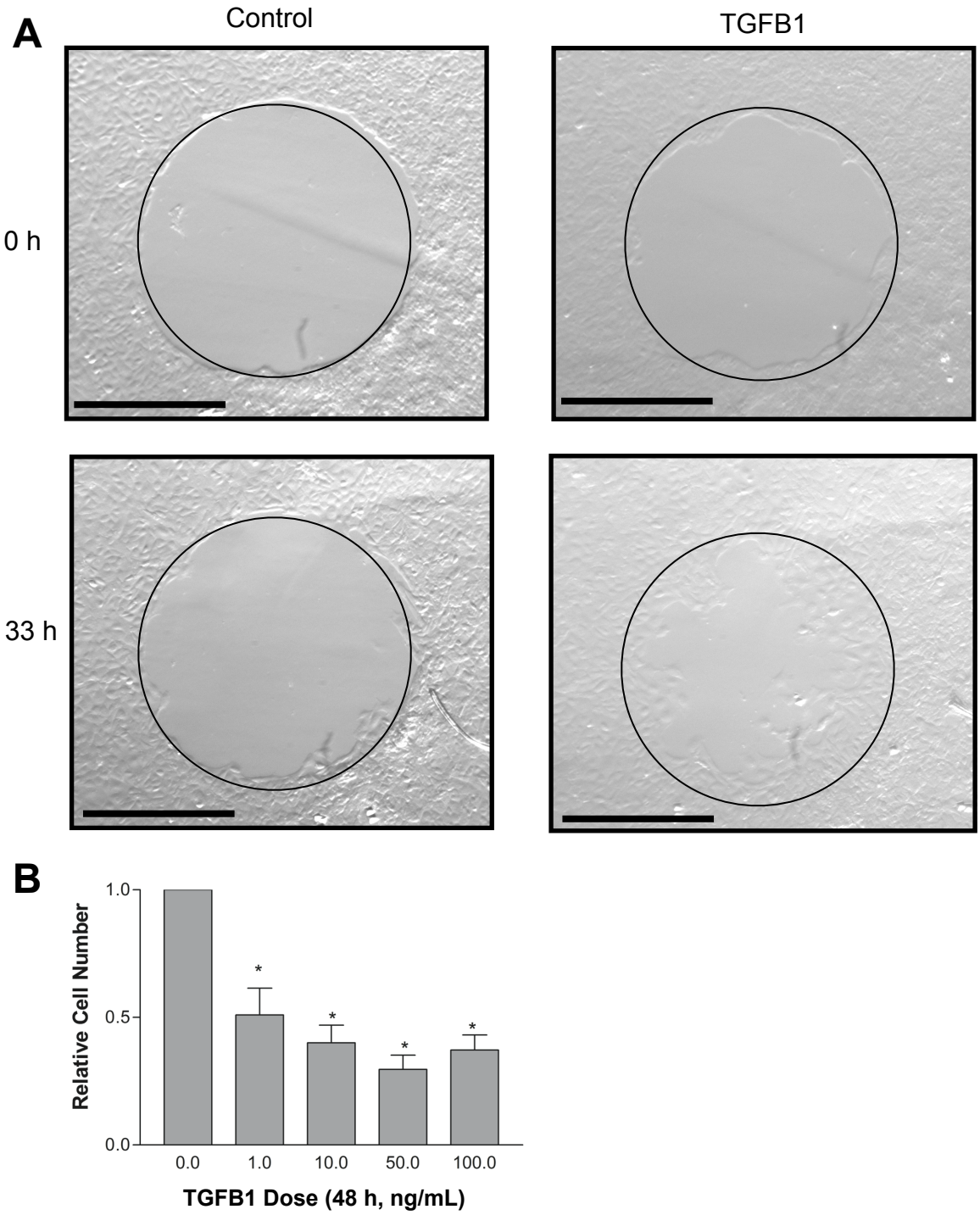


**Figure 3.5: The effect of TGFB1 treatment on migration and proliferation. A:** Gap closure migration assay. Representative phase contrast images of MOSE immediately after the wound (circle) was created (0h) and 33 hours later (33h). MOSE were grown in MOSE media or MOSE media with TGFB1 (10 ng/mL) for 5 days prior to the migration assay and during the migration assay Black bar indicates 250 μm. **B:** An equal number of MOSE cells were grown in a range of TGFB1 concentrations (0-100 ng/mL) until the relative number of viable cells was determined after 48 hours (h). * indicates $p<0.05$ compared to control.

similar levels of SNAIL as uninfected MOSE while MOSE infected with the pBp-SNAIL expressed, on average, 2.6-fold higher levels of SNAIL protein when compared to the vector control (Fig. 3.6A,B). The increase in SNAIL protein coincides with a 2-fold decrease in E-CADHERIN levels (Fig 3.6A,B).

MOSE cells that overexpress SNAIL assumed a distinctive mesenchymal morphology, while cells infected with the vector control maintained an epithelial morphology (Fig. 3.7A). Both the protein expression profile and the morphology of the pBp-SNAIL MOSE cells indicate that overexpression of SNAIL is sufficient to induce an EMT in the MOSE cells. In addition, MOSE cells that overexpress SNAIL had a significantly higher proliferation rate compared to uninfected and pLPCX-infected MOSE cells after 4 days in MOSE media (Fig. 3.7B).

*SNAIL Overexpression Does Not Increase The Percentage Of SCA-1+ Or $FS^{low}$ MOSE*

TGFB1 treatment caused an increase in the proportion of MOSE expressing SCA-1 (Fig. 3.2C), an increase in the percentage of cells in the $FS^{low}$ gate (Fig. 3.2B), and induced an EMT in the MOSE, which included an increase in SNAIL expression (Fig. 3.3). We therefore used flow cytometry to determine if EMT, induced by SNAIL overexpression rather than TGFB1 treatment, was sufficient to increase the number of SCA-1 expressing MOSE. Interestingly, overexpression of SNAIL did not alter the proportion of cells expressing SCA-1 as determined by flow cytometry (Fig. 3.8A), nor did it alter the percentage of $FS^{low}$ MOSE (Fig. 3.8B).

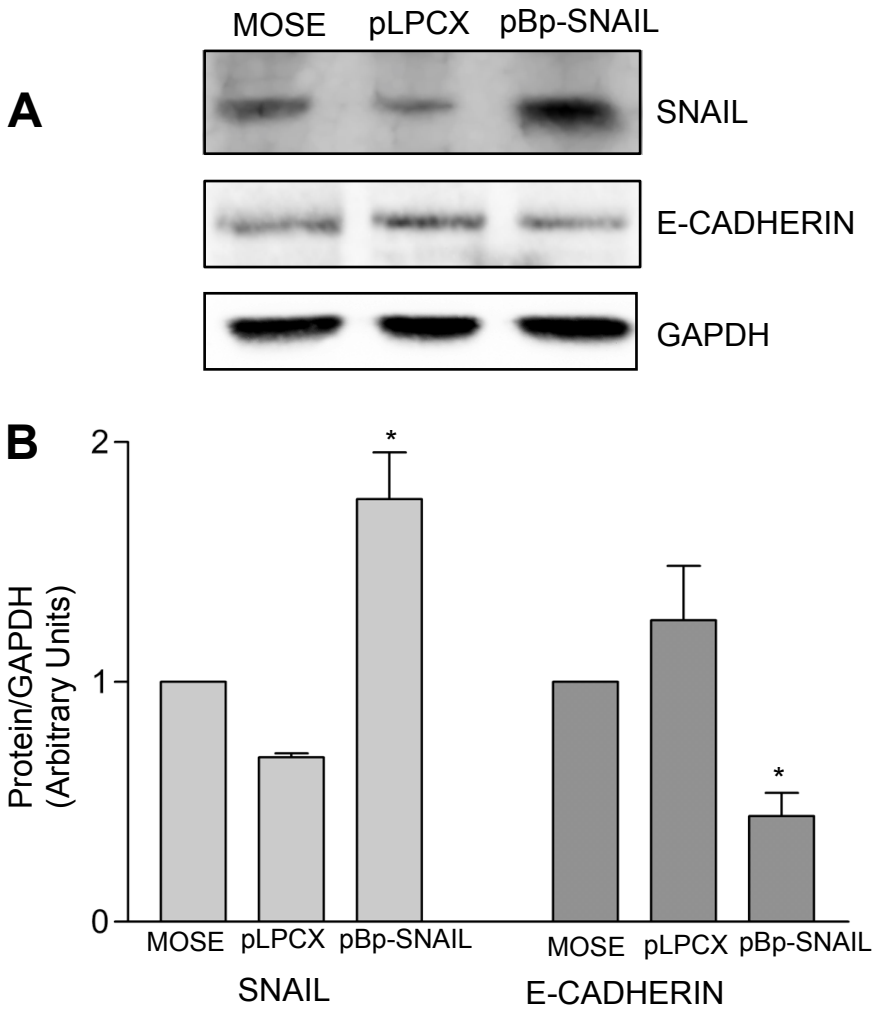


**Figure 3.6: Protein expression analysis in SNAIL-overexpressing MOSE cells.**
MOSE cells were infected with Maloney-based retroviruses encoding for puromycin resistance (pLPCX) or puromycin resistance and SNAIL expression (pBp-SNAIL). Uninfected MOSE were used as a control. pLPCX and pBp-SNAIL infected MOSE were selected in 4 μg/mL puromycin for 4 weeks prior to protein collection. **A:** Representative western blot analysis depicting SNAIL and E-Cadherin expression in control MOSE, pLPCX and pBp-SNAIL infected MOSE. GAPDH was used as a loading control. **B:** Densitometric analysis of four western blots indicative of that shown in A. * indicates $p < 0.05$ compared to control.

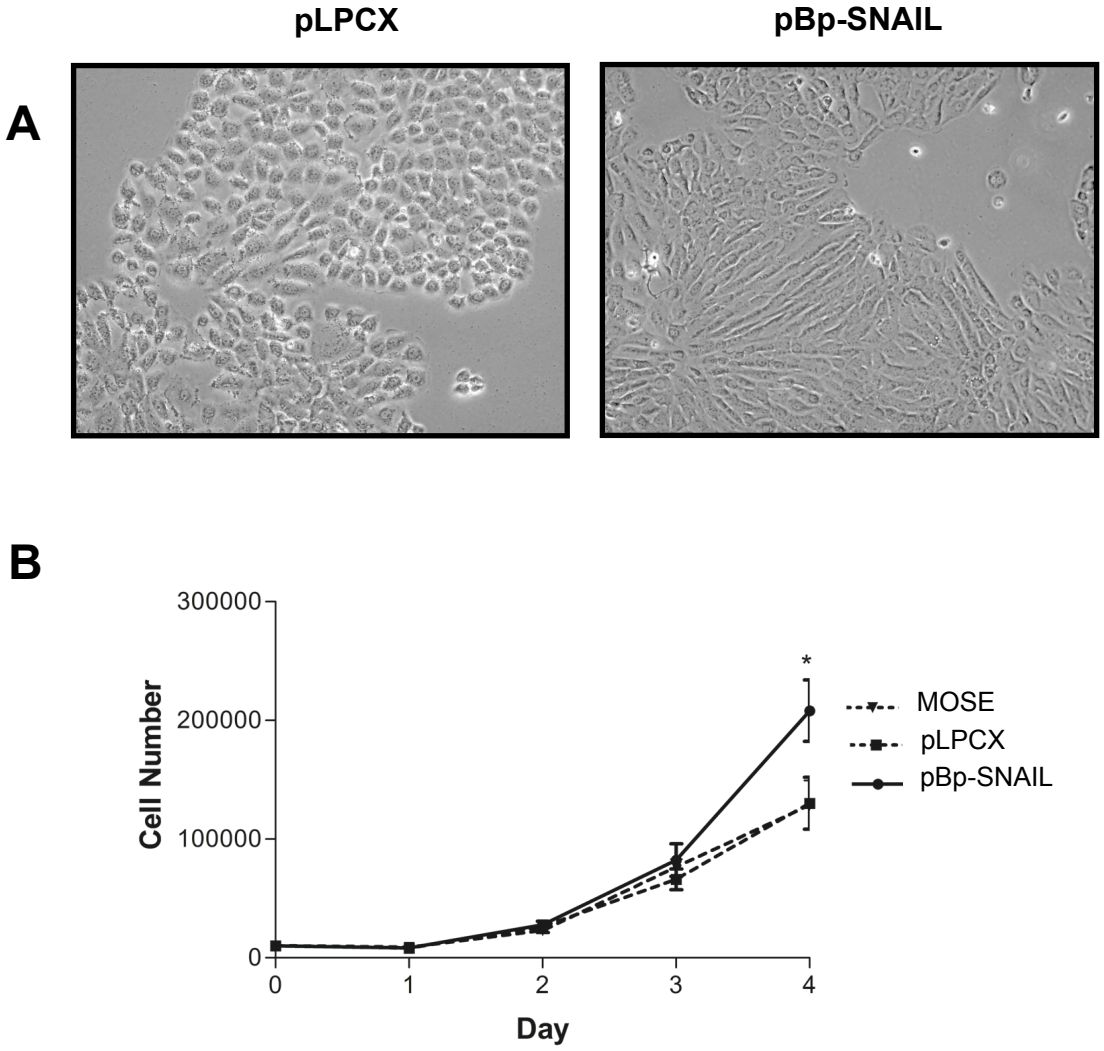


**Figure 3.7: The effect of SNAIL overexpression on MOSE cell morphology and proliferation. A:** Representative phase contrast images of MOSE cells that overexpress SNAIL (pBp-SNAIL) and the vector control (pLPCX). Original magnification is 20x. **B:** A 4-day growth curve comparing the proliferation rate of uninfected MOSE (triangles, MOSE), vector control MOSE (squares, pLPCX) and SNAIL overexpressing MOSE cells (circles, pBp-SNAIL). * indicates $p<0.05$ compared to MOSE and pLPCX.

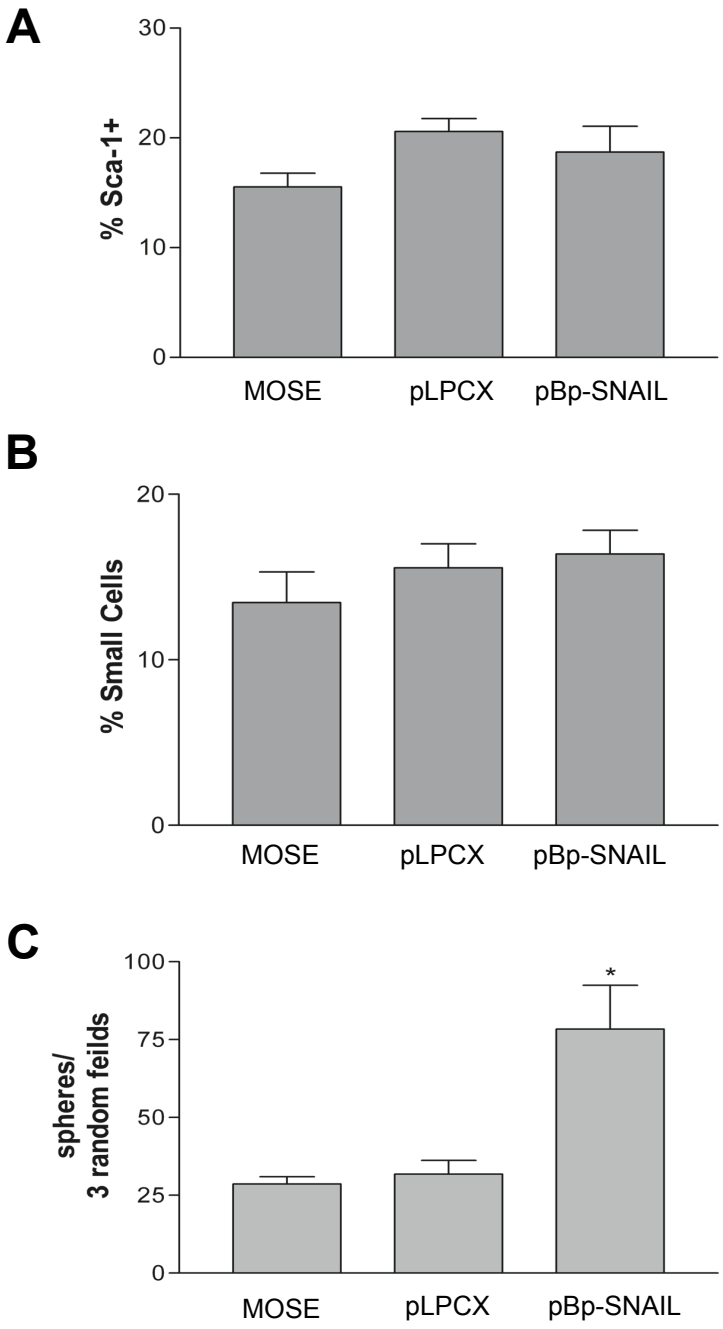


**Figure 3.8: The effect of SNAIL overexpression on SCA-1 surface expression, percentage of FS$^{low}$ (small) cells, and sphere formation. A:** Flow cytometric analysis for SCA-1 surface expression in uninfected MOSE, vector control MOSE (pLPCX) and SNAIL overexpressing MOSE (pBp-SNAIL). **B:** Graphical representation of the average percentage of FS$^{low}$ cells in uninfected MOSE, vector control MOSE (pLPCX) and SNAIL overexpressing MOSE (pBp-SNAIL). **C:** The number of spheres formed from single cells by uninfected MOSE, vector control MOSE and MOSE that overexpress SNAIL (pBp-SNAIL) after one week in methylcellulose. The data shown are means of the number of spheres counted in three random fields in each well, in three independent experiments. * indicates $p<0.05$ compared to MOSE.

*SNAIL Overexpression Increases Sphere Formation*

Since SNAIL overexpression did not increase the percentage of MOSE that express SCA-1 we next determined whether SNAIL overexpression increased sphere formation. Unlike expression of a stem cell marker, sphere formation is a functional test of stemness which has been used extensively to indicate the presence of cells with stem/progenitor cell characteristics in a variety of tissues (Reynolds and Weiss, 1996; Weiss et al., 1996; Dontu et al., 2003; Woodward et al., 2005; Liao et al., 2007). We have previously shown that MOSE progenitor cells have the ability to form spheres and, when treated with TGFB1, show a more than 6-fold increase in the number of spheres that they are able to form (Gamwell et al., 2012). When SNAIL overexpressing cells, the vector controls and normal MOSE were placed into sphere-forming conditions, we found that the pBp-SNAIL MOSE formed 3-fold more spheres than uninfected MOSE or the vector controls (Fig. 3.8C). The results therefore suggest that SNAIL overexpression can increase stemness without any affect on SCA-1 expression.

## 3.5 Discussion

Exposure to TGFB1 caused MOSE to undergo an EMT as seen by a decrease in the expression of epithelial markers (E-Cadherin, Cytokeratin 19), an increase in the expression of mesenchymal markers (Snail), the adoption of a mesenchymal morphology and the acquisition of the ability to migrate. In addition to inducing an EMT, TGFB1 increased the proportion of SCA-1+ MOSE and MOSE that fall within the $FS^{low}$ gate. In comparison, SNAIL overexpression induced an EMT in the MOSE, as evidenced by changes in

morphology and expression of genes associated with epithelial/mesenchymal cells but was not sufficient to increase the proportion of SCA-1+ MOSE although it was sufficient to increase the number of MOSE capable of forming spheres.

SCA-1+ but not SCA-1- MOSE can attach and survive on the surface of the ovary for at least 5 weeks. While not a rigorous demonstration of repopulation ability, these results do indicate that SCA-1+ and SCA-1- MOSE have distinct functional characteristics, and that SCA-1+ cells have greater ability to attach and/or survive transplantation than SCA-1- cells. Moreover, the SCA-1+ cells survived through multiple rounds of natural ovulations. It remains unclear whether the SCA-1+ transplanted cells self-renewed and/or proliferated in association with ovulatory wound repair. This behaviour would best be studied under conditions, not yet developed, where the endogenous epithelium could be removed or destroyed to allow more rigorous limiting dilution and repopulation experiments to be performed.

In agreement with our previous work we have found that TGFB1, which is present in the follicular fluid at ovulation (Fried et al., 1998; Knight and Glister, 2006), expands the SCA-1+ MOSE population. Interestingly, careful flow cytometric characterization of MOSE cells treated with TGFB1 revealed that there are distinct populations of MOSE that can be separated based on their forward scatter. $FS^{low}$ MOSE, which have a smaller cell volume, have a higher proportion of SCA-1+ MOSE compared to $FS^{high}$ MOSE. This indicates that the $FS^{low}$ MOSE may be enriched with cells with progenitor cell characteristics as SCA-1 is a marker for MOSE progenitor cells (Gamwell et al., 2012). With further characterization, FS could prove to be a useful method for isolating MOSE

progenitor cells.

Recently, it has been proposed that both mouse and human OSE may contain cells referred to as "very small embryonic-like stem cells" (VSELs; reviewed in Bhartiya et al., 2012). While it is still a controversial area of research, these VSELs are proposed to have the ability to create or become oocyte-like cells (Parte et al., 2011; Virant-Klun et al., 2011; Bhartiya et al., 2012) in keeping with the reports of other research groups that adult ovaries contain cells that are capable of neo-oogenesis (Johnson et al., 2004; Bukovsky et al., 2008; White et al., 2012). While our results indicate that MOSE with a low FS are enriched with cells that express the MOSE progenitor cell marker SCA-1, further characterization of the $FS^{low}$ MOSE is required before it is known if our findings support the existence of a cell type in the OSE capable of neo-oogenesis.

The EMT is a phenotypic shift where closely associated, stationary epithelial cells take on a more mesenchymal phenotype and gain the ability to migrate (Radisky and LaBarge, 2008). This process plays an important role during embryonic development as well as tissue regeneration and repair in the adult (Radisky and LaBarge, 2008). We found that TGFB1 treatment caused the normally epithelial cobblestone morphology of the MOSE to change to a more scattered and elongated mesenchymal morphology. This morphological shift was accompanied by an increase in *Snail* expression and a decrease in *E-Cadherin* and *Cytokeratin 19*; in essence, the MOSE cells began to express genes seen in mesenchymal cells (*Snail*) and lost the expression of genes normally expressed in epithelial cells (*E-Cadherin, Cytokeratin 19*).

One of the most striking characteristics of mesenchymal cells is their ability to

migrate. MOSE, in culture, are relatively stationary but in response to TGFB1 they gained the ability to migrate. This increase in migration was not due to an increase in proliferation because TGFB1 inhibited MOSE proliferation. On the surface of the ovary, OSE cells undergo an EMT in response to ovulatory wounding (Auersperg et al., 2001; Salamanca et al., 2004; Ahmed et al., 2006; Gotfredson and Murdoch, 2007). Our results suggest that TGFB1, present in the follicular fluid and at the ovulatory wound site, may trigger an EMT in the MOSE surrounding the wound to facilitate their migration to repair the wound. Given that EMT can also contribute to the invasiveness of tumour cells and can increase their metastatic potential, studying this localized EMT may provide some experimental evidence for the incessant ovulation hypothesis of ovarian cancer initiation, which suggests that the process of ovulation is a risk factor for ovarian cancer (Fathalla, 1971).

Growing evidence suggests a role for EMT in the regulation of progenitor or stem cell function. In normal mammary epithelial cells, EMT, when induced by treatment with TGFB1 or the overexpression of Snail, Slug, or Twist, expands a population of cells with characteristics of both mesenchymal cells and stem cells (Mani et al., 2008; Morel et al., 2008; Guo et al., 2012; Palafox et al., 2012). Even more interesting is the observation that EMT expands the stem cell population that shares genetic markers with a breast cancer stem cell population ($CD44^{high}CD24^{low}$). Inducing EMT in breast cancer cells makes them more invasive, metastatic and increases the number of cells that have the breast cancer stem cell-associated $CD44^{high}CD24^{low}$ expression pattern (Hugo et al., 2007; Blick et al., 2010). This implies that there may be a relationship between EMT and cancer stem cells.

It was therefore interesting to find that, in addition to causing an EMT, TGFB1 can

convert SCA-1- MOSE to SCA-1+ progenitor cells (Gamwell et al., 2012). Because the EMT may create cells with a stem/progenitor cell phenotype, we examined the hypothesis that EMT was responsible and sufficient for the TGFB1-mediated increase in MOSE progenitor cells. TGFB1 has a variety of effects on cells. Depending on the context it can induce proliferation, apoptosis, cell cycle arrest or differentiation (Zavadil and Böttinger, 2005). We therefore overexpressed SNAIL in the MOSE cells as a way of inducing an EMT without activating all the additional downstream pathways that are triggered by TGFB1.

SNAIL overexpression did induce an EMT in the MOSE, but it did not exactly phenocopy the effects of TGFB1. SNAIL overexpression caused a downregulation of E-CADHERIN, similar to what was seen when the MOSE were treated with TGFB1. Cobblestone patches of MOSE stretched into elongated mesenchymal cells when SNAIL was overexpressed but the elongation was much more dramatic than was seen with TGFB1 treatment. Interestingly, SNAIL overexpressing MOSE proliferated faster than normal MOSE, which was in direct contrast to the inhibition of proliferation seen as a result of TGFB1 treatment. These differences indicate that, while SNAIL shares some critical functions associated with EMT (change in morphology, gene expression), it also has some actions in MOSE that are quite distinct from TGFB1. While it remains unclear how TGFB1 increases SNAIL expression and at the same time inhibits proliferation, it is clear that there must be other pathways activated by TGFB1 that are able to modulate the actions of SNAIL.

The differences in the effects of SNAIL overexpression and TGFB1 treatment were

also evident when measures of stemness, like SCA-1 surface expression and sphere-forming efficiency, were investigated. While TGFB1 triples the number of MOSE cells that express SCA-1, SNAIL overexpression did not alter the percentage of SCA-1+ MOSE cells. Similarly, while TGFB1 increases the population of $FS^{low}$ MOSE, SNAIL did not alter the percentage of cells with low FS, further strengthening the interpretation that there are notable differences between the effects of EMT induced by TGFB1 and SNAIL overexpression.

The differences seen in the effects of SNAIL and TGFB1 on MOSE cell morphology and proliferation may account for the inconsistency in SCA-1 expression. The EMT induced by TGFB1 is reversible, as the levels of *Snail* and *Cytokeratin 19* return to those of normal MOSE one week after TGFB1 is removed, while in MOSE infected with the pBp-SNAIL vector, SNAIL expression was high for more than four weeks. It has been proposed that the EMT can be classified into three different subtypes (Kalluri and Weinberg, 2009). The first subtype, Type 1, is the EMT that occurs during implantation, embryo formation and organ development. Fibrosis or an invasive phenotype is not associated with this type of EMT and it generates mesenchymal cells that can undergo a mesenchymal to epithelial transition to generate secondary epithelia (Kalluri and Weinberg, 2009).

The second type of EMT, Type 2, is associated with wound healing and inflammation. It generates fibroblasts and, if the inflammatory triggers are not eventually attenuated, the fibrosis can continue and eventually damage the organ. Because tissue damage and inflammation are a consequence of ovulation, and in response the MOSE adopt

a fibroblastic mesenchymal phenotype (Auersperg et al., 2001; Salamanca et al., 2004; Ahmed et al., 2006; Gotfredson and Murdoch, 2007), MOSE are presumably capable of undergoing this type of EMT.

The third type of EMT occurs in neoplastic cells and gives them the ability to invade and metastasize. Even though the three proposed types of EMT have very different functional outcomes, it is currently unclear what signals induce each of the three types or how to distinguish between them in an experimental setting. The fact that in the MOSE, EMT induced by TGFB1 and by SNAIL overexpression have very different functional outcomes (Sca-1 expression, cell size, proliferation) provides further support to the idea that there may be further subtypes of EMT, even within the context of wound repair.

Interestingly, even though cells with the ability to form spheres are more prevalent in the SCA-1+ MOSE cell fraction (Gamwell et al., 2012), SNAIL overexpression caused an increase in the number of spheres formed without increasing the fraction of SCA-1+ cells. This indicates that, while SCA-1 is as of yet the only published MOSE progenitor cell marker, there may be other pathways induced by SNAIL that increase the expression of other, as yet undiscovered, stem/progenitor markers in these cells.

## 3.6. Conclusions

Both TGFB1 and SNAIL overexpression induced an EMT in the MOSE cells, as evidenced by changes in morphology and expression of genes associated with epithelial/ mesenchymal cells. However, only TGFB1 treatment expands the SCA1+ progenitor cell population. Interestingly SNAIL overexpression increased the number of spheres formed by

the MOSE indicating that SNAIL increases the proportion of cells with stem characteristics, even though it did not alter the expression of SCA-1. These results suggest that the EMT seen in the OSE surrounding the ovulatory wound site in vivo may expand the OSE progenitor cell population through signalling pathways that include SNAIL-mediated actions in combination with other, yet to be defined, downstream effects induced by TGFB1.

## 3.7 Acknowledgments

The authors are grateful to Paul Oleynik (StemCore Laboratories, Ottawa, ON), for assisting with the flow cytometry and Dr. Doug Gray (Ottawa Hospital Research Institute, Ottawa, ON) for providing the UbGFP mice.

# CHAPTER 4: TGFB1-MEDIATED DOWNREGULATION OF BRCA1 EXPANDS THE SCA-1+ OSE PROGENITOR CELL POPULATION

Lisa F. Gamwell*[1,2], Olga Collins[1], Denise St Onge[1], Curtis McCloskey[1,2], and Barbara C. Vanderhyden[1,2,]

1. Center for Cancer Therapeutics, Ottawa Hospital Research Institute, Ottawa, ON, Canada, K1H 8L6.

2. Department of Cellular and Molecular Medicine, Faculty of Medicine, University of Ottawa, Ottawa, ON, Canada, K1H 8M5.

Formatted for submission to the journal Stem Cells.

**Contributions of Collaborators:**
Olga Collins performed some of the *Brca1* inactivation, side population analysis and gene expression analysis replicates. Denise St. Onge performed some of the *Brca1* inactivation and gene expression replicates. Curtis McCloskey performed one gene expression analysis replicate.

*While this thesis is submitted under my maiden name Turchet, this manuscript will be published under Gamwell, my married name.

## 4.1 Abstract

Ovulation is the primary non-heritable risk factor for ovarian cancer. Continuous ovulation, with its successive rounds of rupture and repair of the ovarian surface epithelium (OSE), may render the OSE susceptible to malignant transformation. In addition, deleterious germline mutations in the Breast Cancer 1, early onset (*BRCA1*) gene increase a woman's risk of developing ovarian cancer. Recently, an OSE progenitor cell population expressing Stem Cell Antigen-1 (SCA-1, also known as LY6A) has been reported. This population appears to be regulated by ovulation as factors found in the follicular fluid, including TGFB1, have been shown to increase the size of the SCA-1+ population. BRCA1 has been shown to control the size of the progenitor cell population in mammary epithelium, so we therefore hypothesized that the SCA-1 expressing OSE progenitor cell population is regulated by BRCA1. Mouse OSE with inactivated *Brca1* were more stem-like as they had twice the percentage of side population cells, and expressed higher mRNA levels of the known stem cell markers *CD44*, *CD117*, *CD133* and *Sca-1* (2.5-, 10-, 5- and 7-fold respectively) compared to OSE with functional *Brca1*. Inactivation of *Brca1* also increased by 10-fold the number of OSE cells with surface expression of SCA-1 and increased the number of cells with the ability to form spheres 4-fold. In addition, TGFB1 and SNAIL-overexpression decreased BRCA1 protein expression 3-fold and 1.7-fold respectively compared to control. These results indicate that BRCA1 functions as a stem/ progenitor cell regulator in OSE cells, as decreasing the levels of BRCA1 either by TGFB1 treatment or by direct inactivation of *Brca1*, expands the SCA-1+ OSE progenitor cell population.

## 4.2 Introduction

The surface of the ovary is covered by a single layer of epithelial cells, called the ovarian surface epithelium (OSE). When an oocyte is ovulated, the OSE cells at the site of ovulation undergo apoptosis and then OSE cells surrounding the resultant wound proliferate to close the wound (Murdoch, 1998). In addition to their role during ovulation, the OSE is thought to be one of the tissues of origin of human ovarian tumours. When premalignant structures are found in the ovary they often involve hyperplasia or invaginations of the OSE (Bell and Scully, 1994; Tonary et al., 2000).

A mouse OSE (MOSE) stem/progenitor cell population has recently been reported (Szotek et al., 2008; Gamwell et al., 2012). MOSE progenitor cells may be controlled by ovulation as the number of MOSE with progenitor cell characteristics have been found to increase after ovulation (Szotek et al., 2008). Stem Cell Antigen-1 (SCA-1, also known as LY6A) is the only surface marker identified for this progenitor cell population (Gamwell et al., 2012), although recently cell size has been proposed as a marker of both MOSE progenitor cells (Chapter 3) and OSE cells with the ability to produce oocyte-like cells (Parte et al., 2011; Virant-Klun et al., 2011; Bhartiya et al., 2012).

Transforming Growth Factor Beta 1 (TGFB1) expands the SCA-1 expressing (SCA-1+) progenitor cell population in MOSE. TGFB1 is a growth factor found in many tissues, including ovarian follicular fluid (Fried and Wramsby, 1998; Fried et al., 1998; Ouellette et al., 2005; Knight and Glister, 2006; Gamwell et al., 2012) and is therefore present at the ovulatory wound site. When exposed to TGFB1, MOSE assume a more progenitor-like phenotype, as seen by an increase in sphere formation (Gamwell et al.,

2012). This growth factor also expands the SCA-1+ progenitor cell population by converting cells that do not exhibit surface expression of SCA-1 (SCA-1-) into SCA-1+ cells (Gamwell et al., 2012), although the mechanism by which this conversion takes place is unknown.

Ovulation is the primary non-heritable risk factor for ovarian cancer (Fleming et al., 2006). The incessant ovulation hypothesis proposes that continuous ovulation, with its successive rounds of OSE rupture and repair, renders the OSE susceptible to malignant transformation (Fathalla, 1971; Fleming et al., 2006). Support for this hypothesis comes from the observation that intensive egg-laying hens frequently develop ovarian carcinomas (Fredrickson, 1987; Barua et al., 2009). Epidemiological studies indicate that circumstances that decrease the number of ovulations, i.e., pregnancy, use of oral contraceptives, duration of lactation and early menopause, substantially reduce ovarian cancer risk (reviewed in Fleming et al., 2006). Furthermore, although still controversial, some investigators have found an increased risk of ovarian cancer among women treated with ovulation induction drugs in assisted reproduction programs (van Leeuwen et al., 2011).

The risk generated by incessant ovulation may be associated with the formation of inclusion cysts that can develop as a result of the process of ovulation and the pinching off of deep epithelial clefts on the surface of the ovary (Fleming et al., 2006). In mice, repeated rounds of ovulation are associated with a marked increase in MOSE invaginations, stratification and inclusion cysts (Tan et al., 2005; Burdette et al., 2007). Because ovulation and factors in the follicular fluid, such as TGFB1, have been shown to expand the progenitor cell population in the MOSE (Szotek et al., 2008; Gamwell et al., 2012),

understanding the consequence of ovulation on the OSE progenitor cell population may provide insight into the aetiology of ovarian cancer.

The lifetime risk of developing ovarian cancer for women in the general population is 1 in 70 (Weberpals et al., 2008). In women with deleterious germline mutations in the Breast Cancer 1, early onset (*BRCA1*) gene, that risk increases to 1 in 7 (Weberpals et al., 2008). While *BRCA1* mutations occur in only 5-10% of ovarian cancer patients, in 40-72% of ovarian cancers, BRCA1 is rendered dysfunctional through hypermethylation, loss of heterozygosity, or haploinsufficiency (Weberpals et al., 2008). Therefore BRCA1 dysfunction is seen in both hereditary and sporadic forms of ovarian cancer. Although BRCA1 has been implicated in regulating a wide variety of cellular functions, the specific mechanisms by which BRCA1 mutation or dysfunction lead to ovarian cancer remains unexplained.

BRCA1 was originally proposed to function as a breast stem cell regulator by Foulkes (2004). BRCA1 knockdown in mammary epithelial cells leads to an increase in the fraction of cells displaying stem cell markers (Furuta et al., 2005; Liu et al., 2008; Lim et al., 2009; Proia et al., 2011), suggesting that loss of BRCA1 function enhances mammary stem cell characteristics. Current evidence suggests that loss of BRCA1 in mammary tissue may result in the accumulation of genetically unstable breast stem cells, providing prime targets for further carcinogenic events (Furuta et al., 2005; Liu et al., 2008; Lim et al., 2009; Proia et al., 2011). The role of BRCA1 in the regulation of stem cells in other epithelial tissues, like the MOSE, has not yet been investigated. We explored the possibility that loss of BRCA1 in MOSE cells has an impact on the size of the MOSE progenitor cell

compartment and investigated the mechanism by which BRCA1 expression may be regulated in the MOSE.

## 4.3 Materials and Methods

*MOSE Isolation And Culture*

*Brca1*$^{loxP/loxP}$ [FVB;129-*Brca1*$^{tm2Brn}$] mice, bearing loxP sites in introns 4 and 13 of the *Brca1* gene were generously provided by Dr. Anton Berns through the Mouse Models of Human Cancers Consortium Mouse Repository (National Cancer Institute, Frederick, MD) and their use has been previously described (Clark-Knowles et al., 2007; Clark-Knowles et al., 2009). FVB/N mice (Jackson Laboratory, Bar Harbor, ME) were used as non-transgenic controls. All animal experiments described in this study were performed according to the Guidelines for the Care and Use of Animals established by the Canadian Council on Animal Care with protocols approved by the University of Ottawa Animal Care Committee.

MOSE cells were isolated from both strains and cultured as previously described (Gamwell et al., 2012). Briefly, MOSE cells were isolated from 6-week-old female mice using gentle trypsinization (0.25% Trypsin/PBS 0.5 ml/ovary; Invitrogen). For each primary culture, 10–20 mice were used. MOSE were grown in 'MOSE media' and maintained on tissue-culture plates (Becton-Dickinson, Mississauga, ON) as described (Gamwell et al., 2012). All in vitro MOSE experiments were carried out at least three times using a minimum of two different isolations of MOSE cells with a passage number of less than 20.

In addition to MOSE from *Brca1*$^{loxP/loxP}$ and FVB/N mice, MOSE that overexpress

the transcription factor SNAIL (referred to as pBp-SNAIL) and the corresponding vector control (referred to as pLPCX) were used (Chapter 3). The production of these MOSE lines has been previously described (Chapter 3). Briefly, after Maloney-based rotroviruses were produced by cotransfection of 293T/17 cells (American Type Culture Collection, Manassas, VA) with the pBp-SNAIL or pLPX vectors (AddGene, Cambridge, MA and ClonTech, Mountain View, CA , respectively) along with pHIT60, a CMV-driven gag-pol expression plasmid (Soneoka et al., 1995) and pHIT123, a CMV-driven ecotropic env expression plasmid (Soneoka et al., 1995), virus was harvested used to infect two different MOSE primary cultures (200,000 cells). Infections were carried out in duplicate and following infection, cells were selected with 4 μg/ml puromycin. The infected MOSE lines are referred to as pLPCX (vector control, 4 lines total) and pBp-SNAIL (4 lines total).

To test the effects of TGFB1 on RNA and protein expression, MOSE were treated with TGFB1 (10 ng/mL; human TGFB1, Sigma-Aldrich, Oakville, ON) for 7 days as previously described (Gamwell et al., 2012) prior to isolation of RNA and protein.

*Adenovirus Administration*

Recombinant adenoviruses Ad5CMVeGFP (AdGFP) and Ad5CMVCre (AdCre) (Vector Development Laboratory, Houston, TX) were used to express green fluorescent protein (GFP) in the MOSE as a control (AdGFP) or to express Cre Recombinase to excise the portion of the *Brca1* gene between the loxP sites (AdCre). For in vitro infections, 500,000 MOSE cells were infected following an established protocol (Flesken-Nikitin et al., 2003; Clark-Knowles et al., 2007). All experiments were initiated following replating of

the cells 72 h after adenoviral infection.

*DNA Extraction And Detection Of Recombination*

DNA extraction buffer (50 mM KCl, 10 mM Tris–HCl, 2 mM MgCl2, 0.1 mg/ml gelatin, 0.45% Nonidet, and 0.45% Tween-20) containing 40 μg/ml proteinase K (Roche, Mississauga, ON) was added to cells and incubated at 58°C overnight. DNA was precipitated using a standard protocol using saturated NaCl and isopropanol. The DNA pellet was washed with 75% ethanol, air dried, and resuspended in Tris– EDTA (50 mM, pH 6.8).

Cre-mediated excision of exons 5–13 (referred to as $Brca1^{\Delta 5-13}$) was detected by PCR amplification using primers that bind within intron 4 and intron 13. Amplification using primers that bind in intron 4 [Brca1int4fwd (5′ TAT CAC CAC TGA ATC TCT ACC G 3′)] and intron 13 [Brca1int13rev (5′ TCC ATA GCA TCT CCT TCT AAA C 3′)] yields a 600 bp product when recombination has occurred, or no product when recombination has not occurred. Detection of any remaining unrecombined sequence following Cre exposure was performed using primers for exon 11 of Brca1, yielding a 592 bp product (Clark-Knowles et al., 2007).

*Flow Cytometric Analysis*

The percentage of MOSE that fall within the side population (SP) was determined by flow cytometry as previously described (Gamwell et al., 2012). The percentage of cells that exhibit surface expression of SCA-1 was determined using antibodies against SCA-1

and procedures as described in Gamwell et al. (2012).

*Gene Expression Analysis*

RNA was extracted, cDNA was made and gene expression was determined by relative Quantitative PCR (Q-PCR) as previously described (Gamwell et al., 2012). Primers against *CD44*, *CD133*, *CD117*, *Brca1* and *Ppia* (endogenous control) are provided in Table 4.1. Primers against *Sca-1* were described in (Gamwell et al., 2012).

*Western Blot Analysis*

Protein was isolated as described in (Chapter 3). Lysates (60 ng) were run on precast NuPAGE 4-12% Bis-Tris gels (Invitrogen, Burlington, ON) and transferred to Immobilon-P membranes (Millipore, Billerica, MA). All blots were blocked with 5% milk in Tris buffered saline with 0.05% Tween 20 (TBST) for at least 1 hour at room temperature. Antibodies against SNAIL (1:200, Ab82846, AbCam, Toronto, ON), BRCA1 (2 μg/ml, MAB22101, R&D Systems, Burlington, ON) and GAPDH (1:80,000, Ab8245, AbCam) were used. For primary antibodies raised in mice, a rabbit anti-mouse secondary antibody was used (BRCA1 and GAPDH, 1:20,000; Ab6728, Abcam). For primary antibodies raised in rabbits (SNAIL), a donkey anti-rabbit secondary antibody was used (1:10,000, 711-035-152, Cedarlane, Burlington, ON). Both primary and secondary antibodies were diluted in 5% milk in TBST and incubated with the membranes for 1 hour at room temperature. Detection was performed with ECL Plus (GE LifeSciences, Baie d'Urfe, PQ) following the manufacturer's protocol. Images were taken using a DE500

**Table 4.1:** Primer Sequences

| Gene | Forward Primer (5'-3') | Reverse Primer (5'-3') |
|---|---|---|
| *Brca1* | GCT GCA GCT GTG TGG GGG CTT | CCC GAC ACC GGT AGC TGG AT |
| *CD44* | TCC TTC TTT ATC CGG AGC AC | CTC CAT GTA ATG TAG AGA AGT TCT GAG |
| *CD117* | GAT CTG CTC TGC GTC CTG TT | CTT GCA GAT GGC TGA GAC G |
| *CD133* | GAA GGA GCC CAG CTT AGA GG | GGT CAT TCA CTC AAA GTA CCA TCC |
| *Ppia* | AGG GTG GTG ACT TTA CAC GC | GAT GCC AGG ACC TGT ATG CT |

MultiImage FC Light Cabinet and were analyzed using AlphaEase FC (both from Alpha Innotech Corporation, Johannesburg, SA).

*Sphere Formation*

The ability of *Brca1*$^{loxP/loxP}$ and *Brca1*$^{\Delta 5\text{-}13}$ MOSE to form spheres was assessed following the procedures described in Gamwell et al. (2012). Briefly MOSE cells were suspended as single cells in a 1:1 mixture of methylcellulose (to prevent cell aggregation) and progenitor cell media (Gamwell et al., 2012) at a density of 20,000 cells/ml per well of a 12-well tissue culture plate. The bottom of each well was coated with a thin layer of 1% agarose in progenitor cell media to prevent the cells from adhering to the bottom of the culture plate. Sphere formation was monitored using a dissecting microscope, and spheres were counted with the aid of a grid placed under the culture dish.

*Statistical Analyses*

A Student t-test was used to determine statistical significance ($P<0.05$). Error bars indicate the SEM.

## 4.4 Results

*The Percentage Of Cells In The Side Population (SP) Increases When Brca1 Is Inactivated*

When *Brca1*$^{loxP/loxP}$ MOSE were infected with AdCre, Cre recombinase was expressed in the cells and mediated the excision of the regions of the *Brca1* gene flanked by the loxP sites found in intron 4 and 13 (Clark-Knowles et al., 2007). This recombination

was detected by the production of a 600 bp PCR product when primers that bind within the 4th and 13th introns of *Brca1* were used (Fig. 4.1, $Brca1^{\Delta 5\text{-}13}$, recombined). Any unrecombined DNA produced a 592 bp band when primers that bind within exon 11 were used (Figure 4.1, $Brca1^{\Delta 5\text{-}13}$, unrecombined). When $Brca1^{loxP/loxP}$ MOSE were infected with AdGFP, which encodes for GFP rather than Cre recombinase, the DNA is not recombined and a PCR product is detected only with exon 11 primers. The primers for intron 4 and intron 13 bind too far apart on the intact gene for amplification to occur (Fig. 4.1).

MOSE progenitor cells have been shown to be enriched in the SP identified by flow cytometry (Szotek et al., 2008; Gamwell et al., 2012). The SP phenotype is based on the exclusion of the DNA-binding dye Hoechst 33342 (Challen and Little, 2006) and has been used extensively to enrich for stem/progenitor-like cells in both normal and cancerous tissues (Goodell et al., 1996; Wulf et al., 2001; Preffer et al., 2002; Welm et al., 2002; Al-Hajj et al., 2003; Bhatt et al., 2003; Jonker et al., 2005; Haraguchi et al., 2006; Szotek et al., 2006; Ono et al., 2007; Szotek et al., 2008; Hosonuma et al., 2011; Gamwell et al., 2012). Because BRCA1 has been shown to control the size of the progenitor cell population in the mammary gland (Furuta et al., 2005; Liu et al., 2008; Lim et al., 2009; Proia et al., 2011), we determined whether inactivation of *Brca1* in MOSE cells increased the size of the SP. Inactivation of *Brca1* caused a significant, 2-fold increase in the percentage of MOSE that fall within the SP gate (Fig. 4.2 A,B). This indicates that inactivation of *Brca1* may increase the proportion of cells with stem/progenitor cell characteristics.

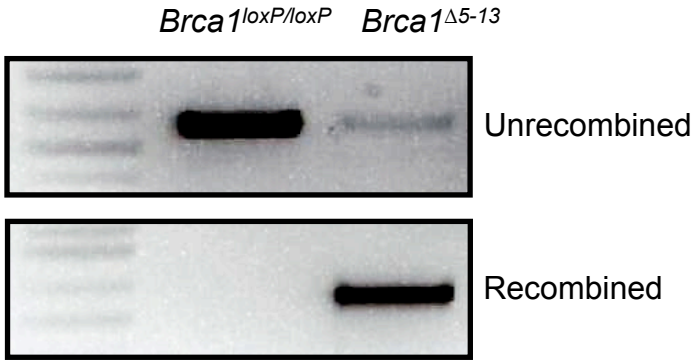


**Figure 4.1: Recombination at loxP sites in the *Brca1* gene.** PCR of genomic DNA extracted from *Brca1*$^{loxP/loxP}$ MOSE cells infected with AdGFP (*Brca1*$^{loxP/loxP}$) or AdCre (*Brca1*$^{\Delta 5\text{-}13}$) to detect recombination at loxP sites within the *Brca1* gene.

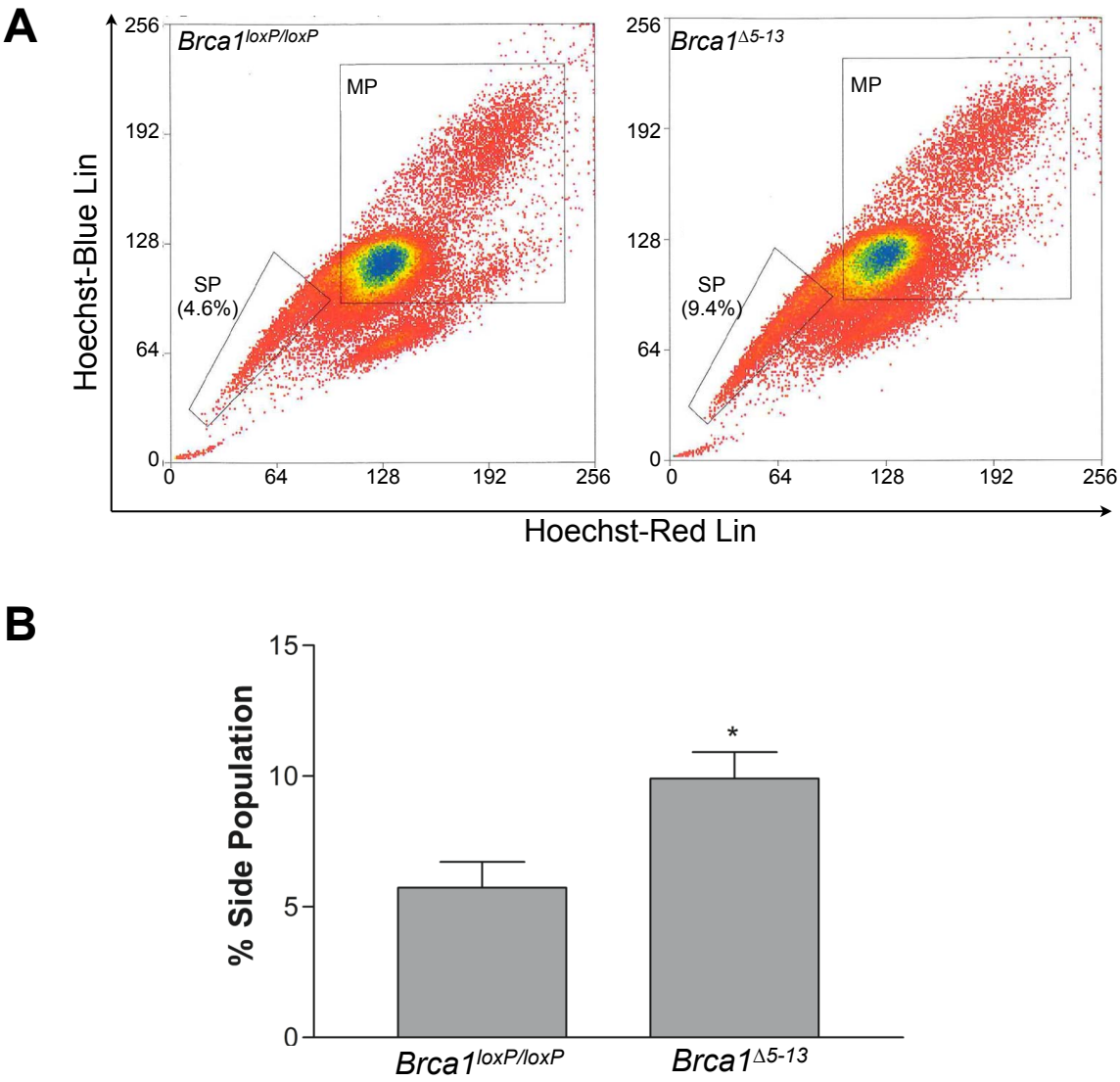


**Figure 4.2: Inactivation of *Brca1* increases the size of the side population. A:** Representative flow cytometry profile of *Brca1*$^{loxP/loxP}$ (control) MOSE or *Brca1*$^{\Delta 5\text{-}13}$ (inactivated *Brca1*) MOSE after staining with Hoechst 33342 dye. SP indicates the side population and MP indicates the main population; the same gates were used for cells with and without BRCA expression. **B:** Graphical representation of the average percentage of side population cells in *Brca1*$^{loxP/loxP}$ and *Brca1*$^{\Delta 5\text{-}13}$ MOSE. * indicates $p<0.05$ compared to control.

*Inactivation Of Brca1 Increases The Expression Of The Stem Cell Markers CD44, CD117, CD133 And Sca-1*

Because inactivation of *Brca1* increased the proportion of cells within the SP, we next determined whether loss of BRCA1 increased the expression of the known stem/ progenitor cell markers CD44, CD117, CD113 and SCA-1. CD44, CD117 and CD133 are stem cell markers in a variety of tissues and are also ovarian cancer stem cell markers (Zhang et al., 2008; Meirelles et al., 2012; Steg et al., 2012) and SCA-1 is a MOSE progenitor cell marker (Gamwell et al., 2012) and is also a marker of progenitor cells in the hematopoietic system, mammary gland, bone, prostate, skeletal muscle, heart, dermis, liver and lung.

Q-PCR measurement of the mRNA levels of *CD44*, *CD117*, *CD133* and *Sca-1* in $Brca1^{loxP/loxP}$ and $Brca1^{\Delta 5\text{-}13}$ MOSE showed that inactivation of *Brca1* significantly increased the mRNA levels of all these stem cell markers compared to control (Fig. 4.3, *CD44*: 3-fold, *CD117*: 10-fold, *CD133*: 5-fold, *Sca-1*: 7-fold).

*Inactivation Of Brca1 Expands The MOSE Progenitor Cell Fraction*

SCA-1 surface expression defines a population of MOSE progenitor cells that are regulated by factors found in the follicular fluid (Gamwell et al., 2012). Because inactivation of *Brca1* caused an increase in the mRNA levels of *Sca-1*, we next determined the effect of *Brca1* inactivation on surface expression of SCA-1 using flow cytometry. MOSE with inactivated *Brca1* exhibited a 10-fold increase in the percentage of cells that express SCA-1 as compared to MOSE with intact *Brca1* (Fig. 4.4A, N=1).

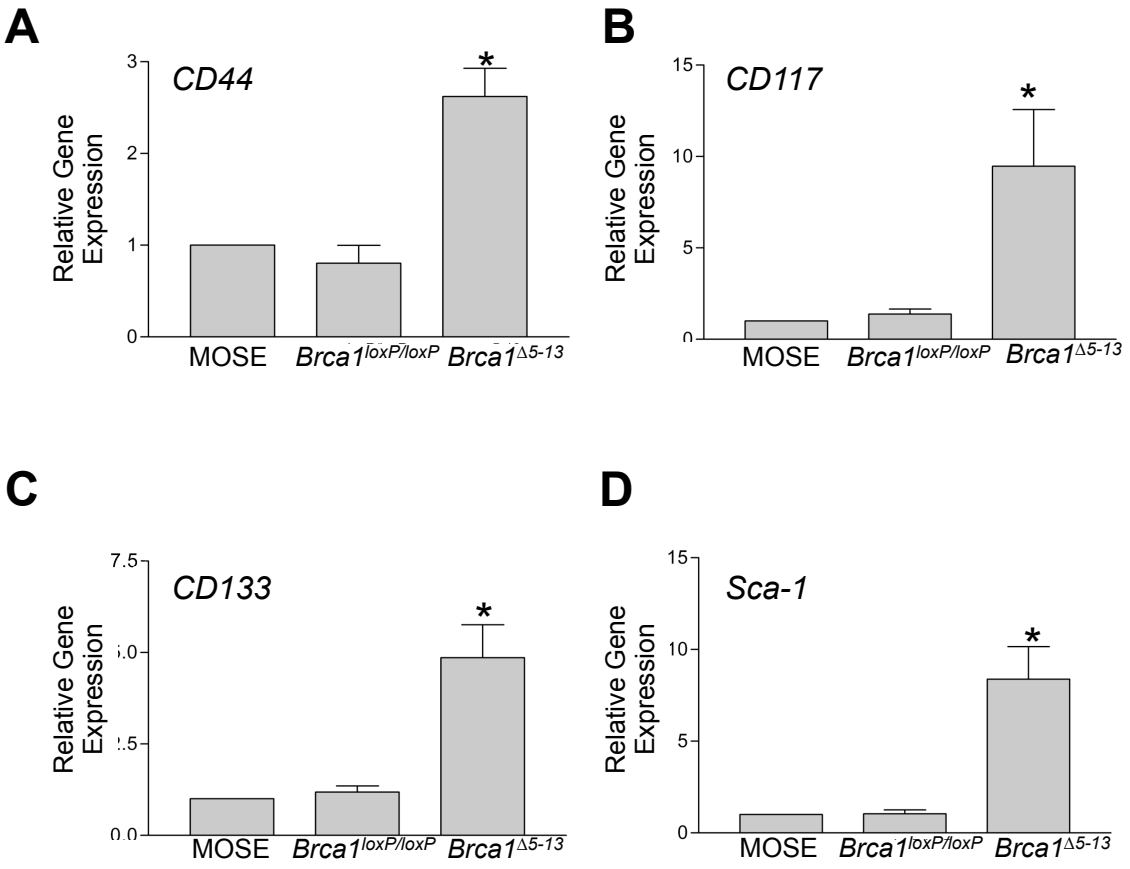


**Figure 4.3: Stem cell marker gene expression analysis in MOSE with inactivated *Brca1*. A-D:**Relative expression of *CD44* (A), *CD117* (B), *CD133* (C), and *Sca-1* (D) mRNA levels in $Brca1^{loxP/loxP}$ MOSE infected with AdGFP ($Brca1^{loxP/loxP}$) or AdCre to inactivate *Brca1* ($Brca1^{\Delta 5\text{-}13}$). mRNA levels are relative to non-transgenic MOSE (MOSE). *indicates $p<0.05$ compared to $Brca1^{loxP/loxP}$.

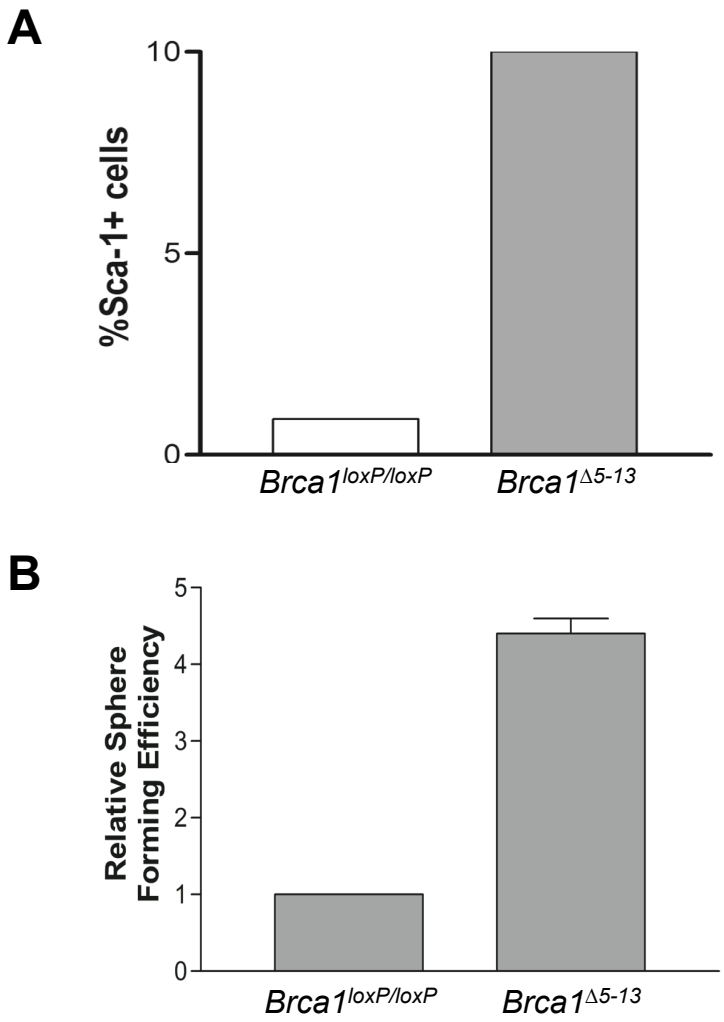


**Figure 4.4: The effect of *Brca1* inactivation on SCA-1 surface expression and sphere formation. A:** Flow cytometric analysis for SCA-1 surface expression in $Brca1^{loxPloxP}$ MOSE and $Brca1^{\Delta 5\text{-}13}$ MOSE (*Brca1* inactivated) (N=1). **B:** The sphere forming efficiency of $Brca1^{\Delta 5\text{-}13}$ MOSE relative to $Brca1^{loxPloxP}$ MOSE. Spheres formed from single cells after 1 week in methylcellulose (N=2).

The capacity for sphere formation has been used to indicate the presence of cells with stem/progenitor cell characteristics in a variety of tissues, including in the MOSE (Reynolds and Weiss, 1996; Weiss et al., 1996; Dontu et al., 2003; Woodward et al., 2005; Liao et al., 2007; Gamwell et al., 2012). In fact, the SCA-1+ MOSE population is enriched with cells with the ability to form spheres (Gamwell et al., 2012). We therefore tested whether the increase in the percentage of SCA-1+ MOSE caused by *Brca1* inactivation resulted in an increase in the number of MOSE that could form spheres. $Brca1^{\Delta 5\text{-}13}$ MOSE formed 4 times more spheres than $Brca1^{loxP/loxP}$ MOSE, which indicates that inactivation of *Brca1* expression may cause an increase in the number of cells with stem-like characteristics.

*TGFB1 Decreases Brca1 mRNA And Protein Expression*

When MOSE are treated with TGFB1, the number of cells with progenitor cell characteristics increases (Gamwell et al., 2012). TGFB1 causes more MOSE to present SCA-1 on their cell surface and a higher proportion MOSE to form spheres (Gamwell et al., 2012). Because inactivating *Brca1* mimics the increase in SCA-1 expression and sphere formation seen when MOSE are treated with TGFB1, we determined whether TGFB1 mediates its effects by decreasing *Brca1* expression. We found that MOSE treated with TGFB1 (10 ng/mL, 7 days), had significantly lower levels of *Brca1* mRNA (Fig. 4.5A) and BRCA1 protein (Fig. 4.5B, C) as seen by Q-PCR and western blot, respectively. TGFB1 caused a 3-fold decrease in both the mRNA and protein levels of BRCA1, indicating that TGFB1 regulates the expression of BRCA1 either directly or indirectly.

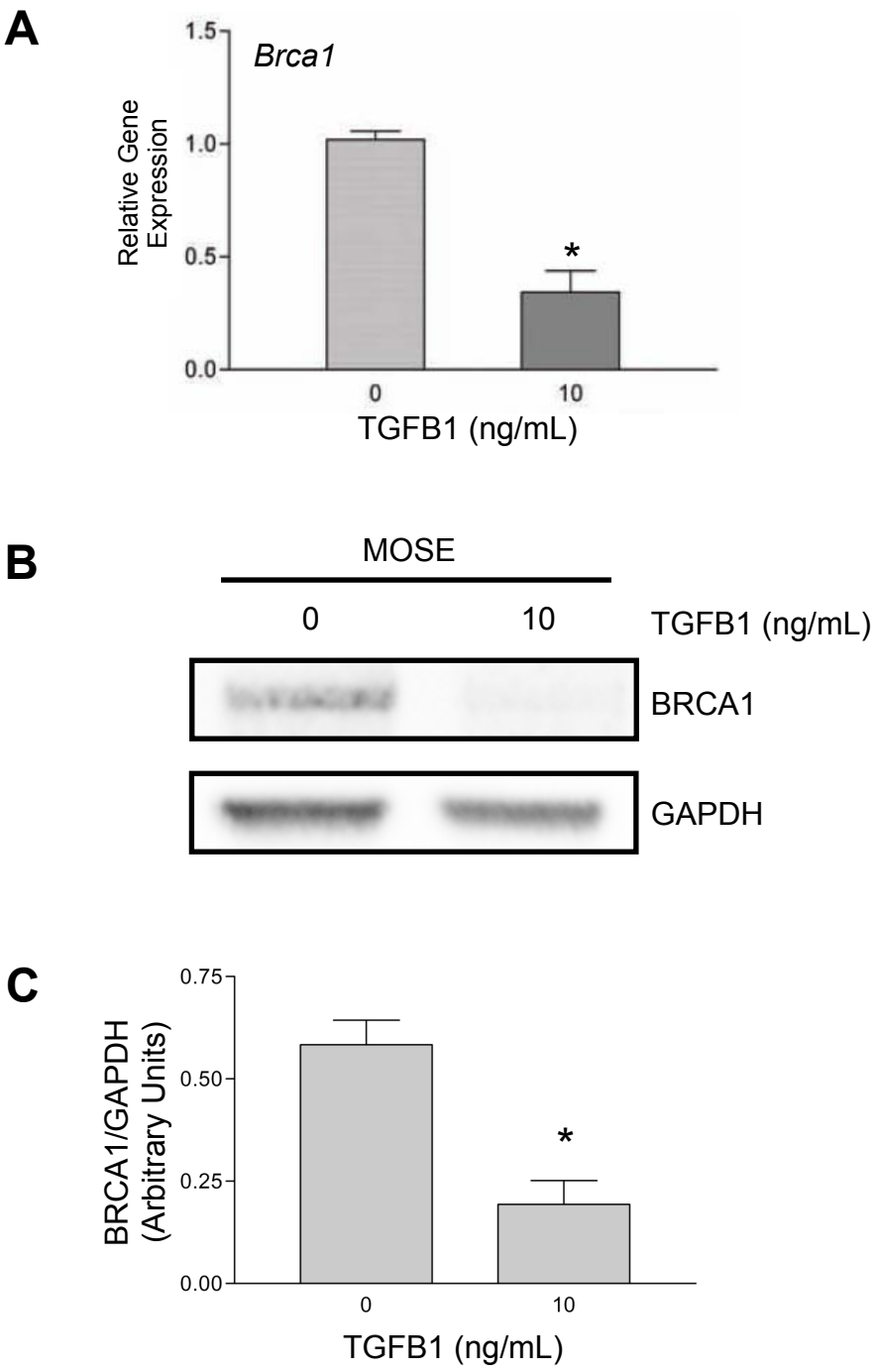


**Figure 4.5: The effect of TGFB1 on BRCA1 mRNA and protein expression. A:** Q-PCR analysis of *Brca1* mRNA levels of MOSE treated with 0 or 10 ng/mL of TGFB1 for 7 days. **B:** Western blot analysis of expression of BRCA1 in MOSE treated with TGFB1 (10 ng/mL, 7 days) and control MOSE. GAPDH was used as a loading control. **C:** Densitometric analysis of three Western blots indicative of that shown in B. * indicates $p < 0.05$ compared to control.

*SNAIL Overexpression Decreases BRCA1 Expression*

TGFB1 can affect a variety of cellular processes including differentiation, proliferation, apoptosis and cellular homeostasis (Kalluri and Weinberg, 2009). It can also cause epithelial cells to adopt a mesenchymal phenotype, termed the epithelial-to-mesenchymal transition (Lee et al., 2006). In the MOSE, TGFB1 induces an EMT, characterized by a shift from an epithelial morphology to a mesenchymal phenotype coupled with an increase in SNAIL expression and a decrease in E-CADHERIN and CK19 expression (Chapter 3).

MOSE that overexpress SNAIL (pBp-SNAIL MOSE) no longer behave as epithelial cells but resemble mesenchymal cells in their morphology and gene expression (Chapter 3). These cells have been previously described (Chapter 3) and are a useful tool to study EMT in isolation of the other effects of TGFB1. We therefore determined whether overexpressing SNAIL caused a decrease in BRCA1 expression by comparing, by western blot, the abundance of BRCA1 protein in pBp-SNAIL MOSE to the vector control pLPCX MOSE. SNAIL overexpression significantly decreased BRCA1 protein 1.7 fold (Fig. 4.6A,B) which suggests that TGFB1 may reduce BRCA1 expression through pathways associated with EMT.

## 4.5 Discussion

We have shown that TGFB1 and SNAIL have the ability to decrease the expression of the potent tumour suppressor BRCA1 in ovarian surface epithelial cells. Furthermore, the consequence of this downregulation, besides the obvious loss of the normal tumour

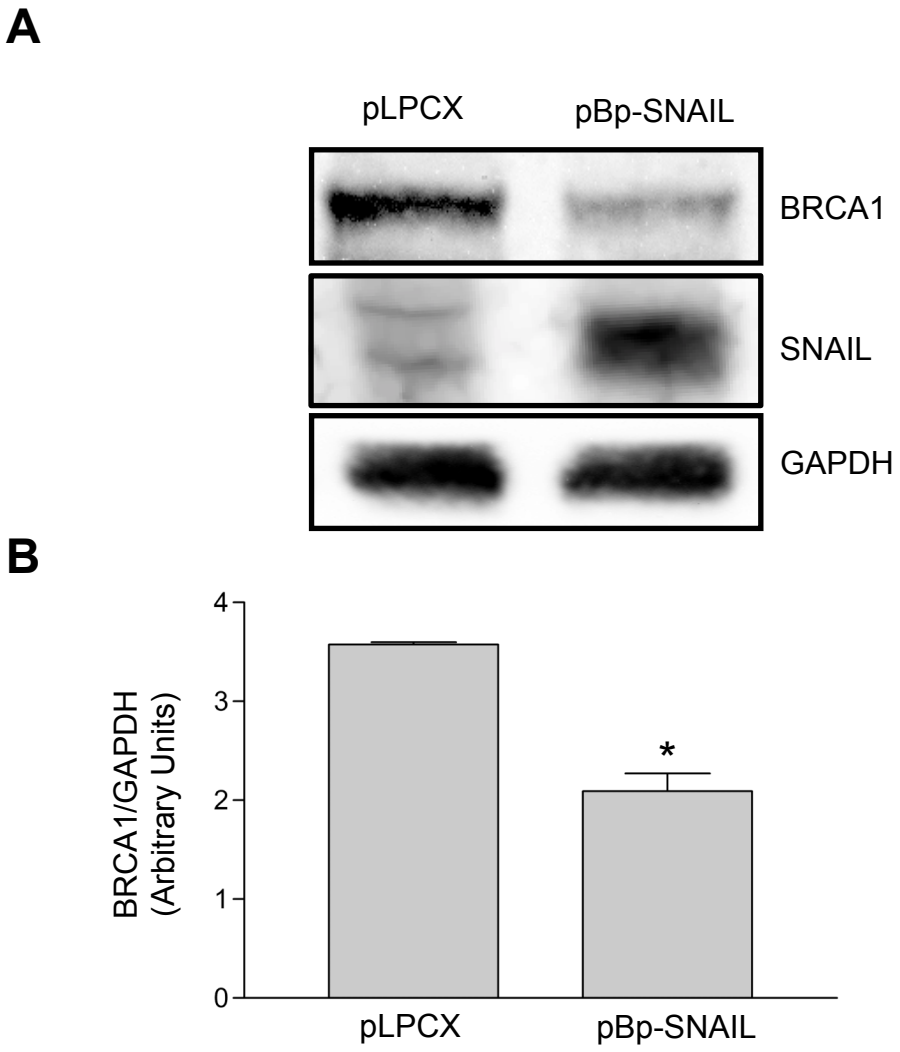


**Figure 4.6: BRCA1 expression in MOSE that overexpress SNAIL A:** Western blot analysis of expression of BRCA1 in MOSE that overexpress SNAIL (pBp-SNAIL) and control MOSE (pLPCX). GAPDH is used as a loading control. **C:** Densitometric analysis of three Western blots indicative of that shown in B. * indicates $p < 0.05$ compared to control.

suppressor function of BRCA1, is an increase in the expression of genes associated with the ovarian cancer stem cell phenotype in the MOSE. In addition, inactivation of *Brca1* resulted in an expansion of the SCA-1+ MOSE progenitor cell population.

To our knowledge, this is the first report that BRCA1 regulates the SP phenotype. SP cells are able to pump out Hoechst dye due to their relatively high level of expression of drug transporters like the ATP-binding cassette (ABC) transporter ABCG2/BCRP1 (breast cancer-resistance protein-1) (Challen and Little, 2006). SP cells have been found in several tissues and cell lines including in the MOSE (Szotek et al., 2008; Gamwell et al., 2012). In the MOSE, the SP is enriched with stem/progenitor-like cells (Gamwell et al., 2012; Szotek et al., 2008). In addition, cancer stem-like cells have been found to be enriched in the SP in a variety of carcinomas including ovarian cancer (Szotek et al., 2006; Hu et al., 2010). The ability of BRCA1 to regulate the size of the SP has implications in both the normal ovary and in ovarian cancer.

In addition to increasing the proportion of cells that have the ability to efflux Hoechst dye, *Brca1* inactivation increased the expression of the ovarian cancer stem cell markers *CD117*, *CD133* and *CD44* (Zhang et al., 2008; Baba et al., 2009; Kusumbe et al., 2009; Meirelles et al., 2012). All three have been proposed to identify ovarian cancer cells that exhibit tumour initiating or cancer stem cell properties. In addition, in the mammary gland and breast cancer cell lines, expression of CD44, CD113 and CD117 has been shown to be controlled by BRCA1 (Furuta et al., 2005; Wright et al., 2008b; Lim et al., 2009; Proia et al., 2011). Our findings that *Brca1* inactivation increases the mRNA levels of these cancer stem cell markers indicates that, similar to what is seen in the breast, BRCA1

controls the size of the MOSE progenitor cell population. Flow cytometric analysis would allow us to determine if *Brca1* inactivation causes an increase in the proportion of MOSE that express the markers, rather than an overall increase in expression.

Human OSE normally do not express CD117 (KIT) unless the OSE are located within preneoplastic lesions like invaginations or inclusion cysts (Tonary et al., 2000). Similarly, a very small percentage of CD117-expressing MOSE can be identified using magnet-assisted cell sorting (Gamwell et al., 2012). The incidence of preneoplastic lesions is increased in mice in which *Brca1* has been inactivated in the MOSE (Clark-Knowles et al., 2007). These inclusions cysts and invaginations are found more frequently in the ovaries of women considered to be at an increased risk for developing ovarian cancer, which includes those with germline *Brca1* mutations (Salazar et al., 1996; Werness et al., 1999; Schlosshauer et al., 2003; Finch et al., 2006). Our results suggest that inactivation of *Brca1* in the MOSE may not only cause an increase in the incidence of preneoplastic lesions (Clark-Knowles et al., 2007), but may also increase the expression of the ovarian cancer stem cell marker CD117.

*Brca1* inactivation caused an increase in *Sca-1* mRNA levels, the number of SCA-1+ MOSE, and the number of MOSE with the ability to form spheres. These results provide further support for the hypothesis that BRCA1 can act as a stem cell regulator (Foulkes, 2004) and show, for the first time, that BRCA1 may regulate progenitor cell populations in other epithelia in the body, notably in ovarian epithelial cells.

*Brca1* inactivation mimicked the effect of TGFB1 on the size of the MOSE progenitor cell population that we have previously reported (Gamwell et al., 2012). We

therefore hypothesized that TGFB1 expands the MOSE progenitor cell population by downregulating BRCA1. TGFB1 is present in the follicular fluid at ovulation and expands the SCA-1+ MOSE progenitor cell population, in part by converting SCA-1- MOSE into SCA-1+ MOSE (Gamwell et al., 2012). TGFB1 caused a decrease in both BRCA1 mRNA and protein, which indicates that in the MOSE, TGFB1 may exert its effects on the progenitor cell population through the downregulation of BRCA1. In fact, inactivating *Brca1* is sufficient to mimic all the observed effects of TGFB1 on SCA-1 expression and sphere formation.

TGFB1 has previously been shown to downregulate *Brca1* mRNA in mammary epithelial cells (Gudas et al., 1996). In this study, the levels of *Brca1* mRNA were linked to the cell cycle. Exponentially dividing cells were found to express the most *Brca1* while senescent cells expressed almost undetectable amounts. These authors proposed that TGFB1 decreased *Brca1* because it caused the cells to senesce (Gudas et al., 1996). Other groups have confirmed that *Brca1* mRNA levels are controlled by the cell cycle and have shown that TGFB1 inhibits *Brca1* mRNA expression through an Rb-dependent pathway (Satterwhite et al., 2000). In that context, our findings that TGFB1 decreases BRCA1 mRNA and protein in MOSE agree with the results of these studies, as TGFB1 also decreases the proliferation rate of the MOSE (Gamwell et al., 2012).

In addition to its effects on the SCA-1+ MOSE population and proliferation, TGFB1 induces an EMT in the MOSE that coincides with an increase in SNAIL expression (Gamwell et al., 2012). Interestingly, unlike TGFB1 treated MOSE, SNAIL overexpressing MOSE have an increased proliferation rate compared to control MOSE (Chapter 3). The

finding in this study that SNAIL-overexpressing MOSE had a lower level of BRCA1 protein expression, despite a higher proliferation rate, goes against the long standing concept that *Brca1* expression is higher in rapidly proliferating cells (Gudas et al., 1996) and suggests that the inverse association between cell cycle progression and BRCA1 expression is not universal.

Recently, SNAIL has been shown to decrease BRCA1 expression in mammary epithelial cells by recruiting the chromatin demethylase, LSD1, and binding to the BRCA1 promoter (Wu et al., 2012). Instead of TGFB1, members of the Wnt pathway were proposed to be the cause of the upregulation of SNAIL protein. We have shown that TGFB1 caused a significant upregulation of SNAIL expression in the MOSE (Gamwell et al., 2012) and that SNAIL was sufficient to cause the decrease in BRCA1 expression seen when MOSE were treated with TGFB1. Our results therefore indicate that a similar pathway could be responsible for controlling *Brca1* expression in the MOSE. Should TGFB1 be shown to reduce BRCA1 expression in the MOSE by altering the methylation of histones in the *Brca1* promoter, it would provide a mechanism by which BRCA1 may be rendered dysfunctional, a characteristic seen in the majority of sporadic ovarian cancers (Weberpals et al., 2008).

Our finding that TGFB1 and SNAIL, which have been shown to cause an EMT in the MOSE (Chapter 3), decrease BRCA1 expression provides preliminary experimental evidence in support of ovulation is a risk factor for ovarian cancer (Fathalla, 1971). Perhaps the EMT induced by ovulation in the MOSE surrounding the wound site causes a decrease in BRCA1 expression. The decreased BRCA1 expression would impair the ability of the

MOSE to repair double stranded DNA breaks which could accumulate in the MOSE when they proliferate to close the ovulatory wound (Burdette et al., 2006) or when they are exposed to reactive oxygen species and inflammatory molecules as a consequence of the ovulatory wound (Murdoch and Martinchick, 2004). The accumulation of DNA damage could then result in the oncogenic transformation of the MOSE. Comparing the expression of BRCA1 in MOSE adjacent to ovulatory wounds sites to those distal to the ovulatory wound would confirm that this relationship between ovulation-induced EMT and BRCA1 expression occurs in vivo.

## 4.6. Conclusions

This work has shown, for the first time, that BRCA1 acts as a stem cell regulator in ovarian epithelial cells. Both TGFB1 and SNAIL, which induce an EMT in the MOSE (Chapter 3), decreased the expression of BRCA1, which suggests that the EMT observed in the OSE at the time of ovulation (Salamanca et al., 2004; Ahmed et al., 2006; Gotfredson and Murdoch, 2007), may result in a decrease in BRCA1 expression. As a result, this study identifies a potential link between the incessant ovulation hypothesis and the BRCA1 dysfunction that is associated with the majority of sporadic ovarian cancers. Further investigations into the consequence of ovulation on the OSE may strengthen this link and further our understanding of the initiating events of this devastating disease.

## 4.7 Acknowledgments

The authors are grateful to Paul Oleynik and Caroline Vergette (StemCore Laboratories,

Ottawa, ON), for assisting with the flow cytometry.

# CHAPTER 5: GENERAL DISCUSSION

The focus of this thesis was to first identify and then characterize a putative stem or progenitor cell population in the OSE. Here we summarize the major findings of this thesis and then discuss our findings in the context of ovulatory wound healing and explore whether our results support the existence of a multipotent or a unipotent progenitor cell in the OSE. We will also discuss whether our findings support the hypothesis that new oocytes can be made in the adult ovary and finally discuss the implications of our results in the initiation of sporadic and hereditary EOC.

## 5.1 Summary of Findings

We have identified a population of SCA-1+ MOSE cells that display progenitor cell activity. We have demonstrated that the behaviour of these putative MOSE progenitor cells is regulated by TGFB1 and LIF, indicating that they may play a role in ovulatory wound healing. Specifically TGFB1 increased the proportion of SCA-1+ cells by converting SCA-1- cells into SCA-1+ cells while LIF induced proliferation in the SCA-1+ and SCA-1- MOSE populations.

Exposure to TGFB1 caused MOSE cells to undergo an EMT as seen by a decrease in the expression of epithelial markers, an increase in the expression of mesenchymal markers, the adoption of a mesenchymal morphology and the acquisition of the ability to migrate. In comparison, SNAIL overexpression induced an EMT in the MOSE, as evidenced by changes in morphology and expression of genes associated with epithelial/ mesenchymal cells but was not sufficient to increase the proportion of SCA-1+ MOSE,

although it was sufficient to increase the number of MOSE capable of forming spheres.

TGFB1 and SNAIL decreased the expression of the potent tumour suppressor BRCA1 in MOSE cells and inactivation of *Brca1* was sufficient to cause an expansion of the SCA-1+ MOSE progenitor cell population. The results presented in this thesis not only identify a cell-surface marker for MOSE with progenitor cell characteristics, but also implicate TGFB1, acting through downregulation of BRCA1 and/or possibly an EMT, as a key regulatory molecule for the progenitor cell population (summarized in Fig. 5.1).

## 5.2 General Discussion

### *5.2.1 Ovulation*

At ovulation, the follicle ruptures, and OSE surrounding the wound site adopt a mesenchymal phenotype and begin to proliferate to heal the wound (Salamanca et al., 2004; Ahmed et al., 2006). We observed an EMT in MOSE cells treated with TGFB1 in vitro. TGFB1 also increased the proportion of SCA-1+ MOSE and converted SCA-1- MOSE into SCA-1+ MOSE in vitro. This indicates that the EMT seen in response to ovulation may enhance the self-renewal of MOSE progenitor cells which would help the ruptured tissue to heal. To confirm that this happens in vivo, immunohistochemistry to detect EMT markers and SCA-1 should be performed at tightly controlled time points after ovulation. The proposed role of LIF and TGFB1 in ovulatory wounding are summarized in Fig. 5.2.

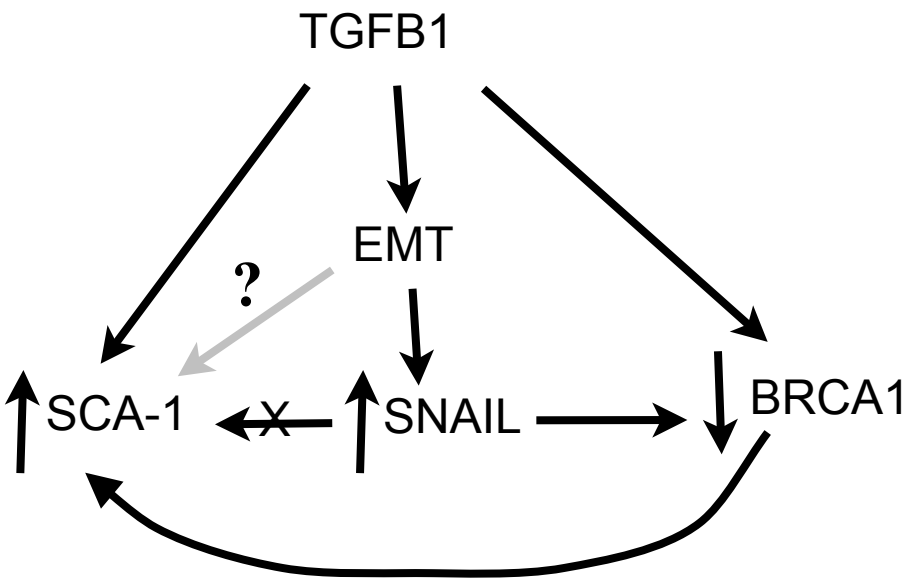


**Figure 5.1: A summary of the major findings of this thesis.** TGFB1 causes an increase in the number of SCA-1+ MOSE, induces an EMT in the MOSE and also decreases BRCA1 expression. The EMT causes an upregulation of SNAIL expression which is sufficient to cause a down-regulation of BRCA1 expression but is not sufficient to increase SCA-1 expression. Inactivation of Brca1 is sufficient to increase SCA-1 expression.

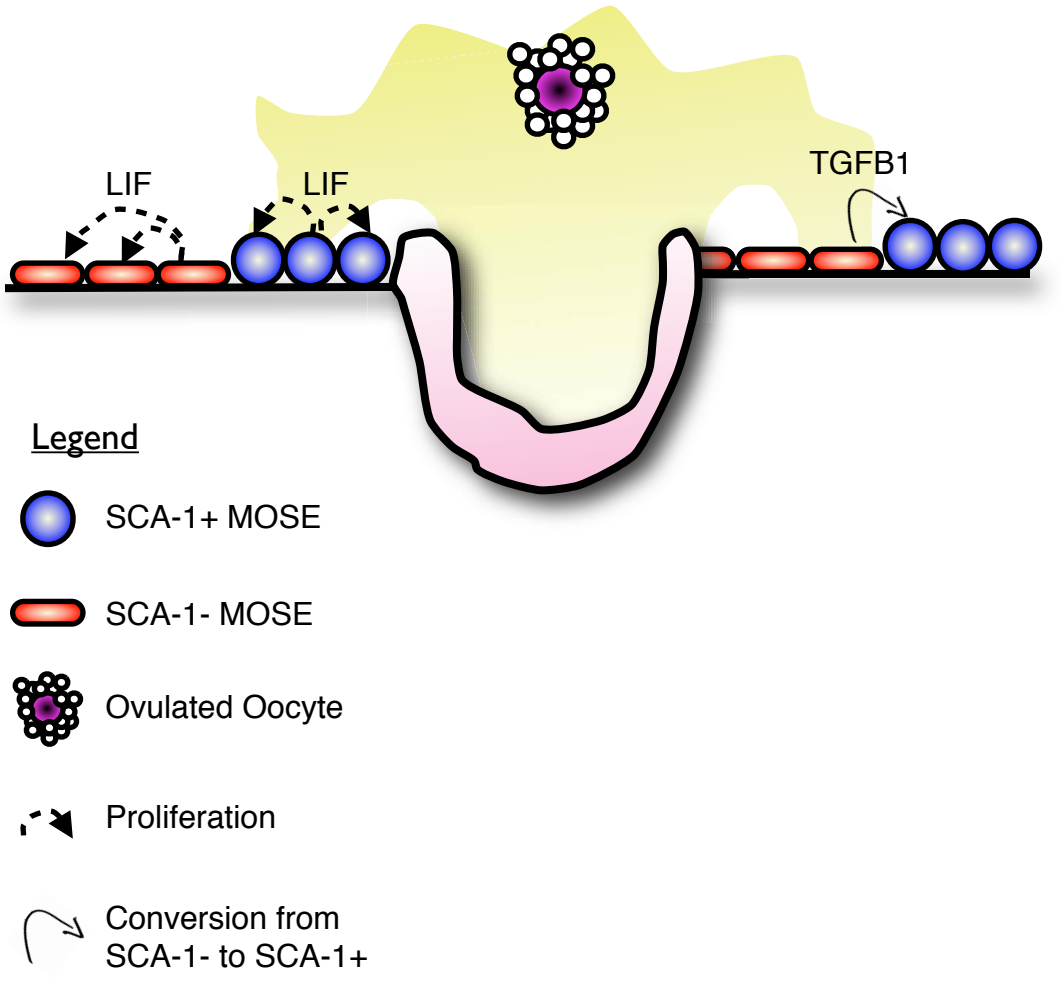


**Figure 5.2: A hypothetical model of the mechanisms controlling ovulatory wound repair, based on the major findings of this study.** During ovulation, follicular fluid is expelled from the follicle and bathes the MOSE surrounding the ovulatory wound. TGFB1 and LIF induce self-renewal of SCA-1+ MOSE progenitor cells while LIF also acts to stimulate proliferation in the MOSE. The data suggest that LIF and TGFB1 act on the MOSE to drive ovulatory wound healing through regulation of a SCA-1+ progenitor cell population.

*5.2.2 Multipotency*

The literature supports the presence of multipotent cells on the surface of the ovary. The OSE can differentiate into mesenchymal cells to heal ovulatory wounds (Salamanca et al., 2004; Ahmed et al., 2006; Gotfredson and Murdoch, 2007) and can adopt aberrant epithelial phenotypes when trapped in inclusion cysts (Maines-Bandiera and Auersperg, 1997; Okamoto et al., 2009; Pothuri et al., 2010; Auersperg, 2011). They may be a source of granulosa cells shortly after birth (Mork et al., 2012) and have even been proposed to have the capacity to differentiate into oocytes (Johnson et al., 2004; Virant-Klun et al., 2008; Virant-Klun et al., 2009; Parte et al., 2011). All of these proposed functions are in addition to the progenitor cell activity required to replace OSE lost during ovulation. Therefore, determining whether OSE cells have the capacity to differentiate into oocytes, granulosa cells or FTE cells would be useful in defining the multipotency of OSE cells.

In this thesis, we have provided evidence of the existence of a progenitor cell on the surface of the ovary. MOSE cells are capable of producing spheres that can be passaged without a significant decline in sphere numbers, which indicates that they can self-renew. SCA-1 surface expression marks a population of MOSE cells that are enriched with cells with this capability. SCA-1+ MOSE cells, but not SCA-1-MOSE cells are also capable of attaching to and surviving on the surface of the ovary through many rounds of ovulation, which while it is not a robust test of repopulation, indicates that the SCA-1+ MOSE population contain cells with some progenitor cell activity. Therefore, while the literature suggests the presence of a multipotent stem cell, from our work we can only conclude that the MOSE contains a unipotent progenitor cell. As SCA-1 is the first reported surface

marker for MOSE cells with progenitor cell characteristics, this thesis comprises the first step in defining a progenitor cell population, or perhaps with more research, a stem cell population, on the surface of the ovary.

*5.2.3 Neo-oogenesis*

While it was not our goal, some of the results presented in this thesis can be interpreted to support the concept that the MOSE contains cells capable of producing oocytes. Using immunohistochemistry for SCA-1 expression, we demonstrated that there are rare cells on the surface of ovary that stain positive for SCA-1 expression. In the same experiments, primary oocytes appeared to stain positive for SCA-1 which implies that primary oocytes express SCA-1. Shared expression of a protein does not always indicate a shared origin, nor does it always demonstrate a lineage relationship. In addition, immunohistochemistry in mouse ovaries, even with an antibody with high specificity, tends to produce background staining in the oocytes. While the positive staining seen in the MOSE has been confirmed by flow cytometry, the apparently positive staining of primary oocytes should be confirmed by another method before conclusions can be made about its validity.

Our finding that SCA-1+ MOSE cells are enriched in the $FS^{low}$ gate can also be interpreted to suggest that SCA-1+ MOSE cells are in some way linked to neo-oogenesis. Our work describing the $FS^{low}$ MOSE population looked at the proportion of $FS^{low}$ (small) cells that express SCA-1. We also observed that TGFB1 caused the percentage of $FS^{low}$ MOSE to increase. A series of recent publications, mostly from affiliated research groups,

have reported the existence of cells with low forward scatter with embryonic stem cell-like characteristics referred to as VSELs that have the capacity to produce oocyte-like cells. VSELs have been reported in the murine bone marrow (Paczkowska et al., 2011), the human OSE (Virant-Klun et al., 2008; Virant-Klun et al., 2009; Parte et al., 2011), the subventricular zone of the murine brain (Zuba-Surma et al., 2009) and human umbilical cord blood (Danova-Alt et al., 2012). Interestingly SCA-1 is reported to be a marker of murine VSELs (Zuba-Surma et al., 2009).

While dead cells were gated out at the beginning of our analysis, it would be crucial to demonstrate that the $FS^{low}$ MOSE are in fact alive and that they can survive in culture. Further characterization is needed to determine whether the $FS^{low}$ MOSE, or SCA-1+ MOSE, are capable of forming oocytes in culture.

In collaboration with Dr. Paul Dyce at Western University, we are testing to determine whether MOSE cells can be differentiated into oocytes in vitro. Dr. Dyce has previously reported the differentiation of oocyte-like cells from fetal porcine skin stem cells (Dyce et al., 2006; Dyce et al., 2011a; Dyce et al., 2011b). Some of the oocyte-like cells were surrounded by cells that were capable of producing estrogen, which indicates that both granulosa and theca cells are present (Dyce et al., 2006). As it stands, the culture system is inadequate to support complete development of competent oocytes from fetal skin stem cells (Dyce et al., 2011b).

Preliminary results indicate that when grown in oocyte differentiation conditions (Dyce et al., 2006; Dyce et al., 2011a; Dyce et al., 2011b), a small proportion of MOSE cells can form oocyte-like cells that express the pluripotency markers *Oct-4* and *Kit* at

much higher levels than MOSE cells grown under normal MOSE conditions (Dyce 2012, unpublished results). In addition, the oocyte-like cells express the oocyte/meiosis-specific markers *Gdf9* and *Scp3*. Interestingly, in oocyte-like cells derived from MOSE cells, SCP3 is properly localized to the chromosomes, while in MOSE cells it is expressed in the cytoplasm (Dyce 2012, unpublished results).

The next goal in this collaboration is to compare the ability of SCA-1+ MOSE to form oocyte-like cells to that of SCA-1- MOSE as well as to compare the capacity for oocyte formation of $FS^{low}$ and $FS^{high}$ MOSE. As with most of the neo-oogenesis work, the ability of a cell to be forced down a specific path of differentiation does not mean it normally makes the end product. Still, finding cell types that can be used to make viable, functional oocytes would have a huge impact on assisted reproductive techniques.

### *5.2.4 The Initiation Of EOC*

Hereditary EOC represents approximately 10% of EOC cases, with the majority of these women carrying germline mutations in the *BRCA1* gene (Weberpals et al., 2008). In addition, in 40-72% of cases of sporadic EOC, BRCA1 is inactivated through hypermethylation, loss of heterozygosity, or haploinsufficiency (Weberpals et al., 2008). Therefore BRCA1 dysfunction is seen in both hereditary and sporadic forms of EOC. Our results predict that in the OSE of *BRCA1* mutation carriers, there are more progenitor cells than in women without germline *BRCA1* mutations.

In both mutation carriers and the general population, ovulation causes OSE cells to replicate (Gaytán et al., 2005; Burdette et al., 2006), undergo an EMT (Salamanca et al.,

2004; Ahmed et al., 2006), and accumulate DNA damage (Murdoch et al., 2001; Murdoch and Martinchick, 2004; Gotfredson and Murdoch, 2007). Our results indicate that LIF may be one of the factors involved in stimulating OSE proliferation and that TGFB1, through the upregulation of SNAIL may induce an EMT. In addition we have shown that both TGFB1 and SNAIL downregulated BRCA1. Therefore, we would expect a lower level of BRCA1 expression and therefore a decreased capacity for DNA repair, in OSE surrounding the ovulatory wound than in those distal to the wound site. In *BRCA1* mutation carriers, who already have a deleterious mutation in one *BRCA1* allele (Weberpals et al., 2008), our work suggests that the EMT associated with ovulation may decrease the expression of BRCA1 from the intact and mutated alleles, further hindering DNA repair. This reduction in BRCA1 function could explain why these women develop EOC at a younger age and are at a higher risk of developing this disease than the general population (Seton-Rogers, 2011).

On the surface of the ovary in response to ovulation a population of cells surround the wound site undergo an EMT (Ahmed et al., 2006). Our results indicate that this may lead to an increase in the number of progenitor cells and a decrease in BRCA1 activity in the OSE. This is occurring when the cells are proliferating to heal ovulatory wounds (Burdette et al., 2006) and are exposed to DNA damaging agents like reactive oxygen species and inflammatory molecules (Murdoch and Martinchick, 2004). This sets up a favourable environment for the accumulation of genetic mutations and malignant transformation.

While a human homologue to SCA-1 has not yet been reported, we found that BRCA1 regulated the expression of other stem cell markers, like *CD44*, *CD117* and

*CD113*, which are expressed in humans and are reported markers of EOC tumour initiating cells (Zhang et al., 2008; Meirelles et al., 2012; Steg et al., 2012). Our work indicates that the regulation of stem cell marker expression in the MOSE may translate to addition markers beyond SCA-1.

## 5.3 Conclusions

Taken together, the results presented in this thesis suggest the presence of a progenitor cell population on the surface of the ovary that plays a role in both ovulation and perhaps the initiation of ovarian cancer. These progenitor cells are enriched in the SCA-1+ MOSE population and are regulated by at least two ovulation-associated factors, LIF and TGFB1. TGFB1 may be acting through two different but interconnected pathways to regulate the MOSE: the EMT and downregulation of BRCA1. In summary, we have shown that the MOSE contains a SCA-1+ progenitor cell population that is expanded by TGFB1 and is normally controlled by BRCA1.

# REFERENCES


Ackerman, R.C., and Murdoch, W.J. (1993). Prostaglandin-induced apoptosis of ovarian surface epithelial cells. Prostaglandins *45*, 475-485.

Adami, H.O., Hsieh, C.C., Lambe, M., Trichopoulos, D., Leon, D., Persson, I., Ekbom, A., and Janson, P.O. (1994). Parity, age at first childbirth, and risk of ovarian cancer. Lancet *344*, 1250-1254.

Ahmed, N., Maines-Bandiera, S., Quinn, M.A., Unger, W.G., Dedhar, S., and Auersperg, N. (2006). Molecular pathways regulating EGF-induced epithelio-mesenchymal transition in human ovarian surface epithelium. Am J Physiol Cell Physiol *290*, C1532-1542.

Ahmed, N., Thompson, E., and Quinn, M. (2007). Epithelial-mesenchymal interconversions in normal ovarian surface epithelium and ovarian carcinomas: an exception to the norm. J Cell Physiol *213*, 581-588.

Al-Hajj, M., Wicha, M.S., Benito-Hernandez, A., Morrison, S.J., and Clarke, M.F. (2003). Prospective identification of tumorigenic breast cancer cells. Proc Natl Acad Sci U S A *100*, 3983-3988.

Anderson, L.D., and Hirshfield, A.N. (1992). An overview of follicular development in the ovary: from embryo to the fertilized ovum in vitro. Md Med J *41*, 614-620.

Arici, A., Oral, E., Bahtiyar, O., Engin, O., Seli, E., and Jones, E.E. (1997). Leukaemia inhibitory factor expression in human follicular fluid and ovarian cells. Hum Reprod *12*, 1233-1239.

Asselin-Labat, M.L., Vaillant, F., Shackleton, M., Bouras, T., Lindeman, G.J., and Visvader, J.E. (2008). Delineating the epithelial hierarchy in the mouse mammary gland. Cold Spring Harb Symp Quant Biol *73*, 469-478.

Attisano, L., and Wrana, J.L. (2002). Signal transduction by the TGF-beta superfamily. Science *296*, 1646-1647.

Auersperg, N. (2011). The origin of ovarian carcinomas: a unifying hypothesis. Int J Gynecol Pathol *30*, 12-21.

Auersperg, N. (2013). The origin of ovarian cancers - hypotheses and controversies Front Biosci *5*, 709-719.

Auersperg, N., Maines-Bandiera, S.L., Dyck, H.G., and Kruk, P.A. (1994). Characterization of cultured human ovarian surface epithelial cells: phenotypic plasticity and premalignant changes. Lab Invest *71*, 510-518.

Auersperg, N., Wong, A.S., Choi, K.C., Kang, S.K., and Leung, P.C. (2001). Ovarian

surface epithelium: biology, endocrinology, and pathology. Endocr Rev *22*, 255-288.

Baba, T., Convery, P.A., Matsumura, N., Whitaker, R.S., Kondoh, E., Perry, T., Huang, Z., Bentley, R.C., Mori, S., Fujii, S.*, et al.* (2009). Epigenetic regulation of CD133 and tumorigenicity of CD133+ ovarian cancer cells. Oncogene *28*, 209-218.

Bamezai, A. (2004). Mouse Ly-6 proteins and their extended family: markers of cell differentiation and regulators of cell signaling. Arch Immunol Ther Exp *52*, 255-266.

Barnett, K.R., Schilling, C., Greenfeld, C.R., Tomic, D., and Flaws, J.A. (2006). Ovarian follicle development and transgenic mouse models. Hum Reprod Update *12*, 537-555.

Barua, A., Bitterman, P., Abramowicz, J.S., Dirks, A.L., Bahr, J.M., Hales, D.B., Bradaric, M.J., Edassery, S.L., Rotmensch, J., and Luborsky, J.L. (2009). Histopathology of ovarian tumors in laying hens: a preclinical model of human ovarian cancer. Int J Gynecol Cancer *19*, 531-539.

Batlle, E., Sancho, E., Francí, C., Domínguez, D., Monfar, M., Baulida, J., and García De Herreros, A. (2000). The transcription factor snail is a repressor of E-cadherin gene expression in epithelial tumour cells. Nat Cell Biol *2*, 84-89.

Bell, D.A., and Scully, R.E. (1994). Early de novo ovarian carcinoma. A study of fourteen cases. Cancer *73*, 1859-1864.

Berchuck, A., Rodriguez, G., Olt, G., Whitaker, R., Boente, M.P., Arrick, B.A., Clarke-Pearson, D.L., and Bast, R.C. (1992). Regulation of growth of normal ovarian epithelial cells and ovarian cancer cell lines by transforming growth factor-beta. Am J Obstet Gynecol *166*, 676-684.

Bhartiya, D., Sriraman, K., and Parte, S. (2012). Stem cell interaction with somatic niche may hold the key to fertility restoration in cancer patients. Obstet Gynecol Int *2012*, 921082.

Bhatt, R.I., Brown, M.D., Hart, C.A., Gilmore, P., Ramani, V.A., George, N.J., and Clarke, N.W. (2003). Novel method for the isolation and characterisation of the putative prostatic stem cell. Cytometry A *54*, 89-99.

Blanpain, C., Horsley, V., and Fuchs, E. (2007). Epithelial stem cells: turning over new leaves. Cell *128*, 445-458.

Blick, T., Hugo, H., Widodo, E., Waltham, M., Pinto, C., Mani, S.A., Weinberg, R.A., Neve, R.M., Lenburg, M.E., and Thompson, E.W. (2010). Epithelial mesenchymal transition traits in human breast cancer cell lines parallel the CD44(hi/)CD24 (lo/-) stem cell phenotype in human breast cancer. J Mammary Gland Biol Neoplasia *15*, 235-252.

Bukovsky, A., Caudle, M.R., Svetlikova, M., and Upadhyaya, N.B. (2004). Origin of germ cells and formation of new primary follicles in adult human ovaries. Reprod Biol Endocrinol *2*, 20.

Bukovsky, A., Gupta, S.K., Virant-Klun, I., Upadhyaya, N.B., Copas, P., Van Meter, S.E., Svetlikova, M., Ayala, M.E., and Dominguez, R. (2008). Study origin of germ cells and formation of new primary follicles in adult human and rat ovaries. Methods Mol Biol *450*, 233-265.

Bukovsky, A., Keenan, J.A., Caudle, M.R., Wimalasena, J., Upadhyaya, N.B., and Van Meter, S.E. (1995). Immunohistochemical studies of the adult human ovary: possible contribution of immune and epithelial factors to folliculogenesis. Am J Reprod Immunol *33*, 323-340.

Burdette, J.E., Kurley, S.J., Kilen, S.M., Mayo, K.E., and Woodruff, T.K. (2006). Gonadotropin-induced superovulation drives ovarian surface epithelia proliferation in CD1 mice. Endocrinology *147*, 2338-2345.

Burdette, J.E., Oliver, R.M., Ulyanov, V., Kilen, S.M., Mayo, K.E., and Woodruff, T.K. (2007). Ovarian epithelial inclusion cysts in chronically superovulated CD1 and Smad2 dominant-negative mice. Endocrinology *148*, 3595-3604.

Calloni, R., Cordero, E.A., Henriques, J.A., and Bonatto, D. (2013). Reviewing and Updating the Major Molecular Markers for Stem Cells. Stem Cells Dev. Epub 2013 Jan 23.

Cano, A., Pérez-Moreno, M.A., Rodrigo, I., Locascio, A., Blanco, M.J., del Barrio, M.G., Portillo, F., and Nieto, M.A. (2000). The transcription factor snail controls epithelial-mesenchymal transitions by repressing E-cadherin expression. Nat Cell Biol *2*, 76-83.

Challen, G.A., and Little, M.H. (2006). A side order of stem cells: the SP phenotype. Stem Cells *24*, 3-12.

Choi, K.C., Kang, S.K., Tai, C.J., Auersperg, N., and Leung, P.C. (2001). The regulation of apoptosis by activin and transforming growth factor-beta in early neoplastic and tumorigenic ovarian surface epithelium. J Clin Endocrinol Metab *86*, 2125-2135.

Clark-Knowles, K.V., Garson, K., Jonkers, J., and Vanderhyden, B.C. (2007). Conditional inactivation of Brca1 in the mouse ovarian surface epithelium results in an increase in preneoplastic changes. Exp Cell Res *313*, 133-145.

Clark-Knowles, K.V., Senterman, M.K., Collins, O., and Vanderhyden, B.C. (2009). Conditional inactivation of Brca1, p53 and Rb in mouse ovaries results in the development of leiomyosarcomas. PloS One *4*, e8534.

Cramer, D.W., and Welch, W.R. (1983). Determinants of ovarian cancer risk. II. Inferences regarding pathogenesis. J Natl Cancer Inst *71*, 717-721.

Cruet, S., Salamanca, C., Mitchell, G.W., and Auersperg, N. (1999). alphavbeta3 and vitronectin expression by normal ovarian surface epithelial cells: role in cell adhesion and cell proliferation. Gynecol Oncol *75*, 254-260.

Danova-Alt, R., Heider, A., Egger, D., Cross, M., and Alt, R. (2012). Very small embryonic-like stem cells purified from umbilical cord blood lack stem cell characteristics. PLoS One *7*, e34899.

Derynck, R., and Zhang, Y.E. (2003). Smad-dependent and Smad-independent pathways in TGF-beta family signalling. Nature *425*, 577-584.

Dontu, G., Abdallah, W.M., Foley, J.M., Jackson, K.W., Clarke, M.F., Kawamura, M.J., and Wicha, M.S. (2003). In vitro propagation and transcriptional profiling of human mammary stem/progenitor cells. Genes Dev *17*, 1253-1270.

Doyle, L.K., and Donadeu, F.X. (2009). Regulation of the proliferative activity of ovarian surface epithelial cells by follicular fluid. Anim Reprod Sci *114*, 443-448.

Dyce, P.W., Liu, J., Tayade, C., Kidder, G.M., Betts, D.H., and Li, J. (2011a). In vitro and in vivo germ line potential of stem cells derived from newborn mouse skin. PLoS One *6*, e20339.

Dyce, P.W., Shen, W., Huynh, E., Shao, H., Villagomez, D.A., Kidder, G.M., King, W.A., and Li, J. (2011b). Analysis of oocyte-like cells differentiated from porcine fetal skin-derived stem cells. Stem Cells Dev *20*, 809-819.

Dyce, P.W., Wen, L., and Li, J. (2006). In vitro germline potential of stem cells derived from fetal porcine skin. Nat Cell Biol *8*, 384-390.

Fathalla, M.F. (1971). Incessant ovulation--a factor in ovarian neoplasia? Lancet *2*, 163.

Finch, A., Shaw, P., Rosen, B., Murphy, J., Narod, S.A., and Colgan, T.J. (2006). Clinical and pathologic findings of prophylactic salpingo-oophorectomies in 159 BRCA1 and BRCA2 carriers. Gynecol Oncol *100*, 58-64.

Fleming, J.S., Beaugié, C.R., Haviv, I., Chenevix-Trench, G., and Tan, O.L. (2006). Incessant ovulation, inflammation and epithelial ovarian carcinogenesis: revisiting old hypotheses. Mol Cell Endocrinol *247*, 4-21.

Flesken-Nikitin, A., Choi, K.C., Eng, J.P., Shmidt, E.N., and Nikitin, A.Y. (2003). Induction of carcinogenesis by concurrent inactivation of p53 and Rb1 in the mouse ovarian surface epithelium. Cancer Res *63*, 3459-3463.

Foulkes, W.D. (2004). BRCA1 functions as a breast stem cell regulator. J Med Genet *41*, 1-5.

Fredrickson, T.N. (1987). Ovarian tumors of the hen. Environ Health Perspect *73*, 35-51.

Fried, G., and Wramsby, H. (1998). Increase in transforming growth factor beta1 in ovarian

follicular fluid following ovarian stimulation and in-vitro fertilization correlates to pregnancy. Hum Reprod *13*, 656-659.

Fried, G., Wramsby, H., and Tally, M. (1998). Transforming growth factor-beta1, insulin-like growth factors, and insulin-like growth factor binding proteins in ovarian follicular fluid are differentially regulated by the type of ovarian hyperstimulation used for in vitro fertilization. Fertil Steril *70*, 129-134.

Furuta, S., Jiang, X., Gu, B., Cheng, E., Chen, P.L., and Lee, W.H. (2005). Depletion of BRCA1 impairs differentiation but enhances proliferation of mammary epithelial cells. Proc Natl Acad Sci U S A *102*, 9176-9181.

Fuxe, J., Vincent, T., and de Herreros, A.G. (2010). Transcriptional crosstalk between TGFbeta and stem cell pathways in tumor cell invasion: Role of EMT promoting Smad complexes. Cell Cycle *9*, 2363-2374.

Gamwell, L.F., Collins, O., and Vanderhyden, B.C. (2012). The Mouse Ovarian Surface Epithelium Contains a Population of LY6A (SCA-1) Expressing Progenitor Cells That Are Regulated by Ovulation-Associated Factors. Biol Reprod *87*, 80.

Gaytán, M., Sánchez, M.A., Morales, C., Bellido, C., Millán, Y., Martín de Las Mulas, J., Sánchez-Criado, J.E., and Gaytán, F. (2005). Cyclic changes of the ovarian surface epithelium in the rat. Reproduction *129*, 311-321.

Goodell, M.A., Brose, K., Paradis, G., Conner, A.S., and Mulligan, R.C. (1996). Isolation and functional properties of murine hematopoietic stem cells that are replicating in vivo. J Exp Med *183*, 1797-1806.

Gotfredson, G.S., and Murdoch, W.J. (2007). Morphologic responses of the mouse ovarian surface epithelium to ovulation and steroid hormonal milieu. Exp Biol Med *232*, 277-280.

Gudas, J.M., Li, T., Nguyen, H., Jensen, D., Rauscher, F.J., and Cowan, K.H. (1996). Cell cycle regulation of BRCA1 messenger RNA in human breast epithelial cells. Cell Growth Differ *7*, 717-723.

Guo, W., Keckesova, Z., Donaher, J.L., Shibue, T., Tischler, V., Reinhardt, F., Itzkovitz, S., Noske, A., Zürrer-Härdi, U., Bell, G.*, et al.* (2012). Slug and Sox9 cooperatively determine the mammary stem cell state. Cell *148*, 1015-1028.

Gwinn, M.L., Lee, N.C., Rhodes, P.H., Layde, P.M., and Rubin, G.L. (1990). Pregnancy, breast feeding, and oral contraceptives and the risk of epithelial ovarian cancer. J Clin Epidemiol *43*, 559-568.

Hanson, P., Mathews, V., Marrus, S.H., and Graubert, T.A. (2003). Enhanced green fluorescent protein targeted to the Sca-1 (Ly-6A) locus in transgenic mice results in efficient marking of hematopoietic stem cells in vivo. Exp Hematol *31*, 159-167.

Haraguchi, N., Utsunomiya, T., Inoue, H., Tanaka, F., Mimori, K., Barnard, G.F., and Mori, M. (2006). Characterization of a side population of cancer cells from human gastrointestinal system. Stem Cells *24*, 506-513.

Havrilesky, L.J., Hurteau, J.A., Whitaker, R.S., Elbendary, A., Wu, S., Rodriguez, G.C., Bast, R.C., Jr., and Berchuck, A. (1995). Regulation of apoptosis in normal and malignant ovarian epithelial cells by transforming growth factor beta. Cancer Res *55*, 944-948.

Hirshfield, A.N. (1991). Development of follicles in the mammalian ovary. Int Rev Cytol *124*, 43-101.

Holmes, C., and Stanford, W.L. (2007). Concise review: stem cell antigen-1: expression, function, and enigma. Stem Cells *25*, 1339-1347.

Horejsí, V., Drbal, K., Cebecauer, M., Cerný, J., Brdicka, T., Angelisová, P., and Stockinger, H. (1999). GPI-microdomains: a role in signalling via immunoreceptors. Immunol Today *20*, 356-361.

Horvay, K., Casagranda, F., Gany, A., Hime, G.R., and Abud, H.E. (2011). Wnt signalling regulates Snai1 expression and cellular localisation in the mouse intestinal epithelial stem cell niche. Stem Cells Dev *20*, 737-745.

Hosonuma, S., Kobayashi, Y., Kojo, S., Wada, H., Seino, K., Kiguchi, K., and Ishizuka, B. (2011). Clinical significance of side population in ovarian cancer cells. Hum Cell *24*, 9-12.

Hsieh, M., Zamah, A., and Conti, M. (2009). Epidermal growth factor-like growth factors in the follicular fluid: role in oocyte development and maturation. Semin Reprod Med *27*, 52-61.

Hu, L., McArthur, C., and Jaffe, R.B. (2010). Ovarian cancer stem-like side-population cells are tumourigenic and chemoresistant. Br J Cancer *102*, 1276-1283.

Hugo, H., Ackland, M.L., Blick, T., Lawrence, M.G., Clements, J.A., Williams, E.D., and Thompson, E.W. (2007). Epithelial--mesenchymal and mesenchymal--epithelial transitions in carcinoma progression. J Cell Physiol *213*, 374-383.

Ismail, R.S., Cada, M., and Vanderhyden, B.C. (1999). Transforming growth factor-beta regulates Kit ligand expression in rat ovarian surface epithelial cells. Oncogene *18*, 4734-4741.

Jarboe, E.A., Folkins, A.K., Drapkin, R., Ince, T.A., Agoston, E.S., and Crum, C.P. (2008). Tubal and ovarian pathways to pelvic epithelial cancer: a pathological perspective. Histopathology *53*, 127-138.

Johnson, J., Bagley, J., Skaznik-Wikiel, M., Lee, H.J., Adams, G.B., Niikura, Y., Tschudy, K.S., Tilly, J.C., Cortes, M.L., Forkert, R.*, et al.* (2005). Oocyte generation in adult

mammalian ovaries by putative germ cells in bone marrow and peripheral blood. Cell *122*, 303-315.

Johnson, J., Canning, J., Kaneko, T., Pru, J.K., and Tilly, J.L. (2004). Germline stem cells and follicular renewal in the postnatal mammalian ovary. Nature *428*, 145-150.

Jonker, J.W., Freeman, J., Bolscher, E., Musters, S., Alvi, A.J., Titley, I., Schinkel, A.H., and Dale, T.C. (2005). Contribution of the ABC transporters Bcrp1 and Mdr1a/1b to the side population phenotype in mammary gland and bone marrow of mice. Stem Cells *23*, 1059-1065.

Kafadar, K.A., Yi, L., Ahmad, Y., So, L., Rossi, F., and Pavlath, G.K. (2009). Sca-1 expression is required for efficient remodeling of the extracellular matrix during skeletal muscle regeneration. Dev Biol *326*, 47-59.

Kalluri, R., and Weinberg, R.A. (2009). The basics of epithelial-mesenchymal transition. J Clin Invest *119*, 1420-1428.

Kindelberger, D.W., Lee, Y., Miron, A., Hirsch, M.S., Feltmate, C., Medeiros, F., Callahan, M.J., Garner, E.O., Gordon, R.W., Birch, C.*, et al.* (2007). Intraepithelial carcinoma of the fimbria and pelvic serous carcinoma: Evidence for a causal relationship. Am J Surg Pathol *31*, 161-169.

King, S.M., Hilliard, T.S., Wu, L.Y., Jaffe, R.C., Fazleabas, A.T., and Burdette, J.E. (2011). The impact of ovulation on fallopian tube epithelial cells: evaluating three hypotheses connecting ovulation and serous ovarian cancer. Endocr Relat Cancer *18*, 627-642.

Knight, P.G., and Glister, C. (2006). TGF-beta superfamily members and ovarian follicle development. Reproduction *132*, 191-206.

Kodaman, P.H., and Behrman, H.R. (2001). Endocrine-regulated and protein kinase C-dependent generation of superoxide by rat preovulatory follicles. Endocrinology *142*, 687-693.

Konishi, I., Kuroda, H., and Mandai, M. (1999). Review: gonadotropins and development of ovarian cancer. Oncology *57 Suppl 2*, 45-48.

Kruk, P.A., and Auersperg, N. (1992). Human ovarian surface epithelial cells are capable of physically restructuring extracellular matrix. Am J Obstet Gynecol *167*, 1437-1443.

Kruk, P.A., and Auersperg, N. (1994). A line of rat ovarian surface epithelium provides a continuous source of complex extracellular matrix. In Vitro Cell Dev Biol Anim *30A*, 217-225.

Kruk, P.A., Uitto, V.J., Firth, J.D., Dedhar, S., and Auersperg, N. (1994). Reciprocal interactions between human ovarian surface epithelial cells and adjacent extracellular matrix. Exp Cell Res *215*, 97-108.

Kusumbe, A.P., Mali, A.M., and Bapat, S.A. (2009). CD133-expressing stem cells associated with ovarian metastases establish an endothelial hierarchy and contribute to tumor vasculature. Stem cells *27*, 498-508.

Laviolette, L.A., Garson, K., Macdonald, E.A., Senterman, M.K., Courville, K., Crane, C.A., and Vanderhyden, B.C. (2010). 17beta-estradiol accelerates tumor onset and decreases survival in a transgenic mouse model of ovarian cancer. Endocrinology *151*, 929-938.

Le Roy, C., and Wrana, J.L. (2005). Clathrin- and non-clathrin-mediated endocytic regulation of cell signalling. Nat Rev Mol Cell Biol *6*, 112-126.

LeClair, K.P., Palfree, R.G., Flood, P.M., Hammerling, U., and Bothwell, A. (1986). Isolation of a murine Ly-6 cDNA reveals a new multigene family. EMBO J *5*, 3227-3234.

Lee, J.M., Dedhar, S., Kalluri, R., and Thompson, E.W. (2006). The epithelial-mesenchymal transition: new insights in signaling, development, and disease. J Cell Biol *172*, 973-981.

Liao, M.J., Zhang, C.C., Zhou, B., Zimonjic, D.B., Mani, S.A., Kaba, M., Gifford, A., Reinhardt, F., Popescu, N.C., Guo, W.*, et al.* (2007). Enrichment of a population of mammary gland cells that form mammospheres and have in vivo repopulating activity. Cancer Res *67*, 8131-8138.

Lim, E., Vaillant, F., Wu, D., Forrest, N.C., Pal, B., Hart, A.H., Asselin-Labat, M., Gyorki, D.E., Ward, T., Partanen, A.*, et al.* (2009). Aberrant luminal progenitors as the candidate target population for basal tumor development in BRCA1 mutation carriers. Nat Med *15*, 907-913.

Liu, S., Ginestier, C., Charafe-Jauffret, E., Foco, H., Kleer, C.G., Merajver, S.D., Dontu, G., and Wicha, M.S. (2008). BRCA1 regulates human mammary stem/progenitor cell fate. Proc Natl Acad Sci U S A *105*, 1680-1685.

Lu, Y., Chu, A., Turker, M.S., and Glazer, P.M. (2011). Hypoxia-induced epigenetic regulation and silencing of the BRCA1 promoter. Mol Cell Bio *31*, 3339-3350.

Ma, X., de Bruijn, M., Robin, C., Peeters, M., Kong, A.S.J., de Wit, T., Snoijs, C., and Dzierzak, E. (2002a). Expression of the Ly-6A (Sca-1) lacZ transgene in mouse haematopoietic stem cells and embryos. Br J Haematol *116*, 401-408.

Ma, X., Robin, C., Ottersbach, K., and Dzierzak, E. (2002b). The Ly-6A (Sca-1) GFP transgene is expressed in all adult mouse hematopoietic stem cells. Stem Cells *20*, 514-521.

Maines-Bandiera, S.L., and Auersperg, N. (1997). Increased E-cadherin expression in ovarian surface epithelium: an early step in metaplasia and dysplasia? Int J Gynecol Pathol *16*, 250-255.

Mani, S.A., Guo, W., Liao, M.J., Eaton, E.N., Ayyanan, A., Zhou, A.Y., Brooks, M., Reinhard, F., Zhang, C.C., Shipitsin, M.*, et al.* (2008). The epithelial-mesenchymal transition generates cells with properties of stem cells. Cell *133*, 704-715.

Marks, J.R., Huper, G., Vaughn, J.P., Davis, P.L., Norris, J., McDonnell, D.P., Wiseman, R.W., Futreal, P.A., and Iglehart, J.D. (1997). BRCA1 expression is not directly responsive to estrogen. Oncogene *14*, 115-121.

Massagué, J. (1992). Receptors for the TGF-beta family. Cell *69*, 1067-1070.

McGee, E.A., and Hsueh, A.J. (2000). Initial and cyclic recruitment of ovarian follicles. Endocr Rev *21*, 200-214.

McGrew, J.T., and Rock, K.L. (1991). Isolation, expression, and sequence of the TAP/ Ly-6A.2 chromosomal gene. J Immunol *146*, 3633-3638.

Meirelles, K., Benedict, L.A., Dombkowski, D., Pepin, D., Preffer, F.I., Teixeira, J., Tanwar, P.S., Young, R.H., MacLaughlin, D.T., Donahoe, P.K.*, et al.* (2012). Human ovarian cancer stem/progenitor cells are stimulated by doxorubicin but inhibited by Mullerian inhibiting substance. Proc Natl Acad Sci U S A *109*, 2358-2363.

Miles, C., Sanchez, M.J., Sinclair, A., and Dzierzak, E. (1997). Expression of the Ly-6E.1 (Sca-1) transgene in adult hematopoietic stem cells and the developing mouse embryo. Development *124*, 537-547.

Mitchell, P.O., Mills, T., O'Connor, R.S., Kline, E.R., Graubert, T., Dzierzak, E., and Pavlath, G.K. (2005). Sca-1 negatively regulates proliferation and differentiation of muscle cells. Dev Biol *283*, 240-252.

Moore, D.J., Markmann, J.F., and Deng, S. (2006). Avenues for immunomodulation and graft protection by gene therapy in transplantation. Transpl Int *19*, 435-445.

Morel, A.P., Lièvre, M., Thomas, C., Hinkal, G., Ansieau, S., and Puisieux, A. (2008). Generation of breast cancer stem cells through epithelial-mesenchymal transition. PLoS One *3*, e2888.

Mork, L., Maatouk, D.M., McMahon, J.A., Guo, J.J., Zhang, P., McMahon, A.P., and Capel, B. (2012). Temporal differences in granulosa cell specification in the ovary reflect distinct follicle fates in mice. Biol Reprod *86*, 37.

Mueller, C., and Roskelley, C.D. (2003). Regulation of BRCA1 expression and its relationship to sporadic breast cancer. Breast Cancer Res *5*, 45-52.

Murdoch, W. (1998). Perturbation of sheep ovarian surface epithelial cells by ovulation: evidence for roles of progesterone and poly (ADP-ribose) polymerase in the restoration of DNA integrity. J Endocrinol *156*, 503.

Murdoch, W., and Van Kirk, E. (2002). Steroid hormonal regulation of proliferative, p53 tumor suppressor, and apoptotic responses of sheep ovarian surface epithelial cells.

Mol Cell Endocrinol *186*, 61-67.

Murdoch, W.J. (1995). Programmed cell death in preovulatory ovine follicles. Biol Reprod *53*, 8-12.

Murdoch, W.J. (1999). Plasmin-tumour necrosis factor interaction in the ovulatory process. J Reprod Fertil Suppl *54*, 353-358.

Murdoch, W.J., and Martinchick, J.F. (2004). Oxidative damage to DNA of ovarian surface epithelial cells affected by ovulation: carcinogenic implication and chemoprevention. Exp Biol Med *229*, 546-552.

Murdoch, W.J., Townsend, R.S., and McDonnel, A.C. (2001). Ovulation-induced DNA damage in ovarian surface epithelial cells of ewes: prospective regulatory mechanisms of repair/survival and apoptosis. Biol Reprod *65*, 1417-1424.

Murdoch, W.J., Van Kirk, E.A., and Shen, Y. (2008). Pathogenic reactions of the ovarian surface epithelium to ovulation, dimethylbenzanthracene, and estrogen are negated by vitamin E. Reprod Sci *15*, 839-845.

Nagy, A., Gertsenstein, M., Vintersten, K., and Behringer, R. (2003). Manipulating the Mouse Embryo: A Laboratory Manual, 3 edn (Cold Springs Harbor, NY: Cold Springs Harbor Laboratory Press).

Nasca, P.C., Greenwald, P., Chorost, S., Richart, R., and Caputo, T. (1984). An epidemiologic case-control study of ovarian cancer and reproductive factors. Am J Epidemiol *119*, 705-713.

Nilsson, E., Doraiswamy, V., Parrott, J.A., and Skinner, M.K. (2001). Expression and action of transforming growth factor beta (TGFbeta1, TGFbeta2, TGFbeta3) in normal bovine ovarian surface epithelium and implications for human ovarian cancer. Mol Cell Endocrinol *182*, 145-155.

Noaksson, K., Zoric, N., Zeng, X., Rao, M.S., Hyllner, J., Semb, H., Kubista, M., and Sartipy, P. (2005). Monitoring differentiation of human embryonic stem cells using real-time PCR. Stem Cells *23*, 1460-1467.

Ohtake, H., Katabuchi, H., Matsuura, K., and Okamura, H. (1999). A novel in vitro experimental model for ovarian endometriosis: the three-dimensional culture of human ovarian surface epithelial cells in collagen gels. Fertil Steril *71*, 50-55.

Okada, S., Nakauchi, H., Nagayoshi, K., Nishikawa, S., Miura, Y., and Suda, T. (1992). In vivo and in vitro stem cell function of c-kit- and Sca-1-positive murine hematopoietic cells. Blood *80*, 3044-3050.

Okamoto, S., Okamoto, A., Nikaido, T., Saito, M., Takao, M., Yanaihara, N., Takakura, S., Ochiai, K., and Tanaka, T. (2009). Mesenchymal to epithelial transition in the human ovarian surface epithelium focusing on inclusion cysts. Oncol Rep *21*,

1209-1214.

Ono, M., Maruyama, T., Masuda, H., Kajitani, T., Nagashima, T., Arase, T., Ito, M., Ohta, K., Uchida, H., Asada, H*., et al.* (2007). Side population in human uterine myometrium displays phenotypic and functional characteristics of myometrial stem cells. Proc Natl Acad Sci U S A *104*, 18700-18705.

Osawa, M., Nakamura, K., Nishi, N., Takahasi, N., Tokuomoto, Y., Inoue, H., and Nakauchi, H. (1996). In vivo self-renewal of c-Kit+ Sca-1+ Lin(low/-) hemopoietic stem cells. J Immunol *156*, 3207-3214.

Osterholzer, H.O., Johnson, J.H., and Nicosia, S.V. (1985). An autoradiographic study of rabbit ovarian surface epithelium before and after ovulation. Biol Reprod *33*, 729-738.

Ouellette, Y., Price, C.A., and Carriére, P.D. (2005). Follicular fluid concentration of transforming growth factor-beta1 is negatively correlated with estradiol and follicle size at the early stage of development of the first-wave cohort of bovine ovarian follicles. Domest Anim Endocrinol *29*, 623-633.

Pacchiarotti, J., Maki, C., Ramos, T., Marh, J., Howerton, K., Wong, J., Pham, J., Anorve, S., Chow, Y.C., and Izadyar, F. (2010). Differentiation potential of germ line stem cells derived from the postnatal mouse ovary. Differentiation *79*, 159-170.

Paczkowska, E., Kawa, M., Klos, P., Staniszewska, M., Sienko, J., and Dabkowska, E. (2011). Aldehyde dehydrogenase (ALDH) - a promising new candidate for use in preclinical and clinical selection of pluripotent very small embryonic-like stem cells (VSEL SCs) of high long-term repopulating hematopoietic potential. Ann Transplant *16*, 59-71.

Palafox, M., Ferrer, I., Pellegrini, P., Vila, S., Hernandez-Ortega, S., Urruticoechea, A., Climent, F., Soler, M.T., Muñoz, P., Viñals, F*., et al.* (2012). RANK induces epithelial-mesenchymal transition and stemness in human mammary epithelial cells and promotes tumorigenesis and metastasis. Cancer Res *72*, 2879-2888.

Palfree, R.G., and Hämmerling, U. (1986). Biochemical characterization of the murine activated lymphocyte alloantigen Ly-6E.1 controlled by the Ly-6 locus. J Immunol *136*, 594-600.

Parte, S., Bhartiya, D., Telang, J., Daithankar, V., Salvi, V., Zaveri, K., and Hinduja, I. (2011). Detection, characterization, and spontaneous differentiation in vitro of very small embryonic-like putative stem cells in adult mammalian ovary. Stem Cells Dev *20*, 1451-1464.

Piek, J.M., van Diest, P.J., Zweemer, R.P., Jansen, J.W., Poort-Keesom, R.J., Menko, F.H., Gille, J.J., Jongsma, A.P., Pals, G., Kenemans, P*., et al.* (2001). Dysplastic changes in prophylactically removed Fallopian tubes of women predisposed to developing ovarian cancer. J Pathol *195*, 451-456.

Pothuri, B., Leitao, M.M., Levine, D.A., Viale, A., Olshen, A.B., Arroyo, C., Bogomolniy, F., Olvera, N., Lin, O., Soslow, R.A.*, et al.* (2010). Genetic analysis of the early natural history of epithelial ovarian carcinoma. PLoS One *5*, e10358.

Preffer, F.I., Dombkowski, D., Sykes, M., Scadden, D., and Yang, Y.G. (2002). Lineage-negative side-population (SP) cells with restricted hematopoietic capacity circulate in normal human adult blood: immunophenotypic and functional characterization. Stem Cells *20*, 417-427.

Proia, T.A., Keller, P.J., Gupta, P.B., Klebba, I., Jones, A.D., Sedic, M., Gilmore, H., Tung, N., Naber, S.P., Schnitt, S.*, et al.* (2011). Genetic predisposition directs breast cancer phenotype by dictating progenitor cell fate. Cell Stem Cell *8*, 149-163.

Purdie, D.M., Bain, C.J., Siskind, V., Webb, P.M., and Green, A.C. (2003). Ovulation and risk of epithelial ovarian cancer. Int J Cancer *104*, 228-232.

Radisky, D.C., and LaBarge, M.A. (2008). Epithelial-mesenchymal transition and the stem cell phenotype. Cell Stem Cell *2*, 511-512.

Reynolds, B.A., and Weiss, S. (1996). Clonal and population analyses demonstrate that an EGF-responsive mammalian embryonic CNS precursor is a stem cell. Dev Biol *175*, 1-13.

Riman, T., Dickman, P.W., Nilsson, S., Correia, N., Nordlinder, H., Magnusson, C.M., and Persson, I.R. (2002). Risk factors for invasive epithelial ovarian cancer: results from a Swedish case-control study. Am J Epidemiol *156*, 363-373.

Risch, H.A. (1998). Hormonal etiology of epithelial ovarian cancer, with a hypothesis concerning the role of androgens and progesterone. J Natl Cancer Inst *90*, 1774-1786.

Risch, H.A., Marrett, L.D., and Howe, G.R. (1994). Parity, contraception, infertility, and the risk of epithelial ovarian cancer. Am J Epidemiol *140*, 585-597.

Risch, H.A., Weiss, N.S., Lyon, J.L., Daling, J.R., and Liff, J.M. (1983). Events of reproductive life and the incidence of epithelial ovarian cancer. Am J Epidemiol *117*, 128-139.

Rodriguez, G.C., Walmer, D.K., Cline, M., Krigman, H., Lessey, B.A., Whitaker, R.S., Dodge, R., and Hughes, C.L. (1998). Effect of progestin on the ovarian epithelium of macaques: cancer prevention through apoptosis? J Soc Gynecol Investig *5*, 271-276.

Romagnolo, D., Annab, L.A., Thompson, T.E., Risinger, J.I., Terry, L.A., Barrett, J.C., and Afshari, C.A. (1998). Estrogen upregulation of BRCA1 expression with no effect on localization. Mol Carcinog *22*, 102-109.

Romero, I., and Bast, R.C. (2012). Minireview: human ovarian cancer: biology, current

management, and paths to personalizing therapy. Endocrinology *153*, 1593-1602.

Rossi, D.J., Jamieson, C.H., and Weissman, I.L. (2008). Stems cells and the pathways to aging and cancer. Cell *132*, 681-696.

Roy, R., Chun, J., and Powell, S.N. (2012). BRCA1 and BRCA2: different roles in a common pathway of genome protection. Nature Rev Cancer *12*, 68-78.

Salamanca, C.M., Maines-Bandiera, S.L., Leung, P.C., Hu, Y.L., and Auersperg, N. (2004). Effects of epidermal growth factor/hydrocortisone on the growth and differentiation of human ovarian surface epithelium. J Soc Gynecol Investig *11*, 241-251.

Salazar, H., Godwin, A.K., Daly, M.B., Laub, P.B., Hogan, W.M., Rosenblum, N., Boente, M.P., Lynch, H.T., and Hamilton, T.C. (1996). Microscopic benign and invasive malignant neoplasms and a cancer-prone phenotype in prophylactic oophorectomies. J Natl Cancer Inst *88*, 1810-1820.

Satterwhite, D.J., Matsunami, N., and White, R.L. (2000). TGF-beta1 inhibits BRCA1 expression through a pathway that requires pRb. Biochem Biophys Res Commun *276*, 686-692.

Savagner, P. (2010). The epithelial-mesenchymal transition (EMT) phenomenon. Ann Oncol *21*, vii89-92.

Schlosshauer, P.W., Cohen, C.J., Penault-Llorca, F., Miranda, C.R., Bignon, Y.J., Dauplat, J., and Deligdisch, L. (2003). Prophylactic oophorectomy: a morphologic and immunohistochemical study. Cancer *98*, 2599-2606.

Seton-Rogers, S. (2011). Ovarian cancer: Driving force. Nature Rev Cancer *11*, 538-539.

Shu, X.O., Brinton, L.A., Gao, Y.T., and Yuan, J.M. (1989). Population-based case-control study of ovarian cancer in Shanghai. Cancer Res *49*, 3670-3674.

Shukovski, L., and Tsafriri, A. (1994). The involvement of nitric oxide in the ovulatory process in the rat. Endocrinology *135*, 2287-2290.

Siemens, C.H., and Auersperg, N. (1988). Serial propagation of human ovarian surface epithelium in tissue culture. J Cell Physiol *134*, 347-356.

Simons, K., and Toomre, D. (2000). Lipid rafts and signal transduction. Nat Rev Mol Cell Biol *1*, 31-39.

Soneoka, Y., Cannon, P.M., Ramsdale, E.E., Griffiths, J.C., Romano, G., Kingsman, S.M., and Kingsman, A.J. (1995). A transient three-plasmid expression system for the production of high titer retroviral vectors. Nucleic Acids Res *23*, 628-633.

Spangrude, G.J., Muller-Sieburg, C.E., Heimfeld, S., and Weissman, I.L. (1988). Two rare populations of mouse Thy-1lo bone marrow cells repopulate the thymus. J Exp Med *167*, 1671-1683.

Spangrude, G.J., Smith, L., Uchida, N., Ikuta, K., Heimfeld, S., Friedman, J., and Weissman, I.L. (1991). Mouse hematopoietic stem cells. Blood *78*, 1395-1402.

Spillman, M.A., and Bowcock, A.M. (1996). BRCA1 and BRCA2 mRNA levels are coordinately elevated in human breast cancer cells in response to estrogen. Oncogene *13*, 1639-1645.

Stanford, W.L., Haque, S., Alexander, R., Liu, X., Latour, A.M., Snodgrass, H.R., Koller, B.H., and Flood, P.M. (1997). Altered proliferative response by T lymphocytes of Ly-6A (Sca-1) null mice. J Exp Med *186*, 705-717.

Stefanová, I., Horejsí, V., Ansotegui, I.J., Knapp, W., and Stockinger, H. (1991). GPI-anchored cell-surface molecules complexed to protein tyrosine kinases. Science *254*, 1016-1019.

Steg, A.D., Bevis, K.S., Katre, A.A., Ziebarth, A., Dobbin, Z.C., Alvarez, R.D., Zhang, K., Conner, M., and Landen, C.N. (2012). Stem cell pathways contribute to clinical chemoresistance in ovarian cancer. Clin Cancer Res *18*, 869-881.

Storm, M.P., Bone, H.K., Beck, C.G., Bourillot, P.Y., Schreiber, V., Damiano, T., Nelson, A., Savatier, P., and Welham, M.J. (2007). Regulation of Nanog expression by phosphoinositide 3-kinase-dependent signaling in murine embryonic stem cells. J Biol Chem *282*, 6265-6273.

Sundfeldt, K., Piontkewitz, Y., Ivarsson, K., Nilsson, O., Hellberg, P., Brännström, M., Janson, P.O., Enerback, S., and Hedin, L. (1997). E-cadherin expression in human epithelial ovarian cancer and normal ovary. Int J Cancer *74*, 275-280.

Szotek, P., Chang, H., Brennand, K., Fujino, A., Pieretti-Vanmarcke, R., Lo Celso, C., Dombkowski, D., Preffer, F., Cohen, K., Teixeira, J*., et al.* (2008). Normal ovarian surface epithelial label-retaining cells exhibit stem/progenitor cell characteristics. Proc Natl Acad Sci U S A *105*, 12469-12473.

Szotek, P., Pieretti-Vanmarcke, R., Masiakos, P., Dinulescu, D., Connolly, D., Foster, R., Dombkowski, D., Preffer, F., Maclaughlin, D., and Donahoe, P. (2006). Ovarian cancer side population defines cells with stem cell-like characteristics and Mullerian Inhibiting Substance responsiveness. Proc Natl Acad Sci U S A *103*, 11154-11159.

Tan, O.L., Hurst, P.R., and Fleming, J.S. (2005). Location of inclusion cysts in mouse ovaries in relation to age, pregnancy, and total ovulation number: implications for ovarian cancer? J Pathol *205*, 483-490.

Tonary, A., Macdonald, E., Faught, W., Senterman, M., and Vanderhyden, B. (2000). Lack of expression of c-KIT in ovarian cancers is associated with poor prognosis. Int J Cancer *89*, 242-250.

Tsirigotis, M., Thurig, S., Dube, M., Vanderhyden, B.C., Zhang, M., and Gray, D.A. (2001). Analysis of ubiquitination in vivo using a transgenic mouse model. BioTechniques

*31*, 120-126, 128, 130.

Tzur, A., Moore, J.K., Jorgensen, P., Shapiro, H.M., and Kirschner, M.W. (2011). Optimizing optical flow cytometry for cell volume-based sorting and analysis. PLoS One *6*, e16053.

van Leeuwen, F.E., Klip, H., Mooij, T.M., van de Swaluw, A.M., Lambalk, C.B., Kortman, M., Laven, J.S., Jansen, C.A., Helmerhorst, F.M., Cohlen, B.J.*, et al.* (2011). Risk of borderline and invasive ovarian tumours after ovarian stimulation for in vitro fertilization in a large Dutch cohort. Hum Reprod *26*, 3456-3465.

Vigne, J.L., Halburnt, L.L., and Skinner, M.K. (1994). Characterization of bovine ovarian surface epithelium and stromal cells: identification of secreted proteins. Biol Reprod *51*, 1213-1221.

Virant-Klun, I., Rozman, P., Cvjeticanin, B., Vrtacnik-Bokal, E., Novakovic, S., Rulicke, T., Dovc, P., and Meden-Vrtovec, H. (2009). Parthenogenetic embryo-like structures in the human ovarian surface epithelium cell culture in postmenopausal women with no naturally present follicles and oocytes. Stem Cells Dev *18*, 137-149.

Virant-Klun, I., Skutella, T., Stimpfel, M., and Sinkovec, J. (2011). Ovarian surface epithelium in patients with severe ovarian infertility: a potential source of cells expressing markers of pluripotent/multipotent stem cells. J Biomed Biotechnol *2011*, 381928.

Virant-Klun, I., Zech, N., Rozman, P., Vogler, A., Cvjeticanin, B., Klemenc, P., Malicev, E., and Meden-Vrtovec, H. (2008). Putative stem cells with an embryonic character isolated from the ovarian surface epithelium of women with no naturally present follicles and oocytes. Differentiation *76*, 843-856.

Weberpals, J.I., Clark-Knowles, K.V., and Vanderhyden, B.C. (2008). Sporadic epithelial ovarian cancer: clinical relevance of BRCA1 inhibition in the DNA damage and repair pathway. J Clin Oncol *26*, 3259-3267.

Weiss, S., Reynolds, B.A., Vescovi, A.L., Morshead, C., Craig, C.G., and van der Kooy, D. (1996). Is there a neural stem cell in the mammalian forebrain? Trends Neurosci *19*, 387-393.

Welm, B.E., Tepera, S.B., Venezia, T., Graubert, T.A., Rosen, J.M., and Goodell, M.A. (2002). Sca-1(pos) cells in the mouse mammary gland represent an enriched progenitor cell population. Dev Biol *245*, 42-56.

Werness, B.A., Afify, A.M., Bielat, K.L., Eltabbakh, G.H., Piver, M.S., and Paterson, J.M. (1999). Altered surface and cyst epithelium of ovaries removed prophylactically from women with a family history of ovarian cancer. Hum Pathol *30*, 151-157.

White, Y.A.R., Woods, D.C., Takai, Y., Ishihara, O., Seki, H., and Tilly, J.L. (2012). Oocyte formation by mitotically active germ cells purified from ovaries of reproductive-age

women. Nature Medicine *18*, 413-421.

Whittemore, A.S. (1993). Personal characteristics relating to risk of invasive epithelial ovarian cancer in older women in the United States. Cancer *71*, 558-565.

Whittemore, A.S., Harris, R., and Itnyre, J. (1992). Characteristics relating to ovarian cancer risk: collaborative analysis of 12 US case-control studies. IV. The pathogenesis of epithelial ovarian cancer. Collaborative Ovarian Cancer Group. Am J Epidemiol *136*, 1212-1220.

Wong, A.S., and Leung, P.C. (2007). Role of endocrine and growth factors on the ovarian surface epithelium. J Obstet Gynaecol Res *33*, 3-16.

Woodward, W.A., Chen, M.S., Behbod, F., and Rosen, J.M. (2005). On mammary stem cells. J Cell Sci *118*, 3585-3594.

Wright, J.W., Pejovic, T., Fanton, J., and Stouffer, R.L. (2008a). Induction of proliferation in the primate ovarian surface epithelium in vivo. Hum Reprod *23*, 129-138.

Wright, M.H., Calcagno, A.M., Salcido, C., Carlson, M., Ambudkar, S., and Varticovski, L. (2008b). Brca1 breast tumors contain distinct CD44+/CD24- and CD133+ cells with cancer stem cell characteristics. Breast Cancer Res *10*, R10.

Wu, Z.Q., Li, X.Y., Hu, C.Y., Ford, M., Kleer, C.G., and Weiss, S.J. (2012). Canonical Wnt signaling regulates Slug activity and links epithelial-mesenchymal transition with epigenetic Breast Cancer 1, Early Onset (BRCA1) repression. Proc Natl Acad Sci U S A *109*, 16654-16659.

Wulf, G.G., Wang, R.Y., Kuehnle, I., Weidner, D., Marini, F., Brenner, M.K., Andreeff, M., and Goodell, M.A. (2001). A leukemic stem cell with intrinsic drug efflux capacity in acute myeloid leukemia. Blood *98*, 1166-1173.

Yang, J., Mani, S.A., Donaher, J.L., Ramaswamy, S., Itzykson, R.A., Come, C., Savagner, P., Gitelman, I., Richardson, A., and Weinberg, R.A. (2004). Twist, a master regulator of morphogenesis, plays an essential role in tumor metastasis. Cell *117*, 927-939.

Zavadil, J., and Böttinger, E. (2005). TGF-beta and epithelial-to-mesenchymal transitions. Oncogene *24*, 5764-5774.

Zhang, S., Balch, C., Chan, M.W., Lai, H.C., Matei, D., Schilder, J.M., Yan, P.S., Huang, T.H., and Nephew, K.P. (2008). Identification and characterization of ovarian cancer-initiating cells from primary human tumors. Cancer Res *68*, 4311-4320.

Zhu, Y., Nilsson, M., and Sundfeldt, K. (2010). Phenotypic plasticity of the ovarian surface epithelium: TGF-beta 1 induction of epithelial to mesenchymal transition (EMT) in vitro. Endocrinology *151*, 5497-5505.

Zou, K., Yuan, Z., Yang, Z., Luo, H., Sun, K., Zhou, L., Xiang, J., Shi, L., Yu, Q., Zhang,

Y., *et al.* (2009). Production of offspring from a germline stem cell line derived from neonatal ovaries. Nat Cell Biol *11*, 631-636.

Zuba-Surma, E.K., Wu, W., Ratajczak, J., Kucia, M., and Ratajczak, M.Z. (2009). Very small embryonic-like stem cells in adult tissues-potential implications for aging. Mech Ageing Dev *130*, 58-66.